CAPITAL UNIVERSITY OF SCIENCE AND
TECHNOLOGY, ISLAMABAD

Improved Attitude Determination using Low-cost MEMS Sensors

by

Shoaib Mansoor

A thesis submitted in partial fulfillment for the
degree of Doctor of Philosophy

in the

Faculty of Engineering
Department of Electrical Engineering

2020

Improved Attitude Determination using Low-cost MEMS Sensors

By

Shoaib Mansoor

Dr. Ahmed El-Mowafy, Associate Professor

Curtin University, Perth, Australia

(Foreign Evaluator 1)

Dr. Fu Li, Professor

BeiHang University, Beijing, China

(Foreign Evaluator 2)

Dr. Aamir Iqbal Bhatti

(Thesis Supervisor)

Dr. Umar Iqbal Bhatti, IST, Islamabad

(Thesis Co-Supervisor)

Dr. Noor Muhammad Khan

(Head, Department of Electrical Engineering)

Dr. Imtiaz Ahmed Taj

(Dean, Faculty of Engineering)

DEPARTMENT OF ELECTRICAL ENGINEERING

CAPITAL UNIVERSITY OF SCIENCE AND TECHNOLOGY

ISLAMABAD

2020

Copyright © 2020 by Shoaib Mansoor

All rights reserved. No part of this thesis may be reproduced, distributed, or transmitted in any form or by any means, including photocopying, recording, or other electronic or mechanical methods, by any information storage and retrieval system without the prior written permission of the author.

Dedicated to my family

CAPITAL UNIVERSITY OF SCIENCE & TECHNOLOGY ISLAMABAD

Expressway, Kahuta Road, Zone-V, Islamabad
Phone:+92-51-111-555-666 Fax: +92-51-4486705
Email: info@cust.edu.pk Website: https://www.cust.edu.pk

CERTIFICATE OF APPROVAL

This is to certify that the research work presented in the thesis, entitled "**Improved Attitude Determination Using Low-cost MEMS Sensors**" was conducted under the supervision of **Dr. Aamer Iqbal Bhatti**. No part of this thesis has been submitted anywhere else for any other degree. This thesis is submitted to the **Department of Electrical Engineering, Capital University of Science and Technology** in partial fulfillment of the requirements for the degree of Doctor in Philosophy in the field of **Electrical Engineering.** The open defence of the thesis was conducted on **01 July, 2020.**

Student Name :	Mr. Shoaib Mansoor (PE141003)	

The Examination Committee unanimously agrees to award PhD degree in the mentioned field.

Examination Committee :

(a)	External Examiner 1:	Dr. Abdul Khaliq, Professor SS CASE IT, Islamabad	
(b)	External Examiner 2:	Dr. Amir Shahzad, NESCOMM, Islamabad	
(c)	Internal Examiner :	Dr. Muhammad Asharaf Professor CUST, Islamabad	
	Supervisor Name :	Dr. Aamer Iqbal Bhatti Professor CUST, Islamabad	
	Name of HoD :	Dr. Noor Muhammad Khan Professor CUST, Islamabad	
	Name of Dean :	Dr. Imtiaz Ahmed Taj Professor CUST, Islamabad	

AUTHOR'S DECLARATION

I, **Mr. Shoaib Mansoor (Registration No. PE141003)**, hereby state that my PhD thesis titled, '**Improved Attitude Determination Using Low-cost MEMS Sensors**' is my own work and has not been submitted previously by me for taking any degree from Capital University of Science and Technology, Islamabad or anywhere else in the country/ world.

At any time, if my statement is found to be incorrect even after my graduation, the University has the right to withdraw my PhD Degree.

(**Mr. Shoaib Mansoor**)

Dated: 1st July, 2020

Registration No : PE141003

PLAGIARISM UNDERTAKING

I solemnly declare that research work presented in the thesis titled "**Improved Attitude Determination Using Low-cost MEMS Sensors**" is solely my research work with no significant contribution from any other person. Small contribution/ help wherever taken has been duly acknowledged and that complete thesis has been written by me.

I understand the zero tolerance policy of the HEC and Capital University of Science and Technology towards plagiarism. Therefore, I as an author of the above titled thesis declare that no portion of my thesis has been plagiarized and any material used as reference is properly referred/ cited.

I undertake that if I am found guilty of any formal plagiarism in the above titled thesis even after award of PhD Degree, the University reserves the right to withdraw/ revoke my PhD degree and that HEC and the University have the right to publish my name on the HEC/ University Website on which names of students are placed who submitted plagiarized thesis.

(**Mr. Shoaib Mansoor**)

Dated: 1st July, 2020

Registration No : PE141003

List of Publications

It is certified that following publication(s) have been made out of the research work that has been carried out for this thesis:-

1. **S. Mansoor**, U.I. Bhatti, A.I. Bhatti, S.M. Dildar Ali, "Improved Attitude Determination by Compensation of Gyroscopic Drift by use of Accelerometers and Magnetometers," *Measurement*, vol. 131, pp.582-589, 2019.

Shoaib Mansoor
(Registration No. PE141003)

Acknowledgements

I would like to thank all the people who helped me and provide me support throughout the entire period of my Ph.D at CUST. First of all I am grateful to my supervisor Professor Aamir Iqbal Bhatti and Co-adviser Dr. Umar Iqbal Bhatti whose guidance and supervision, enable me to conclude my research. Specially, I express my gratitude to Dr. Umar Iqbal Bhatti for both technical and moral support, his precious time and encouragement throughout the research.

I would also thank to my colleagues Mr. Imaran Adil, Syed Dildar Ali, Muhammad Awais, Shafiq Muhammad, Muhammad Arif and Sohail Ahamd for providing me technical support in experimentation, data analysis and testing. I am very thankful to my seniors Dr. Irfan Ahmad for his motivation and Atif Mehmood Chishti for his cooperation.

Finally a lot of thanks to my parents and wife without their support and love I would never be able to reach at this point.

Abstract

Attitude determination is an essential requirement in a wide range of applications like vehicle and space navigation, robotics, virtual environment, surveillance, and Unmanned Air Vehicle. In the standard navigation algorithms, attitude is computed by numeric integration of the gyroscopes (abbreviated as gyros). However, gyros specifically MEMS gyros suffer from large bias errors, which when integrated with time, introduce an unacceptable error in the computed attitude.

For static and low dynamic applications, attitude can also be computed by vector matching using two or more directional vectors. Three accelerometers and three magnetometers rigidly mounted in x, y and z axes can be used as directional vectors to sense gravity and Earth's magnetic field vectors. As the reference vectors of each of these are known, vector matching technique can be used for attitude computation using these sensors. However, the attitude computed via vector matching is noisy as the sensors noise directly appear in the computed attitude. Also, the attitude computed via vector matching is not reliable under accelerated motion and magnetic disturbance as in such cases, the accelerometers will sense linear acceleration in addition to the gravity and the magnetometers will measure nearby magnetic field in addition to the Earth's field.

In the proposed research, we combined both methods and proposed techniques to compute improved attitude under static and dynamic motions. The first method proposed a simplified Quaternion feedback structure for gyro biases estimation and correction. This scheme uses gyros for attitude determination and a combination of accelerometers and magnetometers as aiding sensors for gyros bias errors estimation. The scheme functions in a closed loop by continuously estimating and correcting biases of the gyros. In the other two techniques, we used Kalman filter based data fusion in direct and indirect configurations. These techniques use gyros, accelerometers and magnetometers and fuse their data for error detection and correction. In indirect configuration, error states are estimated which are then used for correction. In the second method, attitude parameters are directly estimated in quaternion form using Kalman filter. Experimental tests have been performed to verify the proposed schemes under static and dynamic conditions

using a self-developed setup consisting of MEMS-based IMU and FPGA based electronics.

Quaternion feedback configuration is also compared with Kalman filter based data fusion algorithm. The proposed quaternion feedback showed comparable results with low computational requirements and lesser probability of instability. It also caters for the effect of linear acceleration during which accelerometer outputs are not reliable for gravity vector sensing.

As in MEMS-based IMU, three-axis gyros, accelerometers and magnetometers are already available; the proposed methods can serve as self-aiding schemes for improved attitude determination.

Contents

List of Figures

List of Tables

Abbreviations

AHRS	Attitude and Heading Reference System
ARW	Angle Random Walk
DCM	Direction Cosine Matrix
ECEF	Earth Centered Earth Fixed Frame
EKF	Extended Kalman Filter
ENU	East North Up
GNSS	Global Navigation Sattellite System
GPS	Global Positioning System
IFOG	Interferrometric Fiber Optic Gyroscope
i-Frame	Inertial Frame
IMU	Inertial Measurement Unit
INS	Inertial Navigation System
KF	Kalman Filter
MEMS	Micromachined Electromechanical System
NED	North East Down
n-Frame	Navigation Frame
QFB	Quaternion Feedback
QUEST	Quaternion Estimator
RI	Rate Integration
RLG	Ring Laser Gyroscope
RMS	Root Mean Square
UAV	Unmanned Air Vehicle

Symbols

g	Acceleration due to gravity
ω	Angular rate
Ω	Angular rate vector
Δq	Attitude Error in Quaternion
$\mathbf{q}^*$	Conjugate of Unit Quaternion
P_k	Error Covariance Matrix
$\hat{a}$	Gravity vector
σ_N	Gyro Noise Density
ψ	Heading angle
$\mathbf{q}^-1$	Inverse of Unit Quaternion
$\hat{m}$	Magnetic Field vector
R	Measurement Covariance Matrix
v_k	Measurement Noise Vector
θ	Pitch angle
Q	Process Covariance Matrix
w_k	Process Noise Vector
β	Real part of Quaternion
$\mathbf{p}$	Rodriguez Parameter
ϕ	Roll angle
$\mathbf{q}$	Unit Quaternion
γ	Vector part of Quaternion

Chapter 1

Introduction

1.1 Background

Navigation is a technique for the determination of position, velocity, and orientation of a moving object with respect to some reference [1]. Navigation is a very ancient skill and an essential for traveling and finding the way from one place to another. Historically mankind used different methods and tools like landmarks, sun and stars for finding position and directions. With the advancement in microelectronics and integrated circuit technology, new methods and tools were developed and today more advanced and sophisticated instruments like Inertial Navigation Systems (INS), Gyrocompass and Global Position Systems (GPS) are available for worldwide Navigation [1].

1.2 Inertial Navigation

Navigation process conducted using inertial sensors is called inertial navigation. The operation of inertial navigation depends upon the laws of classical mechanics as formulated by Issac Newton. According to these laws, a moving body will continue its motion in a straight line unless disturbed by some force acting upon it. Similarly, a force acting on a body will produce an acceleration in that body.

Hence, if the acceleration of a moving body is known, it is possible to calculate the change in velocity and position by successive integration of the acceleration with respect to the time. To get component of acceleration aligned with the reference frame, it is also necessary to track rotation of the body with respect to the reference frame [2].

Hence, for inertial navigation, we need two types of inertial sensors, i.e. accelerometers and gyroscopes (commonly abbreviated to gyros). An accelerometer measures specific force form which acceleration can be inferred, and a gyroscope measures angular rate of rotation.

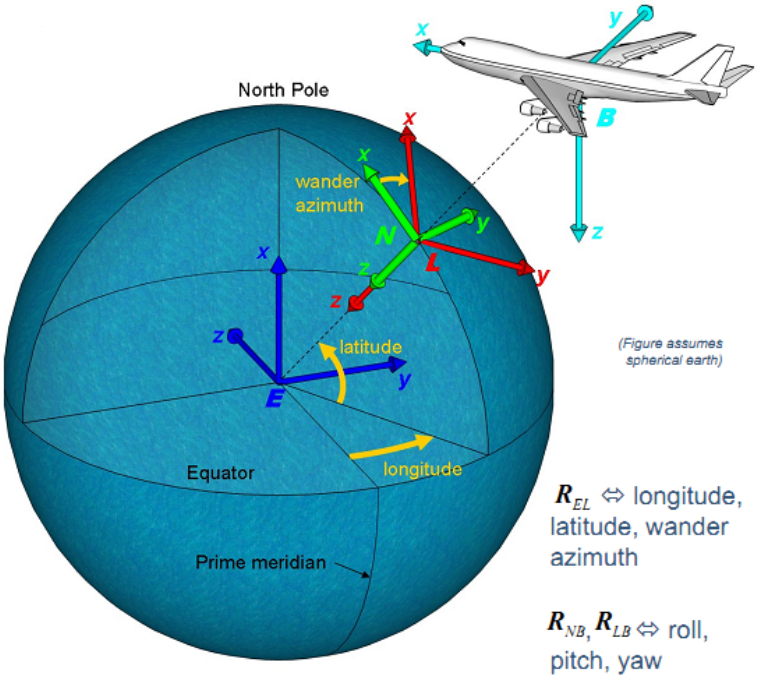

FIGURE 1.1: Navigation Parameters [3]

1.3 Inertial Navigation Systems

Inertial Navigation System uses inertial sensors, i.e. gyroscopes and accelerometers to provide complete navigation information (position, velocity and orientation). Starting from an initial orientation and position, the outputs of gyroscopes are integrated to provide orientation information and the outputs of accelerometers aided by gyros are integrated once to provide velocities and twice to provide

position information.

Inertial Navigation Systems are autonomous systems which rely upon its sensors and does not require any external reference. However, due to imperfection of the sensors, the sensors' errors are also integrated and the navigation solution starts to drift with time. Therefore, in order to provide accurate navigation information for a long periods of time, very high quality sensors with minimum errors are required which are very expensive. The outputs of an Inertial Navigation System with low cost sensors drift within a short period of time. However, some other techniques are available by which the outputs of a navigation systems can be corrected using some external sources which will be discussed later in this chapter. A brief introduction of the accelerometers and gyroscopes and their types are given below.

1.3.1 Accelerometers

As described earlier, inertial navigation depends upon the measurements of acceleration which is integrated successively to compute velocity and position respectively. The device used to measure acceleration is called an accelerometer. Accelerometers measure acceleration in meter per second squared (m/sec^2) or g-force. 1-g is equal to the gravitational acceleration on the Earth, which is approximately 9.8 m/s^2. Depending upon the construction of the device, accelerometers are categorized into two categories [2].

- Mechanical Accelerometers
- Solid State Accelerometers

The traditional mechanical accelerometers work on the principle of a spring mass system in which, the deflection of the spring, proportional to the force acting on the mass is used to measure the acceleration. The technology of mechanical accelerometers is well established. They are available with a dynamic range of few micro-g_s to tens of g_s. For the last few decades, significant advances have been made in the development of solid-state accelerometer in which the mechanical sensing structure

along with the microelectronics readout circuits are developed on silicon[2]. The solid state accelerometer is also called MEMS (Micro-electromechanical systems) accelerometer.

1.3.2 Gyroscopes

A gyroscope is a device used to measure either the angular rate or angle by which a structure or a vehicle rotates about some predefined axis. Gyroscopes have been used in a variety of applications like

- Stabilization
- Autopilot feedback
- Flight path sensor
- Navigation

Conventional mechanical gyroscope mainly consists of a spinning rotor supported by a pair of gimbals. The rotor spinning at high speed makes the use of its inertial properties and tends to maintain its direction of spin. The advancement in fiber optics and silicon technology leads to the development of optical and MEMS gyroscopes, which are now in use for a variety of applications. Depending upon the working principle, gyroscopes are mainly categorized in three [4].

- Mechanical Gyroscopes
- Optical Gyroscopes (Interferometric Fiber Optic Gyros (IFOGs) and Ring Laser Gyros (RLGs)
- Micro-electromechanical Systems (MEMS) gyroscopes

The choice of a type of gyroscope depends upon the application. The first two types are mainly used in inertial navigation. The MEMS gyroscopes are being widely used these days in consumer electronic such as smartphones.

1.4 Types of Inertial Navigation Systems

From an implementation point of view, there are two types of inertial navigation systems. These are

- Stable Platform Systems or Gimbaled Systems
- Strapdown Systems

1.4.1 Stable Platform Systems or Gimbaled Systems

In Stable Platform systems, the sensors are mounted on a set of gimbals such that the platform always remains aligned with the reference frame. This is achieved by a set of motors which rotate the platform when the rotation is sensed by the gyros. As the platform is always aligned with the reference frame, the outputs of accelerometers are directly integrated to compute velocity and position [1]. These systems are complex and their uses are limited to military applications like aircraft, missiles, ships and combat vehicles in the past [5].

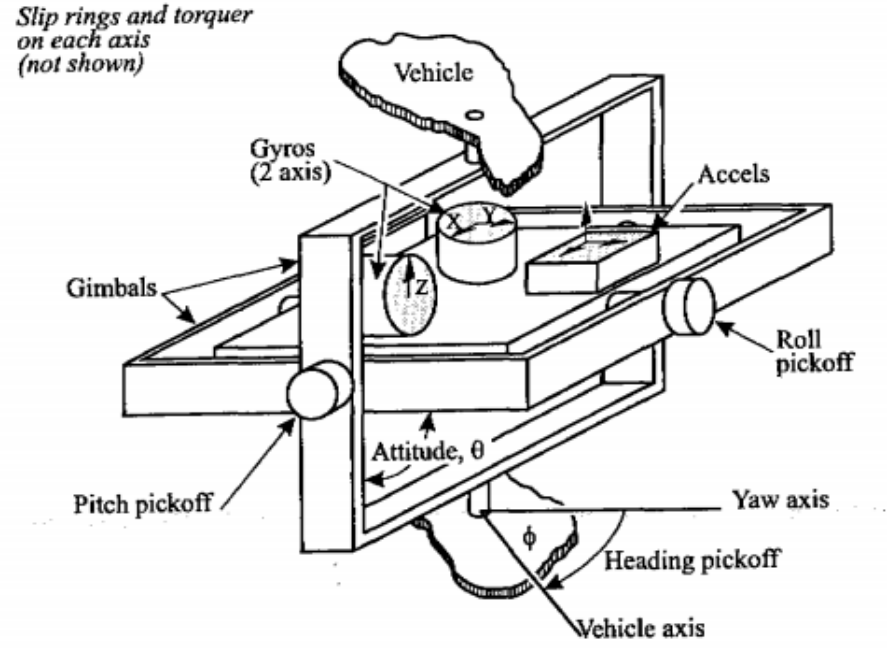

FIGURE 1.2: Gimbaled Systems [6]

1.4.2 Strapdown Systems

With the advancement in Technology, the uses of navigation systems and inertial sensors has rapidly increased especially after arising strapdown systems. In strapdown systems, the sensors are rigidly mounted to the body of the moving platform and the gimbals are replaced by software running in the navigation computer [1]. Rotations rates measured by gyros are used to transform the accelerometer readings from the body frame to the reference frame numerically, instead of physically aligning the accelerometers to the reference frame. After transformation, the accelerometer outputs are integrated to compute velocity and position. Strapdown systems are less-expensive, light weight, small size, low power consumption and more reliable [1].

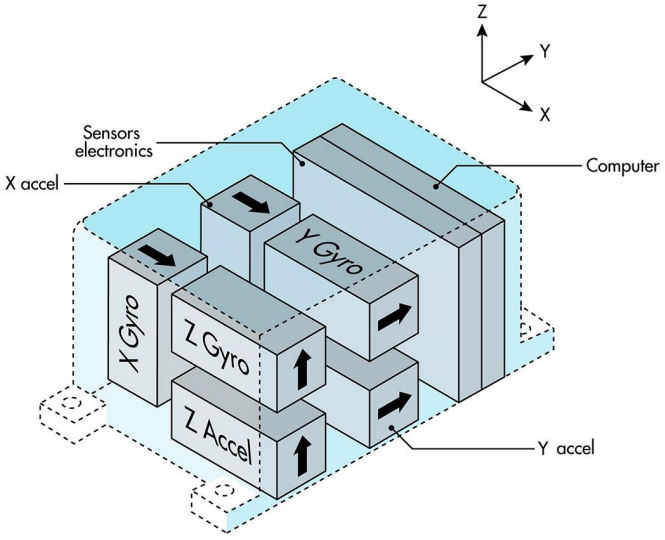

FIGURE 1.3: Strapdown System [6]

Advancement of semiconductor technology resulted in miniature computational hardware and inertial sensors. This made the implementation of strapdwon systems easy which resulted in many new applications such as [2]

- Land vehicle Navigation and Control
- Unmanned Air Vehicles

- Personal Navigation and Transportation
- Surveying and drilling operations
- Smart Phone and Games.

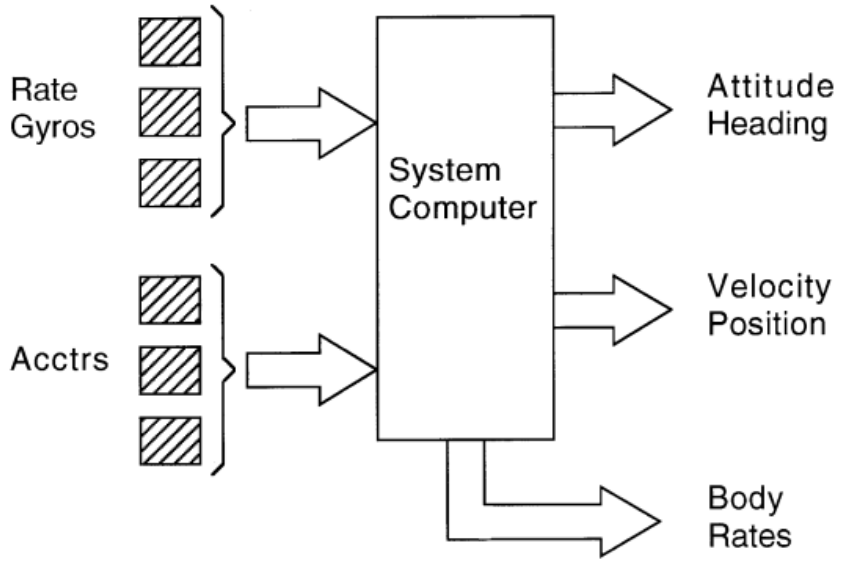

FIGURE 1.4: Schematic Diagram of a Strapdown System [4]

1.5 Inertial Measurement Unit (IMU)

An Inertial Measurement Unit (IMU) consists of three gyros and three accelerometers mounted in orthogonal directions to produce a three-dimensional measurement of specific forces and angular rates. The accelerometers and gyroscopes constitute the inertial sensor assembly (ISA) that is housed along with related electronics in the IMU. The inertial navigation system (INS) comprises the IMU, a computer, mechanization and filtering algorithms. The inertial navigation system (INS) provides position, velocity, and attitude of the host vehicle. Attitude refers to the orientation of a body with respect to some reference frame. Attitude information is very vital in airborne applications where it specifies the manoeuvring and trajectory of the mission. It is also an essential task in a wide range of applications like Unmanned Air Vehicles (UAVs), virtual environment, robotics and head tracking systems [7–9].

1.6 Attitude and Heading Reference System (AHRS)

Attitude and Heading Reference System (AHRS) are basically similar to the inertial navigation systems (INS). The major difference between the two is accuracy and cost of the sensors used [4]. Inertial navigation systems use very high accuracy sensors (both gyros and accelerometers) to provide accurate position, velocity and attitude information without any external reference. Correspondingly the system's cost is high. Attitude and heading reference system (AHRS) uses relatively low performance sensors. Attitude and Heading Reference Systems provide only attitude information for precise orientation. The accelerometers are not of that quality which can be integrated twice to provide precise position. Some other external sources are combined with inertial measurement unit (IMU) for sensor errors' detection and correction which will be discussed later in this chapter.

1.7 External Aiding

The performance of any inertial system is limited by the sensors' errors. Because of the numerical integration involved in the standard navigation algorithms, any error in the sensor outputs will be integrated and introduce error in the computed navigation parameters. For example, any error in the accelerometer outputs will be integrated twice to produce error in the computed position. Similarly gyroscope errors will introduce errors in the attitude as well as in the position. The reason is, in strapdown systems, the attitude computed by the integration of the angular rates given by the gyroscopes will be used to calculate the accelerations in the direction of the reference frame after which, these accelerations will be used for the velocities and position calculation. The errors in inertial sensors can be reduced, but cannot be completely eliminated. Therefore, none of the inertial navigation systems can provide precise navigation information for a long periods of time. As the sensor errors grow with time because of the numerical integration, the

minimum the errors, the lower will be the navigation parameters' drift with time. Inertial navigation systems with high accuracy sensors provide accurate navigation information for long periods while the navigation solution of the low accuracy sensors drifts within a short periods of time. In order for inertial navigation system to provide accurate navigation information for long periods of time, it is necessary to detect and correct the sensors errors. To achieve this task, some external source is required, which can provide a reference for the navigation parameters computed from the inertial navigation systems. This is called external aiding and the systems using aiding are called aided systems.
In aided systems, the navigation parameters are computed using the sensor outputs and compared with that computed from other independent sources. The resulting error is then used to correct the navigation information and the sensor outputs. There are different sources used for aiding. These include

- Global Navigation Satellite Systems (GNSS)
- Magnetometer (Electronic Compass)
- Odometery
- Camera (Visual Navigation)
- Digital Scene Maching
- Air Data System

1.7.1 Global Navigation Satellite Systems (GNSS)

The most widely used source for inertial navigation system's aiding is Global Navigation Satellite System. GNSS provide position in terms of latitude, longitude and altitude plus velocities along north and east directions. Currently there are four satellite systems fully functional. These are GPS from US, GLONASS from Russia, Galileo from European Union and Baidue from China. The most popular of these systems is, American Global Position Systems (GPS). GPS consists of a

constellation of 31 Satellite which are spread in six circular orbits each containing four or more [10]. These satellites transmit encoded radio frequency signals which are received by ground receivers. The ground receiver calculates its own position by using the travel time of the RF signal and the position of the transmitting satellite [1]. To provide precise location, the GPS receiver needs at least four satellite signals. GPS provides absolute position and velocity information which are periodically used to correct the inertial navigation system's parameters.
GPS provides very good navigation parameters in outdoor applications when sufficient number of satellites are available for the receiver. However, it cannot be used for indoor navigation, forest and near tall buildings where satellite signals are weak or not available for the receiver.

1.7.2 Magnetometers

Magnetometers measure the Earth's magnetic field which can be used to find heading relative to the earth's magnetic field. For this purpose three magnetometers mounted in orthogonal directions are required to measure the magnetic fields in X, Y and Z directions. These measurements are used to compute magnetic north, which is converted to the true north and used for aiding [11].
The magnetometer measurements are not very accurate because they are also disturbed by external magnetic fields other than the Earth, due to any nearby metallic structure or current flowing through circuits. It also does not provide position information. However, using magnetometers the system remains autonomous as it does not depend on any external source.

1.7.3 Odometer

Odometer consists of a sensor that measures the rotation of a wheel and provide speed of the host vehicle continuously. The linear distance travelled can be calculated using the rotation data. The speed and distance travelled can be used for aiding inertial navigation systems [12–16]. Odometer provides a low cost

solution with high sampling rate and short term accuracy. However, any small error increases without limits and correspondingly position error increases with the distance travelled [1].

1.7.4 Camera (Visual Navigation)

Camera based systems are also used as aiding sources for inertial navigation systems. Such systems provide position and attitude measurement which can be used for correcting the inertial navigation system outputs [17, 18]. Traditionally, camera based systems are used to navigate over pre-mapped area. The images of the area are stored prior to the flight. During the flight, camera takes pictures which are compared to the pre-saved images from which the position and attitude are calculated.

Camera based systems also suffer from limitations like illumination changes, shadows and snow or water surfaces where no significant difference are found in successive images.

1.7.5 Air Data System

Air data system in aircraft provides pressure altitude, vertical speed and true airspeed, etc. which are used for aiding attitude and heading reference systems [4, 19]. Many manufacturers now provide both air data system and inertial reference system as a single system in one box called Air Data Inertial Reference System (ADIRS). The advantages of such system are lower cost and need less space for installation. In addition, some other sources like SONAR, LIDAR, stars and radars are also used for aiding [13, 15, 20, 21].

The type of aiding source used for error detection and correction depends upon the application. For example,the most widely used aiding source for air-born applications is Global Navigation Satellite System (GNSS). In land navigation, the odometer and magnetometers are also used. Sometimes, multiple aiding sources are used together for better performance and reliability.

1.8 Thesis Organization

The subject of this thesis is improved attitude determination using low cost MEMS sensors by estimating and correcting gyro errors. The types and categories of inertial sensors, inertial sensor errors with their effects, navigation equations, mathematics and techniques for multi-sensor integration for errors estimation and correction are discussed in this thesis. The overall thesis is organized chapter-wise as follows.

Chapter 1 briefly describes the inertial navigation technology and the basic building blocks of the inertial navigation systems. Inertial sensors and systems, their types, the system's aiding and aiding sources are reviewed.

Chapter 2 covers the sensors' errors and their effects on navigation parameters, attitude determination and a survey of previous work done on attitude estimation. Based on the previous work and research gap, the problem is defined with significance and motivation.

Chapter 3 details different attitude representations and navigation mathematics. The relationship between different attitude representations and the merits and demerits of each representation are discussed. Quaternion mathematics used in attitude determination methods is also discussed.

Chapter 4 explores methods of attitude determination based on vector observations and rate sensors.

Chapter 5 proposes multi-sensor integration techniques for better attitude information. Kalman Filter based direct and indirect methods are presented for combining data from gyros, accelerometers and magnetometers. A simplified quaternion feedback algorithm is also proposed for improved attitude determination.

Chapter 6 describes test setup, sensors' calibration and different tests performed to evaluate the attitude determination algorithms. Both Kalman filter based and quaternion feedback multi-sensor algorithms are implemented using real sensors' data. Results' comparison of different attitude determination methods and proposed multi-sensor integration techniques are shown.

Chapter 7 concludes the thesis and suggests some future work.

Chapter 2

Sensor Errors and Attitude Estimation

2.1 Attitude of a Body

Attitude refers to the orientation of a body with respect to some reference frame. To completely describe the orientation of a body in three-dimensional space, three angles need to be specified. These are the roll, pitch and yaw which are the rotation angles of the body frame along X, Y and Z directions (North, East and Down) as shown in Figure 2.1.

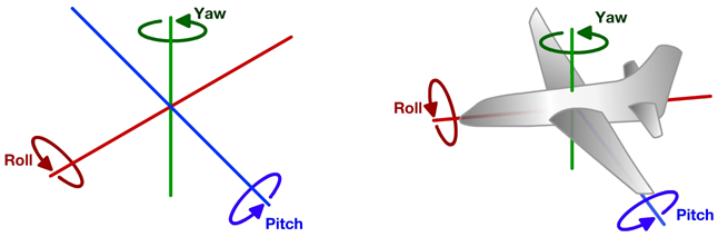

FIGURE 2.1: Attitude Representation in Euler angles

In standard strapdown navigation, the attitude of a body is determined by the rate integration of three orthogonal gyros physically attached to the body starting from a known value. To get the position and velocity three accelerometers are

also attached to the body to measure the acceleration vector. The measured acceleration in the body frame is converted to the reference frame by the use of attitude information. The velocity and position are then computed by single and double integration of the acceleration vector after subtracting the gravity value. Hence, any error in the sensor outputs will be integrated also and introduce an error in the computed parameters.

2.2 Inertial Sensor Errors

Inertial sensors have many associated errors. Some of these are deterministic and some are of stochastic nature. In order to use these sensors effectively in any application, the associated sensor errors need to be understood. Some of the major error characteristics are briefly explained in the following. For details, references [1, 2, 4, 5] can be consulted.

2.2.1 Bias Error

Bias is the signal at the sensor's output when no physical input is present. For example, in case of a gyroscope, the output rate sensed with zero input rate is called bias.
Mathematically, a sensor's output can be expressed as

$$y = f(x) + b$$

where y is the output, x is the input and b denotes the bias error.
Bias error results in accumulated error during the computation process. For example, a constant bias in an accelerometer's output introduces a linear error in velocity and a quadratic error in position. Similarly, a constant bias in a rate gyro's output results in linear error in attitude (heading), a quadratic error in velocity and cubic error in position [22].
To get good performance from inertial sensors, bias error needs to be estimated

and removed from the sensor outputs [23, 24].
Bias error is expressed in deg/h (or deg/sec) and m/sec^2 (or mg_s, ug_s) for gyros and accelerometers respectively. Bias errors can be further characterized as fixed bias, turn-on to turn-on bias and bias drift.

Fixed Bias

Fixed bias refers to the fixed offset in sensor's output when no physical input is present. Almost all sensors show some fixed offset when turned on. The extent of fixed bias depends upon the quality of the sensor. Fixed bias can be easily estimated and corrected by taking a data set for a fixed interval in zero input condition and subtracting mean value of the data from the sensor's output.

Repeatability
(Turn-on to turn-on bias)

Repeatability refers to the ability of a sensor to provide the same output for repeated inputs under the the same environmental conditions. Practically, all sensors show different offset when turned on for repeated times. This is due to the operating principle of the sensors and their intrinsic behavior. Repeatability depends upon the type and quality of the sensors.

Drift (Stability)

Bias drift refers to the variation in a sensor's output over time due to its intrinsic behavior, temperature or any other environmental effect with fixed input. This factor is sometimes called in-run drift or in-run bias stability.
Bias drift defines the quality of the sensors. Good sensors have low bias drift and low performance sensors have relatively high bias drift. It also depends upon the type and working principle of the sensors. The bias and bias drift are shown in Figure 2.2.

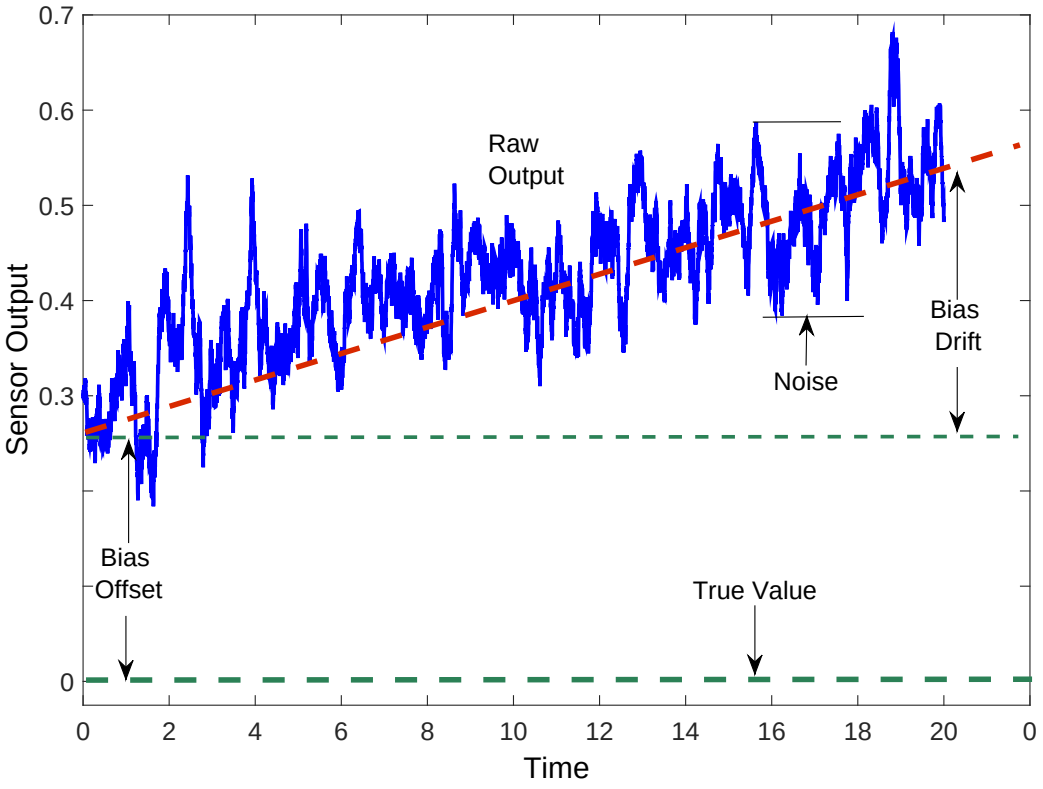

FIGURE 2.2: Bias Error

2.2.2 Scale Factor Error

Scale Factor is the ratio of the change in the output signal of a sensor to the change in the input. For example, in case of a gyro, if the input rate is changed from zero to 1 deg/sec the gyro's output should change accordingly. If the gyro senses a rate of 1 deg/sec, then the ratio of the change in the output to the change in the input is 1 which means that the scale factor is 1. Any variation in this ratio is referred to as a scale factor error. Alternatively, scale factor can also be defined as the slope of the line relating output to the input.

Ideally the scale factor should be unity, but practically sensors show some scaled version of the applied input. For example, in case of a gyro, if the applied rate is 1 deg/sec and the scale factor error of the gyro is 10%, the gyro will show 1.1 deg/sec or 0.9 deg/sec [22]. The scale factor error is expressed in percentage or part per million (PPM). The scale factor error is further characterized as scale factor linearity and asymmetry.

Scale Factor Linearity

Scale factor linearity is the deviation from a straight line relating output to the applied input. Linearity is also expressed in part per million (PPM). Ideally a sensor should have a linear relationship between input and output, and the linearity error should be very small.

Scale Factor Asymmetry

Scale factor asymmetry is the difference between a sensor's output for the same applied input in opposite directions. Normally sensors show some variations in scale factor when the direction of the input is reversed. Scale factor asymmetry also needs to very small for good sensors. Scale factor and scale factor error is shown in Figure 2.3.
Bias and Scale Factor errors are applicable to both gyroscopes and accelerometers. In addition, these errors also have the following general error components [2].

- Temperature induced variations
- Switch on to switch on variations
- In-run variations (For Bias only)

2.2.3 White Noise

The measurement of a sensors contain random noise distributed over all frequencies. Random noise is an intrinsic property of the sensors and related to the manufacturing and operating principles of the devices [1]. Integration of random noise results in random walk (RW) in the computing navigation parameters [22]. Gyro noise results in angle random walk (ARW) and accelerometers noise results in rate random walk (RRW) after integration. Generally inertial sensor manufacturers mention the sensor's noise in term of random walk. For example the noise

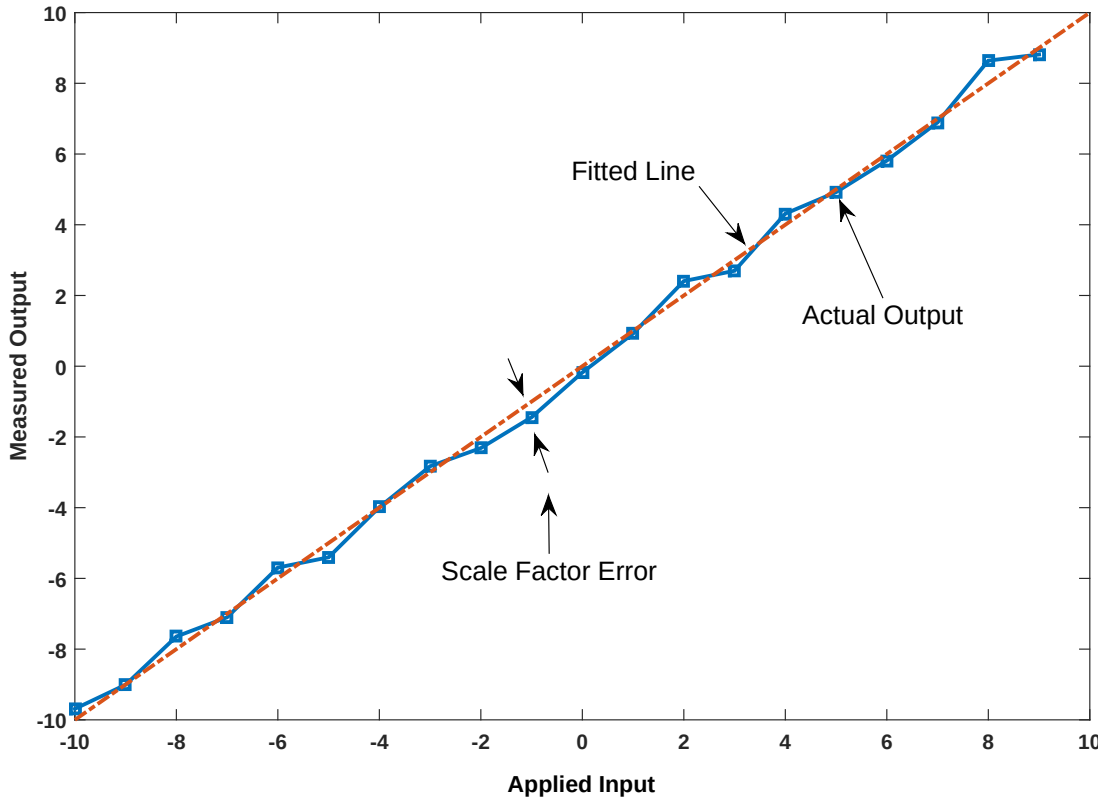

FIGURE 2.3: Scale Factor Error

of a gyro is usually mentioned as angle random walk (ARW) with unit $^\circ/\sqrt{h}$. This means that a gyro with an ARW of $1^\circ/\sqrt{h}$ used for attitude determination will introduce an attitude deviation of 1° after one hour and $1(\sqrt{2}) = 1.414^\circ$ after two hours because of this error [25]. Inertial sensor errors limit the performance of any inertial navigation system. Traditionally, expensive sensors with low errors are being utilized for inertial navigation purposes. However, in recent times a new class of sensors based on Micro-Electromechanical System (MEMS) is also being utilized.

2.3 Micro-Electromechanical Systems (MEMS) Sensors

Micro-Electromechanical Systems are small integrated devices which combine electrical and mechanical components [26]. They are manufactured from silicon as a

base material by etching and batch processing techniques used in Integrated Circuits (ICs) industry. Precise techniques have been developed for silicon machining to fabricate small mechanical structure from silicon or quartz. These provide a significant benefit in cost, size and weight [27]. Low power consumption, rugged construction, low maintenance and high reliability are additional benefits beside cost and size. MEMS devices are one of the most exciting developments in inertial sensors. These devices removed the hurdles in the adoption of inertial sensors for many applications where the cost, size and power consumption are the governing parameters [28–31].

MEMS sensors consist of micro-sensors and micro-electronics fabricated on a single silicon chip. Micro-sensor senses change in the system's environment which is processed by an on-chip micro-electronics to produce a signal proportional to the change detected [26]. The advancement in integrated circuits industry results in rapid transition of MEMS sensors from a research device to practical sensor. Initially the research of MEMS devices was focused on the development of accelerometers for automotive industry. Therefore, first the MEMS accelerometers got the maturity and today MEMS accelerometers with good performance are commercially available. On the other hand MEMS gyroscopes are still under research and the commercially available devices still need significant improvements [2].

MEMS sensors can be categorized into different types like pressure sensors, inertial sensors, micro-fluid bio MEMS and optical MEMS sensors. In the present research, we have been using MEMS inertial sensors, therefore, MEMS inertial sensors are briefly discussed below.

MEMS Accelerometer

Typically a MEMS accelerometer consists of a proof mass and plates suspended in the body of the accelerometer by a mechanical suspension system [26]. The proof mass is connected to movable plates which form a capacitor with fixed plates as shown in Figure 2.4. Upon acceleration, a force acts on the proof mass, making

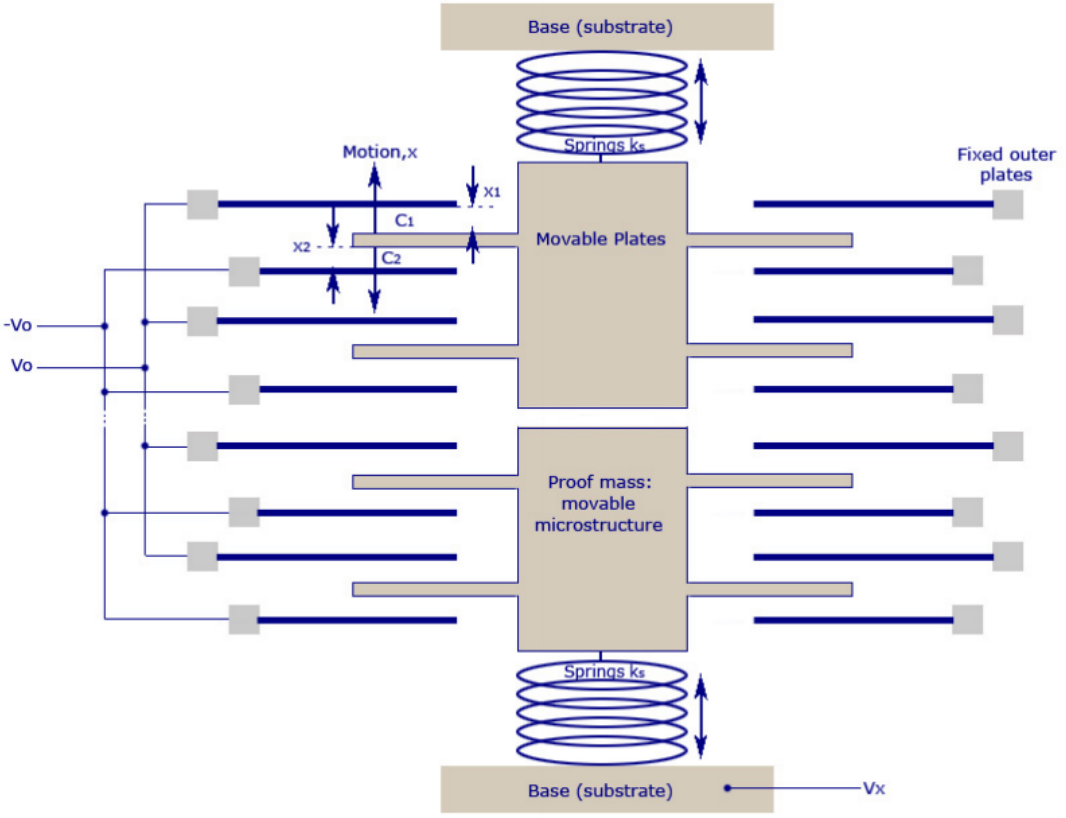

FIGURE 2.4: MEMS Accelerometer [32]

it to move along with the movable plates. The capacitance between fixed and movable plates varies which is proportional to the force acting on the proof mass. The change in capacitance is processed to provide acceleration measurement.

As shown in Figure 2.4 a MEMS accelerometer consists of a number of movable and fixed plates connected in parallel to provide the overall capacitance difference.

MEMS Gyroscope

MEMS gyroscope uses Coriolis acceleration force on a vibrating proof mass to sense angular rate. The Coriolis force generated is perpendicular to both the axis of vibration of the proof mass and the axis along which angular rotation occurs [2]. Let v be the linear velocity of the vibrating proof mass and ω is the angular rate then the Coriolis force generated is given by [33]

$$F_c = -2(v \times \omega)$$

The Coriolis force proportional to the angular rotation rate is sensed by change of capacitance between highly sensitive fixed and movable plates. The change in capacitance is processed and transform to angular rotation rate [2].

MEMS Magnetometer

A magnetometer is a device that measures the strength and direction of the magnetic field. The output of a magnetometer is a combination of both Earth's magnetic field and nearby magnetic field created by other objects. Most of the MEMS magnetic sensors are based on the Hall effect. They work on the principle that an electric field is produced across a conductor through which current is flowing when subjected to a magnetic field [26]. The voltage produced by the electric field is called the Hall voltage which is proportional to the strength of the magnetic field.

MEMS IMU

With the advancement of MEMS technology, it is now possible to fabricate multiple MEMS sensors of different types on a single chip. These days, MEMS-based single package containing three gyros, three accelerometers and three Geomagnetometers are available making a complete MEMS based IMU on a single chip. MEMS IMU is available in different grades like consumer grade, low-cost grade and medium grad [25].

The categorization of the grades is based on the IMU price and specifications. The lowest grade is the cheapest with the lowest specifications and vice versa. The price varies from a few dollars to a few thousand dollars from the lowest to the highest grade. The applications ranges from consumer electronics to medium grade attitude and heading reference systems used in air-born and land applications.

In the present work, we have used a low cost commercially available consumer grade MEMS IMU, which contains tri-axial accelerometer, gyroscope and magnetometer sensors in a single chip.

2.3.1 MEMS Sensor Limitations

MEMS sensors are small sized, low cost, and low power consuming devices, but exhibit different errors. The reason is, the reduction in size of the sensing element imposes limitations on the performance and resolution. Generally, the reduction in size decreases sensitivity and increases noise. Additionally, the effect of temperature further deteriorates the performance because of the change in Young's modules of the silicon with temperature (100 $ppm/^{\circ}C$) [2].
The most dominant errors which MEMS sensors exhibit includes unpredictable bias and scale factor errors [29, 34, 35]. Bias errors of MEMS sensors, especially gyros are higher (from few deg/h upto few deg/sec) as compared to other expensive inertial sensors [30, 35–37]. In addition to the fixed errors, the errors growing with environmental conditions [38] have limited their use to low and medium performance applications so far. In the present research, we have focused on the bias error of the gyros which introduce time growing drift in the attitude.

2.3.2 Bias Error of MEMS Gyros

The bias errors of a MEMS gyro is on the higher side as compared to MEMS accelerometer and Magnetometer. In low-cost consumer grade MEMS-based IMU, it reaches to few deg/sec. Fig 2.5 shows the typical bias characteristic of a low cost MEMS gyro. Gyros with such a high bias error cannot be used for navigation and attitude determination. If the bias error consists of a fixed value, then it can be eliminated by taking a long term data and subtracting the average fixed value from output of the sensor. However, practically a MEMS gyro shows significant variations in its output every time the device is powered on [30]. This turn-on bias is more problematic as compared to the in-run drift. Even in a medium performance gyro, where the in-run drift is less than a deg/h, the turn-on bias is of the order of magnitude. In order to use MEMS gyros with such a large bias error for attitude determination and navigation application, it is necessary to estimate and correct the bias error, both fixed and turn on.

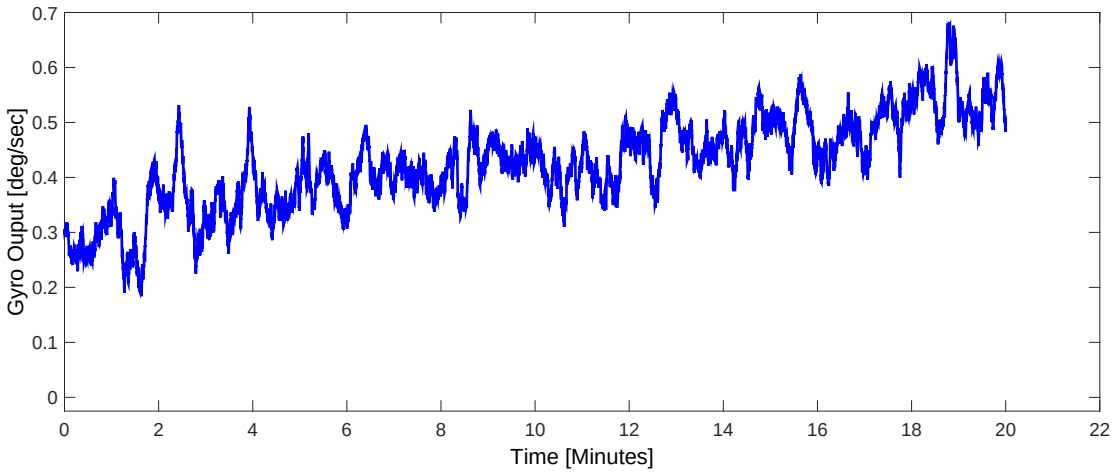

FIGURE 2.5: Bias Error of a MEMS Gyroscope

2.4 Attitude Determination Related work

Attitude is a subset of navigation and is an essential requirement in a wide range of applications like vehicle and space navigation, robotics, virtual environment, surveillance, Unmanned Air Vehicle (UAV) and head tracking systems [7–9]. As mentioned earlier, in a Strapdown INS, the attitude of a body is determined by rate integration of three orthogonal gyros attached to the body starting from a known value. However, it is well-known fact that gyroscopes suffer from bias errors which results in linear attitude drift after numerical integration [4, 39]. Bias errors of MEMS sensors, especially gyros are higher in an order of magnitude as compared to other expensive inertial sensors. A component of bias can be computed in a well arranged inertial navigation laboratory and can be compensated but cannot be removed completely. This determines the performance of an inertial navigation system. Even if the initial bias is measured and compensated to a degree, the in-run bias drift of MEMS sensors is enough to introduce a significant error in navigation parameters.

In the static case, accelerometers can be used to measure the gravity vector from which the tilt angles (pitch and roll) can be calculated and magnetometers can be used to measure the local magnetic field vector from which the heading angle can be calculated [40]. Nevertheless, these sensors are not ideal for dynamic motion

as linear acceleration affects the gravity vector and nearby magnetic fields disturb the magnetometer measurements. Therefore, in many applications, a triad of gyros together with a triad of accelerometers and magnetometers can be used to provide better attitude information [41]. An alternative approach suitable for many applications is known as an integrated solution.

2.4.1 Integrated Solution

Integrated solution employs additional sources of navigation information external from the inertial system. The outputs of inertial navigation system are compared with independent measurements from other external sources and the difference between the two measurements is used to correct the inertial system outputs [1, 2, 4, 5, 42]. Different methods are used to combine inertial system outputs with independent measurements for corrections, including complementary filtering, Kalman filtering, particle filtering and artificial intelligence [1].

Kalman Filter

In conventional work, Kalman filter has been studied extensively for sensors' integration to estimate and compensate inertial sensor errors [8, 9, 41, 41, 43–49]. In general, Kalman filter is an optimal algorithm for estimating error states of a system from noisy measurements. The Kalman filter is used in complementary form in inertial navigation for error states estimation. It functions in two steps. In the first step, the error states are estimated by using state space models of a system. In the second step, the estimated error states are corrected using the available measurements from an independent sources. This is a sequential recursive algorithm which utilizes system models and all available measurements to estimate the current state by appropriately weighing these measurements [1, 50]. Foxlin [8] used a Kalman filter to integrate data from gyroscopes, inclinometers and compass to get an attitude without drift and the acceleration sensitivity of the inclinometers. This technique works well, but suffers from divergence. The

covariance matrices used in Kalman filter formulation need to be tuned to get good static performance and dynamic response. P. Setoodeh et al. [9] did similar work and used wavelet decomposition based approach to estimate the noise covariances but still required experimental tests for tuning parameters which need to remain stable indefinitely. S. Han et al. [41] developed a linear system error model and derived the corresponding observation model to integrate IMU with magnetometers. However, the algorithm seems to be computationally complex as it involves nine states system model. Also, no information is given about the selection of the process and measurement covariance matrices to ensure stability under all conditions. Y. S. Suh at al. [44] used two-step extended Kalman filter which adaptively switches between the steps to compensate external linear acceleration. The author, however modeled angular motion of the body which may not be valid under dynamic conditions. Also, any fixed bias in the gyro outputs is not catered for, which needs to be estimated and corrected if rate integration of the gyros is used for attitude determination. H. Rehbinder et al. [43] modified standard Kalman filter equations and proposed two nonstandard Kalman filters between which switching takes place after detecting linear acceleration to give performance under any kind of rotation or angular motion. The technique, however, used a fusion of accelerometers and gyros data for computation of roll and pitch only and does not address heading determination which is necessary for complete attitude information. Wei Li and Jinling Wang [46] proposed an adaptive Kalman filter for fusion of MEMS-IMU and magnetometer data. The filter gain is adjusted adaptively by changing the measurement covariance matrix parameters according to the dynamic motion sensed by accelerometers. The author, however, used nine states Kalman filter which needs a large hardware resource and difficult to implement with limited hardware resources. R. Mungua [48] proposed Kalman filter in the direct configuration to directly estimate attitude and position states for land vehicle navigation. This approach is different from standard as in most of the literature, Kalman filter is used in indirect configuration to estimate the error states. The author used attitude, gyro rates, gyro biases, accelerations, accelerometer biases, velocities and position in the state vector. The no of states reached to

22 which made the technique complex from the hardware resources point of view. The number of states can be reduced and the technique can be made simplified. However, direct configuration is not recommended as any kind of states divergence leads to complete failure of the system.

Complementary Filter

Complementary filtering is a Multi-Sensor integration scheme used to combine data from two or more sources with different spectral characteristics to generate the output with minimal distortion. The measurement sensors have complementary frequency bands where their outputs are reliable, hence named complementary filter [33]. Figure 2.6 shows the block diagram of a complementary filter.

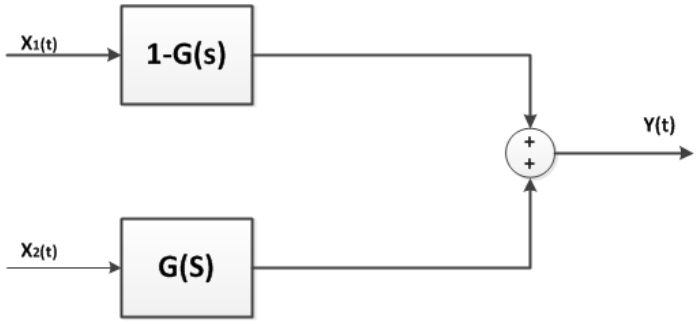

FIGURE 2.6: Complementary Filter for Multiple Measurements

The outputs y(t) is extracted from two sources with different frequency characteristics. The input $x_1(t)$ has a reliable measurement at high frequency while the input $x_2(t)$ has a reliable measurement at low frequency. $x_1(t)$ is passed through a high pass filter $1 - G(s)$ while $x_2(t)$ is passed through a low pass filter. The target is to generate output $y(t)$ reliable, both at low and high frequencies.
Complementary filter is used in [7, 51–53] for Multi-Sensor integration. Euston et al. [7] presented a complementary filter for attitude estimation using gyroscopes and accelerometers. The technique, however, can be used to compute only roll and pitch without heading information. It also requires airspeed information for linear acceleration detection, which is not available in many applications. Q. Yang et al. [51] proposed an adaptive gain Complementary filter for attitude estimation which

fuses data from accelerometers and gyros. The algorithm self adjusts its gain to achieve better performance. The authors claimed comparable performance with Extended Kalman filter. The algorithm, however fuses data from accelerometers and gyros to provide partial attitude information i.e. roll and pitch only. [52] also used a second order complementary filter to combine data from gyros and accelerometers to estimate roll and pitch. The heading information is extracted by using measurements of magnetic field from digital compass. Yu Xu et al. [53] used two complementary filters for attitude, velocity and position estimation and proposed a miniaturized inertial navigation system for rotary-wing UAVs. The first complementary filter combines data from rate gyros and vector based attitude determination system. The second complementary filter fuses data from accelerometers and GPS for position and velocity estimation. The author claimed simplified system having small size and low cost with good static and dynamic response.

Other techniques used for Multi-Sensor integration like linear observers are used in [54–57]. The advantages of such methods are lower computational complexity and global or semi-global stability analysis. H. Fourati et al. [54] presented rigid body quaternion based attitude estimation for Bio-logging applications using nonlinear observer. The author used gyroscopes for attitude update and a combination of accelerometer and magnetometer readings for correction in the proposed attitude observer. With lower computational requirement, the scheme works both under static and accelerated motion conditions. However the observer gain needs to be tuned for accuracy and stability. M.D. Hua et al. [55] proposed two attitude observers for accelerated bodies based on IMU and GPS data fusion and showed rigorous stability convergence analysis. The proposed technique, however, used GPS for linear velocity measurement to estimate the vehicle's acceleration, which is not suitable for low-cost applications where the GPS receiver is not available. H.F. Grip et al. [56] proposed an observer for attitude and gyro bias estimation which used gyroscopes, accelerometers, and magnetometers. This observer is then used in cascade to construct a second observer for GNSS/INS integration. The proposed design is verified through flight simulation, but the effect of error sources

(accelerometer bias, magnetic disturbances, GPS failure) and the performance is not evaluated. Honglei et al. [57] proposed a second order sliding mode observer for attitude estimation with application of quadrotor. The authors claimed that the proposed observer is effective and can meet the requirement for control application with less computational burden.

[58] presented a new framework of drift-free attitude determination by using gyroscopes and two directional vectors sensed by three-axes accelerometers and magnetometers. This technique computes attitude via two directional vectors using vector matching [59–63] and via rate integration using gyros' data. The two attitudes computed from these different approaches are compared and the resulting error is used to estimate the biases for gyros which are continuously fed back to the attitude algorithm. The effects of linear acceleration and magnetic disturbance are compensated by weight adjustment of the vectors used in the vector matching.

2.4.2 Vector Matching

Attitude determination through vector matching has been rigorously studied since 1960s for spacecraft applications [59–63]. This method uses two or more vectors and their mathematical models to compute the orientation of a body with respect to some reference. For example, if an acceleration vector is known with three accelerometers and a magnetic field vector is known with three magnetometers showing magnetic field in three X, Y and Z directions mounted on a body and the references of these two vectors are known, we can compute the orientation of the body in the form of quaternions, Euler angles or a rotation matrix.

The first and simplest method used for attitude determination by vector matching is the Triad algorithm [62]. This method is simple and straightforward, but it does not give an optimal solution because it does not assign equal values to the two vectors used. It is always assumed while using the Triad algorithm that one of the two available vectors is more accurate. Moreover, if more than two vectors are available for measurement then this method cannot be used. Other efficient and

accurate methods for attitude determination by vector matching developed while finding the solution of Wahba's Problem.

Wahba's Problem

In 1965, Grace Wahba [59] formulated a problem of finding an orthogonal matrix that minimizes the loss function

$$J = \frac{1}{2}\sum_{k=1}^{N} w_k \mid v_{b(k)} - Rv_{i(k)} \mid^2 \tag{2.1}$$

Where J is the loss function to be minimized, k is the number of observations, $v_{b(k)}$ is the measurement vector in a body frame, and $v_{i(k)}$ is the reference vector in the inertial frame, w_k is a weight constant for each vector observation and $R \in \Re^{3\times3}$ is the attitude matrix to be determined. Wahbas Problem has been extensively researched since 1965 to find the attitude matrix R which minimizes this loss function and different solutions are presented [60–64]. Among these, P. Davenport's q-method [60] and Shuster's QUEST [62] are well known. Later F. L Markley [63] presented a method based on singular value decomposition which requires no approximations and is more numerically stable.

Vector matching technique is very useful and provides drift free attitude. However, the performance depends on the sensors used for vector measurements. First of all, the noise of the sensors is very critical. As the attitude is calculated sample by sample, the sensors' noise used for the vector measurements directly appear in the computed attitude. The lower the sensors' noise, the lower will be the noise in the computed attitude. Other factors which influence this method, are the disturbances or false measurements. The sensors used for vector measurements should correctly measure the observation vector not the disturbances from the environment. For example, if the gravity vector is used in the vector matching and accelerometers are used for the gravity measurement, then the accelerometers should measure the gravity only. However, if the body on which the accelerometers are fixed for gravity measurement moves with certain acceleration, then the accelerometers will sense the body's acceleration in addition to the gravity. In such

case, the gravity vector measurement will not be accurate enough to be used for attitude determination. Similarly, if the Earth's magnetic field is used as vector a measurement in this method, then the magnetometers used should measure only the Earth's magnetic field and reject all other fields available in the environment. The gravity and magnetic field are the absolute quantities available on the surface of the Earth whose measurement and reference vectors are available. Therefore, we have to use these measurements if we want to use vector matching for the attitude determination. Because of these limiting factors, the use of vector matching technique is mostly limited to the static environment where the effects of linear acceleration and magnetic disturbances are minimum.

2.5 GAP Analysis

From the literature review, it has been concluded that attitude can be computed by rate integration of gyros and by vector matching using directional vectors. Each method has its merits and demerits. In the gyros integration method, the bias error in the outputs of the gyros will grow with time and will introduce a significant error in the computed attitude. Besides, any fixed error, gyros exhibit unpredictable bias drift, which varies with environmental conditions especially with temperature.

On the other hand, two or more directional vectors which have fixed references like gravity and magnetic field can be used for attitude determination. Gravity and magnetic field vectors can be sensed by three accelerometers and three magnetometers mounted in X, Y, and Z directions respectively. The attitude computed by vector matching is, however, not suitable under dynamic linear acceleration motion and strong magnetic interference.

Generally, to provide drift free attitude both under static and dynamic conditions, attitude is computed using rate integration of gyros and additional sources are used to estimate and correct the attitude and sensor errors. Tradition GNSS/GPS integration is used through the Kalman filter for multi-sensor integration. Although the Kalman filter is an optimal linear estimator which gives best results, it has

some associated convergence problem [5]. It works on the linear system model. If the system is nonlinear, Kalman filter does not remain optimal [2]. As most of the systems in the universe are nonlinear in nature, system modeling is very critical. Generally, a system is modeled by a linear model and it is supposed that the conditions for linearity hold over a relatively short interval of time. Any discrepancy in the system model (unstable or marginally stable states) leads to divergence [5]. Kalman filter performance also depends upon a-priori information. Poor a-priori information related to process and measurement covariance matrices also lead to divergence. Moreover, the implementation requires higher dimensional matrices and complicated vector operations, which are especially challenging with very limited hardware resources and suffer numerical instabilities.

GNSS/GPS receiver is not suitable for low-cost and indoor applications. As additional sensors like accelerometers and magnetometers are also available in today's MEMS-based IMU; these sensors can also be used for aiding. However, the use of accelerometers and magnetometers will be limited to the static and magnetic disturbance free environment. Also multi-sensor integration through Kalman filter is not suitable with limited hardware resources. Therefore, other integration techniques with lower computational complexity also need to be evaluated.

2.5.1 Problem Statement

The proposed research is focused on "*Improved (Drift and noise free) attitude determination using low cost MEMS IMU containing tri-axial gyroscope, accelerometer and magnetometer sensors by overcoming the limitations of accelerometers and magnetometers and provide performance both in static and dynamic environment.*" To achieve this, attitude will be primarily computed by the rate integration of gyros and a combination of accelerometers and magnetometers will be used as adding sensors for gyro biases estimation. The effects of environmental disturbance on accelerometers and magnetometers will be catered for by a linear acceleration isolation framework and calibration of the magnetometers before use. Hence, the

proposed research will result in a self-aiding scheme for drift free attitude under static and dynamic conditions using a single chip, low-cost MEMS-based IMU.

2.6 Motivation and Research Contribution

As mentioned earlier MEMS gyros cannot be used in un-aided mode because of their intrinsic bias errors. To use MEMS gyros for attitude determination and navigation, additional aiding is required. In AHRs and Navigation systems, the aiding is mostly achieved through GNSS/GPS for sensors' errors estimation and correction [5, 39, 42, 47, 65–67]. Inertial sensors and GPS data are combined through data fusion algorithms using Kalman filter. GNSS/GPS integration, however, has the following limitations.

- GNSS/GPS receiver module used for INS aiding is an expensive component as compared to the MEMS IMU itself, hence not suitable for cost-effective solutions.
- GNSS/GPS signals are not always available, especially in a crowded area with skyscraper buildings, forests, bad weather conditions and inside the buildings [68].
- GNSS/GPS signals can be jammed and denied any time by the GPS service provider.
- Kalman filter which is mostly used for multi-sensor integration, suffers from implementation complexity and requires non-intuitive tuning procedures [5, 69].

The proposed research suggests a passive type aiding which does not require any external aiding source and with no tendency toward jamming or unavailability. MEMS-based IMU has already embedded accelerometers and magnetometers with bounded and limited errors. Using all the nine sensors available in a MEMS-based IMU, an improved attitude determination framework is proposed suitable

for space, land vehicle, control, and indoor applications. The quaternion feedback method proposed in this research for multi-sensor integration is also computationally simple with no tuning process required.
Following are the main contribution of this research work.

- Study, implementation and comparison of attitude determination methods.
- Development of simplified quaternion feedback algorithm for drift free and low noise attitude determination.
- Development of Kalman filter based algorithm for drift and noise free attitude in direct and indirect configuration with minimum number of states.
- Evaluation and testing of algorithm on real sensors' data under static and dynamic conditions.
- Comparison of quaternion feedback algorithm with Kalman filter based algorithm under static and dynamic conditions.

The above mentioned work is performed using a self developed test setup containing MEMS based IMU with nine sensors (three gyros, three accelerometers, three magnetometers) integrated with field programmable gate array (FPGA) based digital electronics.

Chapter 3

Navigation Mathematics and Attitude Representation

3.1 Introduction

Navigation parameters (velocity, position and orientation) are always defined with respect to some reference [50]. For example, inertial sensors provide measurements in the inertial frame which are resolved in the body frame and further transformed to the the navigation frame. Navigation algorithm also involves a transformation from one frame to another. In this chapter, reference frames commonly used in navigation are explained, then different types of attitude representation, their properties and inter-conversion from one form to another are discussed. Finally, some navigation mathematics and sensors' measurements are presented.

3.2 Reference Frames

The following co-ordinate (reference) frame are commonly used in navigation algorithms.

Inertial Frame (i-frame)

Inertial frame (i-frame) is defined as stationary, with respect to the fixed stars. Its origin is at the center of the earth and Z-axis coincides with the rotation axis of the Earth. X-axis points toward the vernal equinox in the equatorial plane and Y-axis is perpendicular to both X and Z axes to complete right handed system.

Earth Centered Earth Fixed Frame (ECEF frame)

Earth Centered Earth Fixed frame has its origin at the center of the earth, Z-axis coincides with the rotation axis of the Earth, X-axis points toward the intersection of equatorial plane and Greenwich meridian and Y-axis is orthogonal to both X and Z axes. The ECEF frame is fixed to the Earth. Hence it rotates with the Earth's rotation along the Z-axis (Earth spin axis).

Navigation Frame (n-frame)

The navigation frame (n-frame) is centred to the navigation system installed on the vehicle, but it does not rotate with the vehicle. The X-axis is aligned to the north, Y-axis is aligned to the east and Z-axis points downward along the gravity vector. This convention is called NED (North East Down) frame. In some cases ENU (East North Up) convention is also used in which X-axis points to the east, Y-axis points towards the north and Z-axis points upward. The different reference frames are shown in Figure 3.2.

3.2.1 Body Frame

The body frame (b-frame) is centered to the host vehicle and its axes are aligned to the principle axes of the vehicle. X-axis aligns to the longitudinal axis (roll axis), Y-axis points towards the transverse axis (pitch axis) and Z-axis points downwards (yaw axis). The rotation along these axes are called roll, pitch and yaw angles.

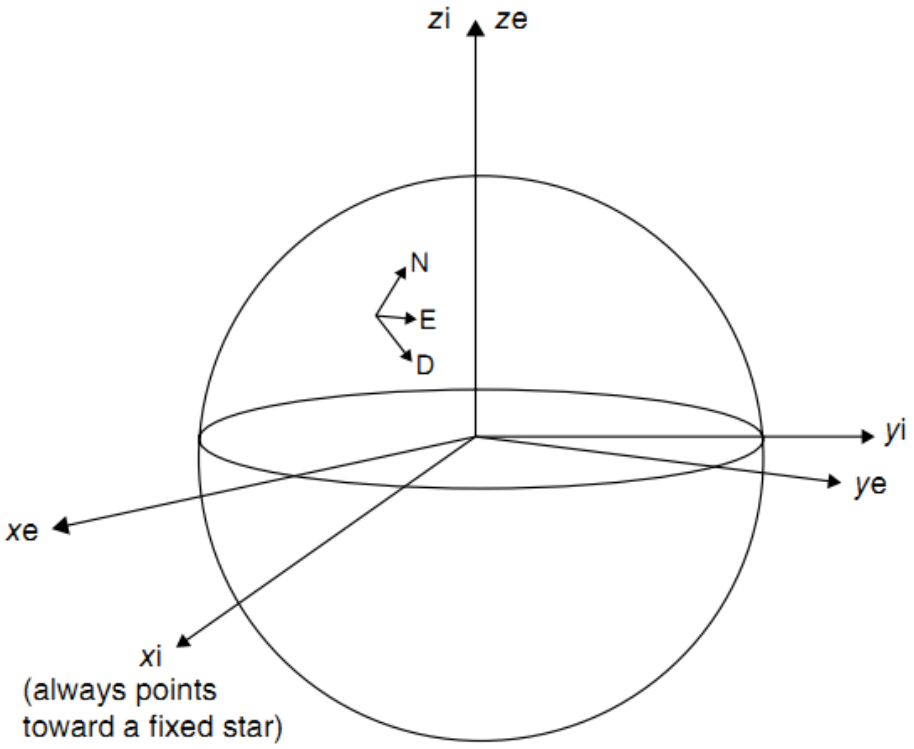

FIGURE 3.1: i-frame, ECEF-frame and n-frame[70]

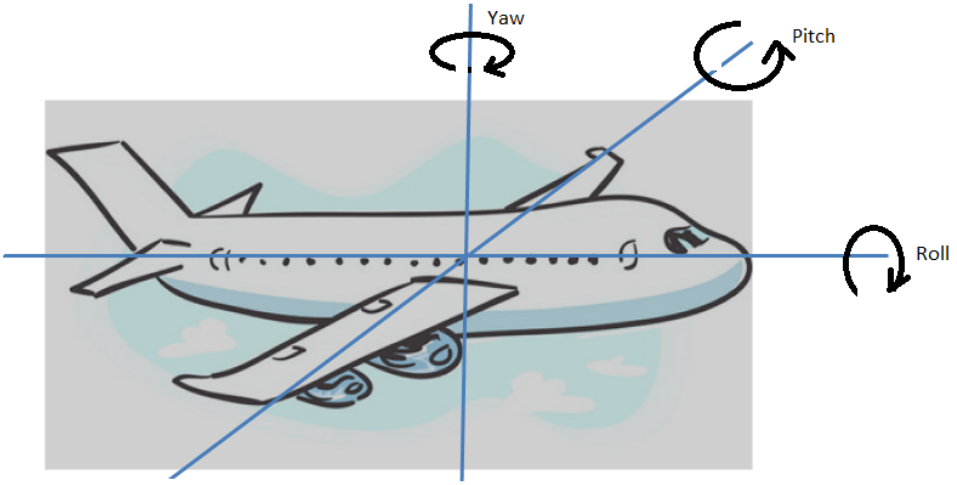

FIGURE 3.2: The Body frame

3.3 Attitude Representation

Different mathematical representations are used to define the attitude of a body with respect to a reference frame. In a strapdown systems, the parameters associated with each representation are stored within a computer and updated as the body moves by using the measurements from the gyroscopes. The following three representations are generally used for attitude representation [2].

- Direction Cosine
- Euler Angles
- Unit Quaternion

3.3.1 Direction Cosine Matrix (DCM)

Direction cosine matrix is a transformation matrix between any two frames with three orthogonal axes. It is composed by the direction cosines between the axes of the initial reference frame and the axes of the target reference frame.
For example, a unit vector v_b in the body frame can be converted to a unit vector v_i in the inertial frame using the DCM matrix ${C_b}^i$.

$$v_i = C_b^i v_b \tag{3.1}$$

The columns of the DCM matrix represent unit vectors in the body axes projected along the reference axes. The elements in the ith row and jth column represents the cosine of the angle between the $i-axis$ of the reference frame and the $j-axis$ of the body frame. The general representation of the DCM matrix is given by

$$C_b^i = \begin{bmatrix} c_{11} & c_{12} & c_{13} \\ c_{21} & c_{22} & c_{23} \\ c_{31} & c_{32} & c_{33} \end{bmatrix} \tag{3.2}$$

The DCM update equation is given by

$$\dot{C}_b^i = C_b^i \Omega_{ib}^b \tag{3.3}$$

where Ω_{nb}^b is the skew-symmetric form of the angular velocity vector of the b-frame relative to the i-frame, as resolved in the b-frame, and

$$\Omega_{nb}^b = \begin{bmatrix} 0 & -r & q \\ r & 0 & -p \\ -q & p & 0 \end{bmatrix} \tag{3.4}$$

where p, q and r are the angular rates of the b-frame measured by gyros with respect to the i-frame.

3.3.2 Euler Angles

In Euler angle representation, the orientation of a body is represented by three angles called roll, pitch and yaw. The body is assumed to be in parallel to the axis of the reference frame and a series of rotation brings it to the present orientation [4].

Clockwise rotation about Z-axis through angle =

$$\psi = \begin{bmatrix} \cos\psi & \sin\psi & 0 \\ -\sin\psi & \cos\psi & 0 \\ 0 & 0 & 1 \end{bmatrix} \tag{3.5}$$

Clockwise rotation about Y-axis through angle=

$$\theta = \begin{bmatrix} \cos\theta & 0 & -\sin\theta \\ 0 & 1 & 0 \\ \sin\theta & 0 & \cos\theta \end{bmatrix} \tag{3.6}$$

Clockwise rotation about X-axis through angle =

$$\phi = \begin{bmatrix} 1 & 0 & 0 \\ 0 & \cos\phi & -\sin\phi \\ 0 & \sin\phi & \cos\phi \end{bmatrix} \tag{3.7}$$

The order of rotation is very important because the different order will result in different orientations. Transformation from one frame to another can be expressed as a product of individual rotation matrices.

$$C_b^n = \begin{bmatrix} \cos\psi & \sin\psi & 0 \\ -\sin\psi & \cos\psi & 0 \\ 0 & 0 & 1 \end{bmatrix} \begin{bmatrix} \cos\theta & 0 & -\sin\theta \\ 0 & 1 & 0 \\ \sin\theta & 0 & \cos\theta \end{bmatrix} \begin{bmatrix} 1 & 0 & 0 \\ 0 & \cos\phi & -\sin\phi \\ 0 & \sin\phi & \cos\phi \end{bmatrix} \tag{3.8}$$

$$C_b^n = \begin{bmatrix} \cos\theta\cos\psi & -\cos\phi\sin\psi + \sin\phi\sin\theta\cos\psi & \sin\phi\sin\psi + \cos\phi\sin\theta\cos\psi \\ \cos\theta\sin\psi & \cos\phi\cos\psi + \sin\phi\sin\theta\sin\psi & -\sin\phi\cos\psi + \cos\phi\sin\theta\sin\psi \\ -\sin\theta & \sin\phi\cos\theta & \cos\phi\cos\theta \end{bmatrix} \tag{3.9}$$

The Euler angles update relation with body angular rates is given by [2]

$$\begin{bmatrix} \dot{\phi} \\ \dot{\theta} \\ \dot{\psi} \end{bmatrix} = \begin{bmatrix} 1 & \sin\phi\tan\theta & \cos\phi\tan\theta \\ 0 & \cos\phi & -sin\phi \\ 0 & \sin\phi\ sec\theta & \cos\phi\sec\theta \end{bmatrix} \begin{bmatrix} \omega_x \\ \omega_y \\ \omega_z \end{bmatrix} \tag{3.10}$$

where $\begin{bmatrix} \omega_x & \omega_y & \omega_z \end{bmatrix}^t$ are the angular rates measured by gyros mounted in X, Y and Z directions.

The Euler angles can be computed by numeric integration of Equation 3.10 starting from initial values. However, the process fails when $\theta = 90$ as both $\tan\theta$ and $\sec\theta$ becomes infinity. Hence, the use of Euler angles are limited to pitch angle of < 90 to avoid mathematical singularities. Euler angles are easy to visualize, but suffer from singularities as discussed.

Relation between Euler angles and DCM

The relationship between DCM and Euler angle is given by

$$C_b^n = \begin{bmatrix} \cos\theta\cos\psi & -\cos\phi\sin\psi + \sin\phi\sin\theta\cos\psi & \sin\phi\sin\psi + \cos\phi\sin\theta\cos\psi \\ \cos\theta\sin\psi & \cos\phi\cos\psi + \sin\phi\sin\theta\sin\psi & -\sin\phi\cos\psi + \cos\phi\sin\theta\sin\psi \\ -\sin\theta & \sin\phi\cos\theta & \cos\phi\cos\theta \end{bmatrix} \tag{3.11}$$

The Euler angles can be computed from DCM matrix using the following relations

$$\phi = \tan^{-1}[\frac{c_{32}}{c_{33}}] \tag{3.12}$$

$$\theta = \sin^{-1}[-c_{31}] \tag{3.13}$$

$$\psi = \tan^{-1}[\frac{c_{21}}{c_{11}}] \tag{3.14}$$

3.3.3 Quaternion

To overcome the limitation of the pitch angle, a fully manoeuvrable system for attitude representation is required. This can be achieved by using quaternions. A quaternion is a four parameter representation invented by Sir Willian R. Hamilton in 1843. It is based on the idea that a transformation from one coordinate frame to another can be expressed in terms of a single rotation about a suitably positioned axis [4]. The quaternion denoted by $\mathbf{q}$ is a four element vector, the elements of which are functions of this vector and the magnitude of rotation.

$$\mathbf{q} = \begin{bmatrix} a \\ b \\ c \\ d \end{bmatrix} = \begin{bmatrix} (\cos\theta/2) \\ (\theta_x/\theta)\sin(\theta/2) \\ (\theta_y/\theta)\sin(\theta/2) \\ (\theta_z/\theta)\sin(\theta/2) \end{bmatrix} \tag{3.15}$$

where θ_x, θ_y and θ_z are the components of the angle vector Θ and θ is the magnitude of Θ.

Quaternions are very useful for analysing rotation in three dimensions. Being a 4-tuple, it is more concise representation of attitude than a rotation matrix.

3.4 Quaternion Mathematics

Quaternion can be considered as a hyper complex number with a real part and three dimensional imaginary part.

$$\mathbf{q} = a + \hat{i}b + \hat{j}c + \hat{k}d \tag{3.16}$$

3.4.1 Addition

Quaternions are added component wise. Let $p = a + \hat{i}b + \hat{j}c + \hat{k}d$ and $q = e + \hat{i}f + \hat{j}g + \hat{k}h$ be two quaternions, their addition gives

$$\mathbf{p} + \mathbf{q} = (a + e) + \hat{i}(b + f) + \hat{j}(c + g) + \hat{k}(d + h) \tag{3.17}$$

3.4.2 Multiplication

The product of two quaternions is based on the following rules suggested by Hamilton

$$\hat{i}^2 = \hat{j}^2 = \hat{k}^2 = -1$$

$$\hat{i}\hat{j} = \hat{k} = -\hat{j}\hat{i}$$

$$\hat{j}\hat{k} = \hat{i} = -\hat{k}\hat{j}$$

$$\hat{k}\hat{i} = \hat{j} = -\hat{i}\hat{k}$$

Hence the product of two vectors

$$\mathbf{q}.\mathbf{p} = (a + \hat{i}b + \hat{j}c + \hat{k}d)(e + \hat{i}f + \hat{j}g + \hat{k}h)$$

$$= (ea - bf - cg - dh) + (af + be + ch - dg)\hat{i} + (ag + ce - bh + df)\hat{j} + (ah + de + bg - cf)\hat{k} \tag{3.18}$$

In matrix form the quaternion product can be expressed as

$$\mathbf{q}.\mathbf{p} = \begin{bmatrix} a & -b & -c & -d \\ b & a & -d & c \\ c & d & a & -b \\ d & -c & b & a \end{bmatrix} \begin{bmatrix} e \\ f \\ g \\ h \end{bmatrix} \tag{3.19}$$

It can be seen that the product of two quaternions is also a quaternion with a real and imaginary part. Quaternion multiplication is not commutative i.e.

$$\mathbf{q}.\mathbf{p} \neq \mathbf{p}.\mathbf{q} \tag{3.20}$$

3.4.3 Conjugate and Norm of a Quaternion

The conjugate of a quaternion $\mathbf{q} = a + \hat{i}b + \hat{j}c + \hat{k}d$ is given by

$$\mathbf{q^*} = a - \hat{i}b - \hat{j}c - \hat{k}d \tag{3.21}$$

and its norm is given by

$$|\mathbf{q}| = \sqrt{a^2 + b^2 + c^2 + d^2} \tag{3.22}$$

3.4.4 Inverse of a Quaternion

To find the inverse of a quaternion $\mathbf{q} = a + \hat{i}b + \hat{j}c + \hat{k}d$, we multiply it with its conjugate. To find the inverse of a quaternion $\mathbf{q} = a + \hat{i}b + \hat{j}c + \hat{k}d$ we multiply it with its conjugate.

$$\mathbf{q}.\mathbf{q^*} = (a + \hat{i}b + \hat{j}c + \hat{k}d)(a - \hat{i}b - \hat{j}c - \hat{k}d)$$

$$= (aa - bb\hat{i}^2 - cc\hat{j}^2 - dd\hat{k}^2) + (-ab + ba - bc + cb)\hat{i} +$$

$$(-ac + ca + bd - bd)\hat{j} + (-ad + da - bc + cb)\hat{k}$$

$$\mathbf{q}.\mathbf{q}^* = a^2 + b^2 + c^2 + d^2$$

$$\mathbf{q}.\mathbf{q}^* = |\mathbf{q}|$$

$$\mathbf{q}^{-1} = \frac{\mathbf{q}^*}{|\mathbf{q}|} \tag{3.23}$$

3.5 Unit Quaternion and Vector rotation

A quaternion with its norm $|\mathbf{q}|$ equal to 1 is called unit quaternion. This is the necessary condition for quaternion to be used for attitude representation and vector rotation [71, 72]. For unit quaternion $\mathbf{q}^{-1} = \mathbf{q}^*$ as $|\mathbf{q}| = 1$. A vector in three dimension is called pure quaternion with real part equal to zero. Suppose we have a vector $\mathbf{q}^b$ and we want to express it in reference frame as $\mathbf{q}^r$. First we convert the vector in corresponding quaternion with real part equal to zero.

$$\mathbf{q}^b = \hat{i}x + \hat{j}y + \hat{k}z$$

$$\mathbf{q}^{b'} = 0 + \hat{i}x + \hat{j}y + \hat{k}z$$

and then rotate the vector using rotation vector $\mathbf{q}$ using conjugate operation

$$\mathbf{q}^{r'} = \mathbf{q}\ \mathbf{q}^{b'}\mathbf{q}^* \tag{3.24}$$

$$= (a + \hat{i}b + \hat{j}c + \hat{k}d)(0 + \hat{i}x + \hat{j}y + \hat{k}z)(a - \hat{i}b - \hat{j}c - \hat{k}d)$$

$$= 0 + [(a^2 + b^2 - c^2 - d^2)x + 2(bc - ad)y + 2(bd + ac)z]\hat{i}$$

$$+[2(bc + ad)x + ((a^2 - b^2 + c^2 - d^2))y + 2(cd - ab)z]\hat{j}$$

$$[2(bd - ac)x + 2(cd + ab)y + 2(a^2 - b^2 - c^2 + d^2)z]\hat{i}$$

in matrix form

$$\mathbf{q}^{r'} = \mathbf{C}'\mathbf{q}^{b'} \tag{3.25}$$

where

$$\mathbf{C}' = \begin{bmatrix} 0 & 0 \\ 0 & \mathbf{C} \end{bmatrix} \quad \mathbf{q}^{b'} = \begin{bmatrix} 0 \\ \mathbf{q}^b \end{bmatrix}$$

and

$$\mathbf{C} = \begin{bmatrix} (a^2+b^2-c^2-d^2) & 2(bc-ad) & 2(bd+ac) \\ 2(bc+ad) & (a^2-b^2+c^2-d^2) & 2(cd-ab) \\ 2(bd-ac) & 2(cd+ab) & (a^2-b^2-c^2+d^2) \end{bmatrix} \tag{3.26}$$

Alternatively, we can write

$$\mathbf{q}^r = C\mathbf{q}^b \tag{3.27}$$

where the matrix $\mathbf{C}$ is equivalent to Direction Cosine Matrix (DCM) C_b^n.
The quaternion update relation with angular rates is given by [2]

$$\dot{\mathbf{q}} = \frac{1}{2}\,\mathbf{Q}_q \begin{bmatrix} 0 \\ \Omega \end{bmatrix} \tag{3.28}$$

where $\mathbf{Q}_q = \begin{bmatrix} a & -b & -c & -d \\ b & a & -d & c \\ c & d & a & -b \\ d & c & b & a \end{bmatrix}$ and $\Omega = \begin{bmatrix} \omega_x & \omega_y & \omega_z \end{bmatrix}^t$

3.6 Relationship between DCM, Euler angles and Quaternion

From equation 3.2, 3.11 and 3.26 it can be seen that the DCM matrix can be expressed in terms of Euler angles and quaternion i.e.

$$C_b^n = \begin{bmatrix} c_{11} & c_{12} & c_{13} \\ c_{21} & c_{22} & c_{23} \\ c_{31} & c_{32} & c_{33} \end{bmatrix}$$

$$= \begin{bmatrix} \cos\theta\cos\psi & -\cos\phi\sin\psi + \sin\phi\sin\theta\cos\psi & \sin\phi\sin\psi + \cos\phi\sin\theta\cos\psi \\ \cos\theta\sin\psi & \cos\phi\cos\psi + \sin\phi\sin\theta\sin\psi & -\sin\phi\cos\psi + \cos\phi\sin\theta\sin\psi \\ -\sin\theta & \sin\phi\cos\theta & \cos\phi\cos\theta \end{bmatrix}$$

$$= \begin{bmatrix} (a^2+b^2-c^2-d^2) & 2(bc-ad) & 2(bd+ac) \\ 2(bc+ad) & (a^2-b^2+c^2-d^2) & 2(cd-ab) \\ 2(bd-ac) & 2(cd+ab) & (a^2-b^2-c^2+d^2) \end{bmatrix} \tag{3.29}$$

By comparing these three equations, it can be seen that the quaternion can be expressed in terms of DCM elements or Euler angles. some of these inter-conversion are expressed below.

3.6.1 Quaternion in Terms of DCM Elements

If the rotation matrix is known, the corresponding quaternion parameters can be computed as [1, 2]

$$\begin{aligned} a &= \frac{1}{2}\sqrt{(1+c11+c22+c33)} \\ b &= \frac{1}{4a}(c32-c23) \\ c &= \frac{1}{4a}(c13-c31) \\ d &= \frac{1}{4a}(c21-c12) \end{aligned} \tag{3.30}$$

3.6.2 Quaternion in Terms of Euler angles

If the Euler angles are known, the quaternion parameters can be computed as

$$\begin{aligned} a &= \cos\frac{\phi}{2}\cos\frac{\theta}{2}\cos\frac{\psi}{2} + \sin\frac{\phi}{2}\sin\frac{\theta}{2}\sin\frac{\psi}{2} \\ b &= \sin\frac{\phi}{2}\cos\frac{\theta}{2}\cos\frac{\psi}{2} - \cos\frac{\phi}{2}\sin\frac{\theta}{2}\sin\frac{\psi}{2} \\ c &= \cos\frac{\phi}{2}\sin\frac{\theta}{2}\cos\frac{\psi}{2} + \sin\frac{\phi}{2}\cos\frac{\theta}{2}\sin\frac{\psi}{2} \\ d &= \cos\frac{\phi}{2}\cos\frac{\theta}{2}\sin\frac{\psi}{2} + \sin\frac{\phi}{2}\sin\frac{\theta}{2}\cos\frac{\psi}{2} \end{aligned} \tag{3.31}$$

3.7 Advantages of Quaternion

Quaternions offer certain advantages over DCM and Euler angles [1, 50]. These include

- Only four parameters need to be computed instead of six which are required when a rotation matrix is computed using directional cosines.
- No singularity problem exists using quaternions which occurred with Euler angles.
- Computation is simple and numerically more stable.
- The main disadvantage of quaternion is its difficulty to visualize as compared to the Euler angles and re-normalization during computation [1].

3.8 Sensors Measurements

For strapdown Inertial Navigation systems two types of inertial sensors, i.e. gyroscopes and accelerometers are required. However, recent development in MEMS technology results in a miniaturized single chip package containing additional sensors like Magnetometers and pressure sensors. In the present research, we have been using MEMS based IMU with nine sensors, i.e. three gyros, three accelerometers and three magnetometers. Therefore, we will discuss the measurement model of these three types of sensors.

3.8.1 Rate Gyro

A Gyro measures angular rate of the body on which it is mounted with respect to the inertial frame. The measurement of a gyro can be modeled by the following equation [73].

$$\omega_g = \omega + \omega_b + n_\omega \tag{3.32}$$

where

ω_g is the gyro output

ω is the actual angular rate

ω_b is the gyro bias

n_ω is the wide-band output noise of the gyro. The gyro bias ω_b is a slow time varying and may be considered constant. Therefore, we can assume

$$\dot{\omega_b} \approx 0$$

3.8.2 Accelerometer

An accelerometer measures specific force which includes both linear acceleration of the body on which it is mounted as well as the gravitational acceleration g [74] with respect to the inertial frame. The output of an accelerometer can be expressed as

$$\alpha_{acc} = \alpha + g + \alpha_b + n_\alpha \tag{3.33}$$

where

α_{acc} is the accelerometer output.

α is the true linear acceleration of the body.

g is the acceleration due to gravity.

α_b is the accelerometer bias

n_α is the output noise of the accelerometer

Under static and no accelerated motion, an accelerometer senses only the gravity component along its sensitive axis. In that case the output of the accelerometer can be modeled as

$$\alpha_{acc} = g + \alpha_b + n_\alpha \tag{3.34}$$

3.8.3 Magnetometer

Magnetometers measure strength of the magnetic field around the surrounding environment of the body on which they are mounted. The magnetometer output

can be modeled as

$$m_g = m_B + m_b + n_m \tag{3.35}$$

where

m_g is the magnetometer output.

m_B is the true or actual magnetic field

m_b is the magnetometer bias

n_m is the magnetometer output noise

Magnetometers are used in navigation to measure the Earth's magnetic field which in turn is used to compute magnetic north. As the angle between magnetic north and true north is fixed with respect to the location, the true north can be estimated using magnetic north.

Chapter 4

Methods of Attitude Determination

In the standard navigation algorithm, the attitude of a moving body is determined by integration of angular rate sensors mounted on the body. However, for spacecraft attitude determination, methods based on vector observations measured by sensors are used [62, 64, 75–79]. The sensors used are magnetometers, accelerometers, sun sensors, star tracker and GPS. The choice of sensors depends upon the availability and applications.

The sensors used for attitude determination can be categorized in two types. The first type provides absolute measurements, whereas the second type provides relative measurements. Absolute measurement sensors provide measurements with respect to some absolute reference like three magnetometers mounted in orthogonal directions provide measurement with respect to the Earth's magnetic field in the X, Y and Z directions. Relative measurement sensors include gyroscopes, which provide angular rate or angle starting from a known position or angle respectively. For attitude determination using vector observations, sensors with absolute measurements are used.

In the proposed research, we used both methods and combine them to provide better attitude information under static as well as dynamic environment. In the

preceding section the two methods (gyros integration and vector observations) of attitude determination are discussed in details.

4.1 Attitude Determination by Vector Observations (Vector Matching)

For attitude determination using vector observations, at least two vector observations and their reference vectors are required. For example, the two vectors used may be the gravity vector and magnetic field vector. The magnetic field vector can be measured by three axes magnetometer and gravity vector can be measured by three axes accelerometer. These sensors will provide orthogonal measurements of the acceleration and magnetic field in three dimensional space. As the reference of these two vectors are known (will be discussed in the next section), attitude determination methods calculate the attitude using the deviation of the measurement vector from the reference vector.

4.1.1 Reference Vectors

In the proposed research we used magnetic field and gravity vector as two observations. Earth has a strong magnetic field distributed in X, Y and Z directions (North, East and down). It is a vector quantity. At each point in the space or on the surface, it has a strength and direction. Consider Figure 4.1 which describes the Earth's magnetic field and its components. In this figure **X**, **Y**and **Z** are the strengths of Magnetic field in three orthogonal directions. **F** is the total field strength, **H** is the field strength in the horizontal plane, **D** is the angle of declination, which is defined as the angle between the true north and magnetic north, and **I** is the angle of inclination defined as the angle between the horizontal plane and total field **F**. These components are interrelated by the following relations

Total Field Strength $\mathbf{F} = \sqrt{\mathbf{X}^2 + \mathbf{Y}^2 + \mathbf{Z}^2}$

Horizontal Field Strength $\mathbf{H} = \sqrt{\mathbf{X}^2 + \mathbf{Y}^2}$

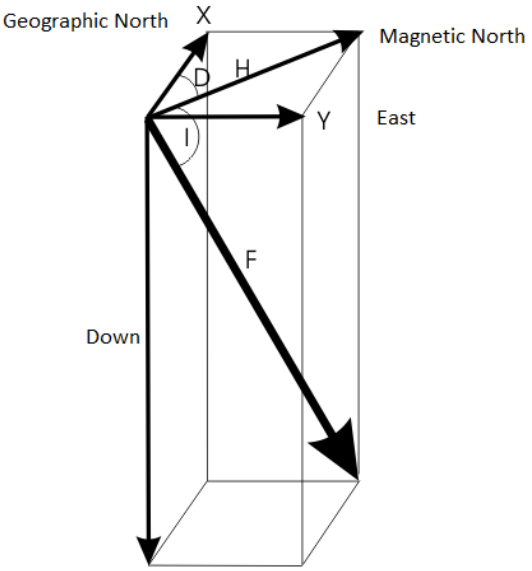

FIGURE 4.1: Earth's Magnetic Field Components [80]

Angle of Declination $\mathbf{D}$=$\tan^{-1}(\frac{\mathbf{Y}}{\mathbf{X}})$
Angle of Inclination $\mathbf{I}$=$\tan^{-1}(\frac{\mathbf{Z}}{\mathbf{H}})$
North $(\mathbf{X}) = \mathbf{H}cos(\mathbf{D})$
East $(\mathbf{X}) = \mathbf{H}sin(\mathbf{D})$

If the total strength of the field $\mathbf{F}$ and the angle of inclination $\mathbf{I}$ is known, then the reference vector can be calculated as

$$B_r = \mathbf{F}\begin{bmatrix}\cos(\mathbf{I}) & 0 & sin(\mathbf{I})\end{bmatrix}^t \tag{4.1}$$

Alternatively, the reference vector for the Earth's magnetic field can be calculated using online magnetic field calculator [81, 82] which uses International Geomagnetic Reference Field model (IGRF). This model needs the location information in the form of latitude, longitude and altitude over the sea level. The magnetic reference field is fixed with the location.
Earth has also a gravitational acceleration due to its mass attraction. The gravitational acceleration acts downward i.e. normal to the surface of the Earth in Z-axis. The gravity in X and Y directions are zero (North and East). Hence, the

reference vector for gravity in NED frame is given by

$$g_r = \begin{bmatrix} 0 & 0 & -g \end{bmatrix}^t \tag{4.2}$$

where "g" is called acceleration due to gravity. The value of g varies with respect to the location on the surface of the Earth and with height above it. The exact value of "g" on a specific location can be calculated using gravity model. The details of the gravity model can found in references [1, 2].

4.1.2 Triad Algorithm

The first and simplest method used for three axis attitude determination using vector matching is Triad Algorithm. This method computes attitude in the form of a rotation matrix which is equivalent to finding the orientation of a body with respect to some reference frame.

Consider two measurement vectors such as gravity $\hat{a}$ and Earth's magnetic field $\hat{m}$. The measured components of these vectors in the body frame with respect to the inertial frame are denoted by m_b and a_b. The corresponding reference vectors in inertial frame are m_i and a_i. The rotation matrix satisfies the following relations.

$$m_b = C_i^b(m_i) \tag{4.3}$$

and

$$a_b = C_i^b(a_i) \tag{4.4}$$

Triad algorithm is based on constructing two triads of orthonormal vectors from the available vector information which are components of the same reference frame. Consider this reference frame as F_t. This reference frame is constructed by assuming that one of the two available vectors is more correct than the other. Suppose the gravity vector is more accurate such that when we find the rotation matrix, equation 4.4 is exactly satisfied. We take this vector as the first base vector of our

reference frame F_t.

$$\hat{t_1} = \hat{a}$$

$$t_{1b} = a_b$$

$$t_{1i} = a_i$$

The second base vector of F_t is constructed as a unit vector perpendicular to both the available measurement vectors $\hat{a}$ and $\hat{m}$.

$$\hat{t_2} = \hat{a} \times \hat{m}$$

$$t_{2b} = \frac{a_b \times m_b}{|a_b \times m_b|}$$

$$t_{2i} = \frac{a_i \times m_i}{|a_i \times m_i|}$$

The third base vector of F_t is constructed as a unit vector perpendicular to both t_1 and t_2 to complete the Triad.

$$\hat{t_3} = \hat{t_1} \times \hat{t_2}$$

$$t_{3b} = \frac{t_{1b} \times t_{2b}}{|t_{1b} \times t_{2b}|}$$

$$t_{3i} = \frac{t_{1i} \times t_{2i}}{|t_{1i} \times t_{2i}|}$$

Now we construct two rotation matrices using the three basis vectors of our frame F_t.

$$C_t^b = \begin{bmatrix} t_{1b} & t_{2b} & t_{3b} \end{bmatrix} \; and \; C_t^i = \begin{bmatrix} t_{1i} & t_{2i} & t_3 i \end{bmatrix}$$

To get the rotation matrix, we multiply these two matrices

$$C_i^b = C_t^b C_i^t = \begin{bmatrix} t_{1b} & t_{2b} & t_{3b} \end{bmatrix} \begin{bmatrix} t_{1i} & t_{2i} & t_3 i \end{bmatrix}^t \tag{4.5}$$

C_i^b is the attitude matrix from which the attitude can be found in Euler angles or quaternion as desired. This completes the Triad Algorithm. Because the algorithm is simple, it has been widely used in many spacecraft missions and still in use in many applications for three axis attitude determination [62]. The drawback of

Triad algorithm is that, it does not give equal weights to the two measurement vectors. We have to suppose that one measurement is more accurate than the other. Therefore, it does not provide optimal solution. Moreover, if more than two vectors are available for measurements then this method cannot be used.

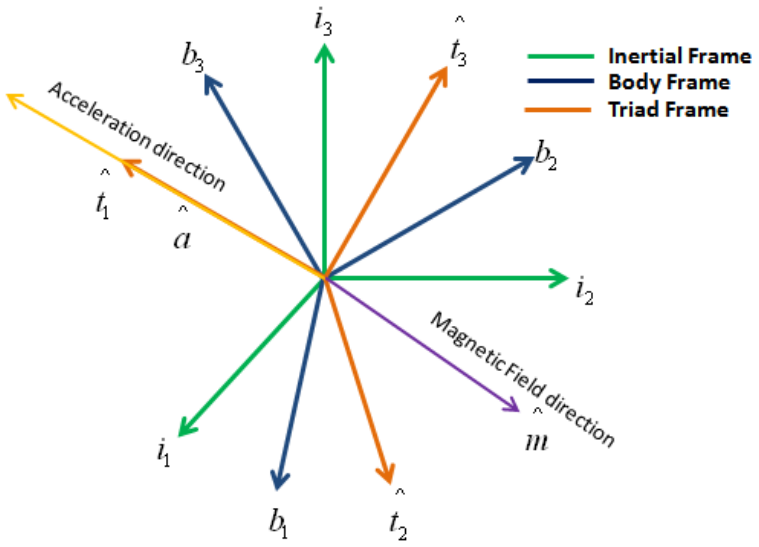

FIGURE 4.2: Triad Frame

4.1.3 Davenport q-method

P. Davenport [60] showed that the quadratic loss function given by Equation (2.1) in the attitude matrix could be transformed into a quadratic loss function in the corresponding quaternions and presented a method called q-method. This method transforms the Wahba's problem into a largest eigenvalue problem, where the associated eigenvector corresponds to the attitude in the form of quaternion [61].

This method evolved as a solution to the Wahba's problem. Consider the loss function proposed by Wahba (Equation 2.1).

$$J = \frac{1}{2}\sum_{k=1}^{N} w_k \mid v_{b(k)} - C v_{i(k)} \mid^2$$

Expanding the loss function

$$\begin{aligned} J &= \frac{1}{2}\sum_{k=1}^{N} w_k (v_{b(k)} - C v_{i(k)})^t (v_{b(k)} - C v_{i(k)}) \\ J &= \frac{1}{2}\sum_{k=1}^{N} w_k (v_{b(k)}^t v_{b(k)} + v_{i(k)}^t v_{i(k)} - 2 v_{b(k)}^t C v_{i(k)}) \end{aligned}$$

The vectors are supposed to be normalized i.e.

$$v_{b(k)}^t v_{b(k)} = v_{i(k)}^t v_{i(k)} = 1$$

Hence, the loss function becomes

$$\begin{aligned} J &= \sum_{k=1}^{N} w_k (1 - v_{b(k)}^t C v_{i(k)}) \\ J &= \sum_{k=1}^{N} w_k (1 - J_R) \end{aligned}$$

where

$$J_R = \sum_{k=1}^{N} w_k (v_{b(k)}^t C v_{i(k)}) \tag{4.6}$$

Now minimizing J is the same as maximizing J_R.

To solve this optimization problem, Davenport replaced the rotation matrix C by its corresponding quaternion $\bar{q} = \begin{bmatrix} \mathbf{q}^T & q_4 \end{bmatrix}$ using the relation [83]

$$C = (q_4^2 - \mathbf{q}^t\mathbf{q})I + 2\mathbf{q}^t\mathbf{q} - 2q_4\mathbf{q}^\times \tag{4.7}$$

with the constraint

$$\mathbf{q}^t\mathbf{q} = 1$$

The substitution of C in terms of $\bar{\mathbf{q}}$ in equation 4.6 leads to

$$J(q) = \bar{\mathbf{q}}^t K \bar{\mathbf{q}} \tag{4.8}$$

where K is a 4×4 matrix given by

$$K = \begin{bmatrix} s - \sigma \mathrm{I} & z \\ z^t & \sigma \end{bmatrix} \tag{4.9}$$

with

$$\begin{aligned} B &= \sum_{k=1}^{N} w_k (v_{b(k)} {v_{i(k)}}^t) \\ s &= B + B^t \\ z &= \begin{bmatrix} B_{23} - B_{32} & B_{31} - B_{13} & B_{12} - B_{21} \end{bmatrix}^t \\ \sigma &= tr(B) \end{aligned}$$

To maximize $J(q)$, we may take its derivative with respect to $\bar{\mathbf{q}}$, but as $\bar{\mathbf{q}}$ is subjected to the constraint $\mathbf{q}^t\mathbf{q} = 1$, we can take a new function $J^{'}(q)$ using Lagrange multiplier [84]

$$J^{'}(q) = \bar{\mathbf{q}}^t K \bar{\mathbf{q}} - \lambda \bar{\mathbf{q}}^t \bar{\mathbf{q}} \tag{4.10}$$

Differentiating Equation 4.10 shows that $J^{'}(q)$ has a stationary value when

$$K\bar{\mathbf{q}} = \lambda \bar{\mathbf{q}} \tag{4.11}$$

Equation 4.11 shows the eigenvalue problem. Hence, the optimal attitude can be computed by computing eigenvector of K matrix.

However, K matrix has four eigenvalues. In order to find which eigenvalue will result in optimal attitude, consider the gain function again

$$\begin{aligned} J(q) &= \bar{\mathbf{q}}^t K \bar{\mathbf{q}} \\ &= \bar{\mathbf{q}}^t \lambda \bar{\mathbf{q}} \\ &= \lambda \bar{\mathbf{q}}^t \bar{\mathbf{q}} \\ &= \lambda \end{aligned}$$

The maximum value of λ which is the eigenvalue of K matrix will maximize the gain function. Hence, the eigenvector corresponding to the this largest eigenvalue will result in optimal estimate of the attitude.

4.1.4 QUEST

The q-Method provides optimal attitude by computing the eigenvalue and eigenvector of K matrix. Computing eigenvalues and corresponding eigenvectors are numerically intensive processes. To simplify the process and increase the numeric efficiency, M.D. Shuster proposed a method which was named QUEST [62]. This method is relatively simple and numerically less intensive.

Recalling the loss function given by Equation 2.1

$$\begin{aligned} J &= \frac{1}{2}\sum_{k=1}^{N} w_k \mid v_{b(k)} - Cv_{i(k)} \mid^2 \\ J &= \sum_{k=1}^{N} w_k(1 - v_{b(k)}^t C v_{i(k)}) \\ J &= \sum_{k=1}^{N} w_k(1 - J_R) \end{aligned}$$

where

$$J_R = \sum_{k=1}^{N} w_k(v_{b(k)}^t C v_{i(k)})$$

Let $J_R = \lambda_{opt}$

Hence, the loss function becomes

$$J = \sum_{k=1}^{N} w_k - \lambda_{opt} \tag{4.12}$$

$$\lambda_{opt} = \sum_{k=1}^{N} w_k - J \tag{4.13}$$

$$\tag{4.14}$$

J being the loss function needs to be minimized, hence the approximate eigenvalue can be calculated as

$$\lambda_{opt} \approx \sum_{k=1}^{N} w_k \tag{4.15}$$

For many applications this estimated eigenvalue provides sufficient accuracy. After estimating the eigenvalue, the next step is to calculate the corresponding eigenvector. One simplified way to calculate the eigenvector is to convert the eigenvalue problem to corresponding Rodriguez parameter [85]

$$p = \frac{\bar{\mathbf{q}}}{q_4}$$

The eigenvalue problem in terms of Rodriguez parameter then becomes

$$\mathbf{p} = [(\lambda_{opt} + \sigma)I - S]^{-1} Z \tag{4.16}$$

As the matrix inversion is an intensive numeric process, the above equation can be rearranged and solved by Gauss elimination [86] or other numerical method as

$$\mathbf{p}[(\lambda_{opt} + \sigma)I - S] = Z \tag{4.17}$$

Once the Rodriguez parameter has been calculated, the optimal attitude in terms of quaternion can be calculated as

$$\bar{\mathbf{q}} = \frac{1}{\sqrt{1 + \mathbf{p}^t \mathbf{p}}} \begin{bmatrix} \mathbf{p} \\ 1 \end{bmatrix} \tag{4.18}$$

4.2 Attitude Determination using Gyroscopes

As mentioned earlier that in the standard navigation algorithm, gyros are used whose outputs are integrated to find the attitude information. For this purpose, three gyros are mounted in orthogonal directions to provide measurement in three dimensions. The gyros can be either single axis or three axes in single chip as in the case of MEMS based IMU.

For attitude determination using gyros, the initial estimate of the attitude is necessary. Once the initial estimate is known, the attitude update can be calculated using the relation

$$\dot{\Theta} = \Theta\Omega \tag{4.19}$$

In matrix form using Euler angles the above equation can be written as

$$\begin{bmatrix} \dot{\phi} \\ \dot{\theta} \\ \dot{\psi} \end{bmatrix} = \begin{bmatrix} 1 & \sin\phi\tan\theta & \cos\phi\tan\theta \\ 0 & \cos\phi & -sin\phi \\ 0 & \sin\phi\ sec\theta & \cos\phi\sec\theta \end{bmatrix} \begin{bmatrix} \omega_x \\ \omega_y \\ \omega_z \end{bmatrix} \tag{4.20}$$

In quaternion form, the attitude update relation is given by

$$\dot{\mathbf{q}} = \frac{1}{2}\mathbf{q} \cdot \Omega_q \tag{4.21}$$

$\mathbf{q} = \begin{bmatrix} q_1 & q_2 & q_3 & q_4 \end{bmatrix}$ is the attitude in the form of quaternion, $\bar{\Omega_q} = \begin{bmatrix} 0 & \omega_x & \omega_y & \omega_z \end{bmatrix}$ is also a quaternion with real part equal to zero and ω_x, ω_y and ω_z are rate outputs of the gyros mounted in orthogonal directions X, Y and Z. The above equation can be expressed in matrix form as

$$\dot{\mathbf{q}} = \begin{bmatrix} \dot{q_1} \\ \dot{q_2} \\ \dot{q_3} \\ \dot{q_4} \end{bmatrix} = 0.5 \begin{bmatrix} q_1 & -q_2 & -q_3 & -q_4 \\ q_2 & q_1 & -q_4 & q_3 \\ q_3 & q_4 & q_1 & -q_2 \\ q_4 & -q_3 & q_2 & q_1 \end{bmatrix} \begin{bmatrix} 0 \\ \omega_x \\ \omega_y \\ \omega_z \end{bmatrix} \tag{4.22}$$

The above equations can be solved using suitable hardware to provide attitude in the form of Euler angles or quaternion starting from an initial estimate [2]. The main drawback of this method is that any error typically bias at the gyro outputs also integrates along with the actual rate. The error accumulates with time and drifts beyond acceptable limits after some time depending upon the sensors' accuracy.

In summary, attitude determination by vector matching requires at least two sensor measurements for measurement vectors. The reference vectors for these measurements are calculated using the available mathematical models. The simplest

method using vector matching is the Triad algorithm. Many other more accurate methods like q-method and QUEST evolved as a result of finding the solution of Wahba's Problem. Triad algorithm uses two vector measurements with one measurement supposed to be more accurate than the other. Other methods like q-method and QUEST can handle more than two vectors and weight all the available information equally. Hence, they provide better results by making optimal use of the available information.

Chapter 5

Multi-Sensor Integration

As discussed in the previous chapters that attitude can be computed by integration of gyroscopes starting from an initial estimate and also by vector matching using directional vectors such as gravity and magnetic field vectors measured by three axes accelerometers and magnetometers. The attitude computed by integration of gyroscopes is accurate and low noise for a short interval of time. However, because of the integration involved in the computation process, any bias error is also integrated and the error grows with time resulting an unbounded drift in the computed attitude. On the other hand, the attitude computed by vector matching is accurate without any drift with time, but suffered from high noise depending upon the noise of the sensors used. Also under dynamic conditions, the sensors will not provide true information about the directional vectors because the sensor measurements will also include dynamic environmental measurements. To provide attitude estimation which is accurate under all dynamic and environmental conditions and drift free with time, the information from multiple sensors are combined together using Multi-Sensor integration techniques.

In the proposed research, we will use Multi-Sensor integration techniques to combine data from gyroscopes, accelerometers and magnetometers for improved attitude determination. The two techniques used for Multi-Sensor integration are based on Kalman Filter and Quaternion feedback configuration. These techniques will be discussed in details in the upcoming sections.

5.1 Quaternion Feedback Configuration

In the present research, we proposed a method similar to [58] with some modifications for Multi-Sensor integration. This method is simpler as compared to the Kalman Filter and suitable for drift free attitude determination using MEMS based IMU containing magnetometers in addition to the gyros and accelerometers. A block diagram of the proposed technique is shown in Figure 5.1. In the proposed scheme, gyros are used as primary sensors for attitude determination. Attitude is computed by rate integration of the gyro outputs as performed in the standard navigation algorithm. However, bias error of gyros will also be integrated along with the actual rate resulting continuous drift in the computed attitude. To get drift free attitude, the gyro biases need to be estimated and corrected. To achieve this task, attitude is also computed by vector matching using accelerometers and magnetometers. This attitude is noisy, but drift free and therefore, taken as a reference. The attitude computed by the rate integration is compared with this reference attitude and the resulting attitude error is used to estimate the gyro biases. The estimated gyro biases are continuously fed back and subtracted from the gyro outputs. Hence, only the actual rate information free from the bias error is integrated which results in improved computed attitude without drift. Because of rate integration, the noise in the gyro outputs also filter out, providing a low noise attitude in addition to the drift free.

The attitude computed from both types of sensors is in quaternion form and normalized to unity magnitude. When a unit quaternion says q_1 is multiplied with another unit quaternion q_2 after taking inverse of the second (inverse of a unit quaternion being equal to its conjugate), their quaternion multiplication yields another quaternion which corresponds to error between the two.

$$\Delta q = q_1 . q_2^{-1} \tag{5.1}$$

As the attitude error is in the quaternion form which is continuously fed back, we called this scheme as quaternion feedback configuration.

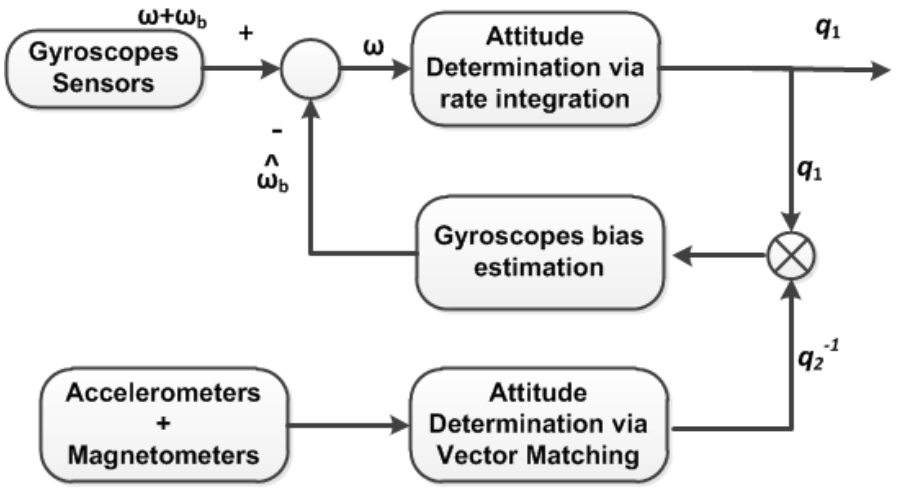

FIGURE 5.1: Block Diagram of Quaternion Feedback Configuration

5.1.1 Reference Attitude

The reference attitude q_2 is computed by the vector matching technique. Different techniques of attitude determination using vector matching have already been discussed in chapter 4. We used Davenport q- method for the reference attitude (q_2) generation. As discussed in section 4.1.3, the optimal attitude can be computed by computing eigenvector of K matrix given by

$$K = \begin{bmatrix} s - \sigma \mathrm{I} & z \\ z^t & \sigma \end{bmatrix} \tag{5.2}$$

with

$$B = \sum_{k=1}^{N} w_k (v_{b(k)} {v_{i(k)}}^t) \tag{5.3}$$

$$s = B + B^t \tag{5.4}$$

$$z = \begin{bmatrix} B_{23} - B_{32} & B_{31} - B_{13} & B_{12} - B_{21} \end{bmatrix}^t \tag{5.5}$$

$$\sigma = tr(B) \tag{5.6}$$

The two vectors used for observations are gravity g_b and azimuth m_b which are measured by three-axes accelerometers and magnetometers in the body frame.

The reference vectors for these measurements in inertial frame are given by

$$g_r = \begin{bmatrix} 0 & 0 & -g \end{bmatrix}^t$$

and

$$m_r = M \begin{bmatrix} \cos\delta & 0 & sin\delta \end{bmatrix}^t$$

These reference vectors are discussed in details in Chapter 4. The parameters used for calculating B matrix given by Equation (5.3) are $N = 2$, $w_1 = w_2 = 0.5$, $v_{b(1)} = m_b$, $v_{b(2)} = g_b$, $v_{i(1)} = m_r$ and $v_{i(2)} = g_r$.
Once the B matrix and K matrix are calculated, the reference attitude is given by

$$q_2 = eigen\ vector(K) \tag{5.7}$$

5.1.2 Attitude Error

Attitude q_1 computed by the rate integration of gyros is multiplied with q_2^{-1} computed by the vector matching to generate the attitude error. Both q_1 and q_2 are in quaternion form which results in better numeric stability and easy implementation as no trigonometric function are involved. Also q_1 and q_2 are normalized to the unit quaternion before multiplication. The attitude error is given by

$$\Delta q = q_1 . q_2^{-1} \tag{5.8}$$

The product of two quaternions is also a quaternion. Therefore Δq which is the attitude error is also a quaternion.
Let the real part is denoted by $\Delta\beta$ and the vector part by $\Delta\gamma$. When the two quaternions represent the same attitude, i.e. $q_1 = q_2$ their product results in

$$\Delta\beta = 1 \ \ and \ \ \Delta\gamma = 0$$

Hence, to make the two attitudes coincides i.e. to make q_1 to track the reference altitude q_2 the necessary condition is

$$\Delta\gamma = 0$$

5.1.3 Bias Compensator/Controller

The accelerometers and magnetometers are properly calibrated before use for computing the reference attitude. Hence, it is assumed that the difference between the two attitudes q_1 and q_2 is mainly due to the bias error of the gyros. With no bias error the two attitudes q_1 and q_2 will be equal.

Hence, the objective is to design a bias compensator which construct a rate vector ω_{comp} such that $q_1 \rightarrow q_2 \; as \; t \rightarrow \infty$ using the attitude error. When $q_1 \rightarrow q_2$ the rate vector $\omega_{comp} \rightarrow \omega_b$ which will be fed back for compensation.

For the bias estimation and compensation, the vector part of the attitude error $\Delta\gamma$ will be used as we have established the necessary condition $\Delta\gamma = 0$ for the two attitudes to coincide. The requirements for compensator are to estimate the bias vector and retain the estimated value once the condition ($\Delta\gamma \rightarrow 0$) is achieved. Therefore, the following compensator is proposed which include the proportional and integral terms

$$\omega_{comp} = k_1\Delta\gamma + \frac{k_2}{s}\Delta\gamma \tag{5.9}$$

Where $k_1,\ k_2 > 0$. Once the required condition $\omega_{comp} \rightarrow \omega_b$ is achieved, the vector part of attitude error $\Delta\gamma \rightarrow 0$ and the integral term will preserve the estimated bias.

5.1.4 Effect of Linear Acceleration

The reference attitude q_2 will be relatively accurate under static and low acceleration linear motion. However, during the linear accelerated motion, the accelerometers will also measure linear acceleration in addition to the gravity. Therefore, they will not provide precise information about the gravity vector and the attitude

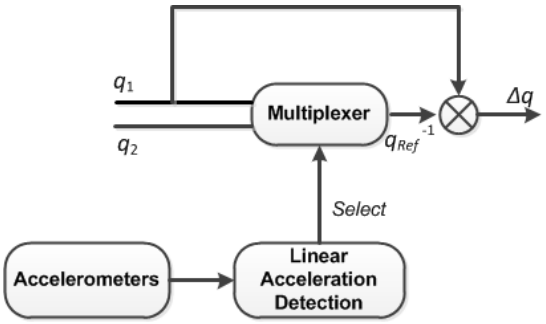

FIGURE 5.2: Linear Acceleration Detection and Correction Scheme

q_2 computed through vector matching will not be reliable. In such case, q_2 cannot serve as a reference attitude for bias estimation of the gyros.

To handle the effect of linear acceleration, it is first necessary to detect the acceleration. To use the accelerometers for the gravity vector sensing, the accelerometer outputs are normalized with gravitational acceleration. With normalized accelerometer outputs, the necessary condition for acceleration free movement is given by [43, 44]

$$a_x^2 + a_y^2 + a_z^2 = 1$$

This means that if no accelerated motion exists, then the accelerometers will sense only gravitational acceleration. On the other hand, under accelerated motion, the accelerometers will sense linear acceleration in addition to the gravity and in such case, the magnitude of gravity vector will be > 1. Hence, we can establish a necessary condition for the acceleration detection as

$$a_x^2 + a_y^2 + a_z^2 - 1 > \varepsilon \tag{5.10}$$

Where ε is the threshold which depends upon the maximum allowable linear acceleration component and the accelerometers' noise. Using the condition given by Equation 5.10, a multiplexed framework is proposed as shown in Fig 5.2. The reference attitude can be selected either q_2 or q_1 in this multiplexed scheme. Under normal condition, i.e. when no accelerated motion is detected, q_2 will be selected as reference attitude and will be multiplied by q_1 to generate the attitude error. When the linear acceleration is detected, the proposed scheme will pass q_1 for

reference attitude. When q_1 is multiplied by its own inverse, the resulting attitude error will be zero. In such case, the previously estimated bias will be preserved because of the integral term embedded in the compensator. Hence, the proposed algorithm works both under zero acceleration and accelerated motion conditions.

5.2 Kalman Filter

In 1960 R.E. Kalman presented a recursive algorithm for optimal state estimation which became a topic of extensive research, especially after the advancement in digital computing [87, 88]. This algorithm is known as Kalman Filter and is widely used in radar tracking, adaptive equalization of telephone channels, equalization of channel dispersion, spacecraft orbit determination and inertial navigation etc. [5, 89].

Kalman Filter is a set of mathematical equations that provide an optimal way to estimate the states of a process by minimizing the mean square error. Kalman Filter is very powerful because it takes into account the past, present and even the future estimate of the states [88]. In assisted inertial navigation, Kalman Filter is used as a tool to integrate data from multiple sensors to estimate accurate navigation states such as velocities, position and attitude.

5.2.1 Kalman Filters equations

The detailed derivation of the Kalman Filter equations can be found in references [5, 10, 88, 89]. In the following section, we describe the basic Kalman Filter equations. Consider the discrete time dynamic model of a system

$$x_{k+1} = \mathbf{F}x_k + Bu_k + w_k \tag{5.11}$$

where $\mathbf{F}$ is $n \times n$ state transition matrix

B is $n \times p$ matrix which relates the input control vector u to the state x

and w_k is $n \times 1$ process noise vector with covariance Q. Suppose a subset of

the states is available for measurements which can be expressed by the following equation

$$y_k = \mathbf{H}x_k + v_k$$

where y_k is the $m \times 1$ measurement vector and $\mathbf{H}$ is the $m \times n$ observation matrix. v_k is the measurement noise vector with covariance R. Kalman Filter works in two steps. The first step is called time update or prediction and the second step is called observation or measurement update [88].

Time update (Prediction)

At time $t = k$, we estimate the state vector using state space model of the system and call it $\hat{x_k^-}$.

$$\hat{x_k^-} = \mathbf{F}x_{k-1} + Bu_k \tag{5.12}$$

and also update the error covariance matrix

$$P_k^- = \mathbf{F}P_{k-1}\mathbf{F}^t + Q \tag{5.13}$$

Measurement update(Correction)

When the measurement is available at time $t = k$ we update our estimate using the relation

$$\hat{x_k} = \hat{x_k^-} + K_k(y_k - \mathbf{H}\hat{x_k^-}) \tag{5.14}$$

where K_k is called Kalman gain given by

$$K_k = P_k^-\mathbf{H}^t[\mathbf{H}P_k^-\mathbf{H}^t + R_k]^{-1} \tag{5.15}$$

Kalman gain determines how much the measurements will contribute to update the estimate.

Once the estimated states are updated using the available measurements, the error

covariance matrix is updated for the next cycle as

$$P_k = [I - K_k \mathbf{H}] P_k^- \tag{5.16}$$

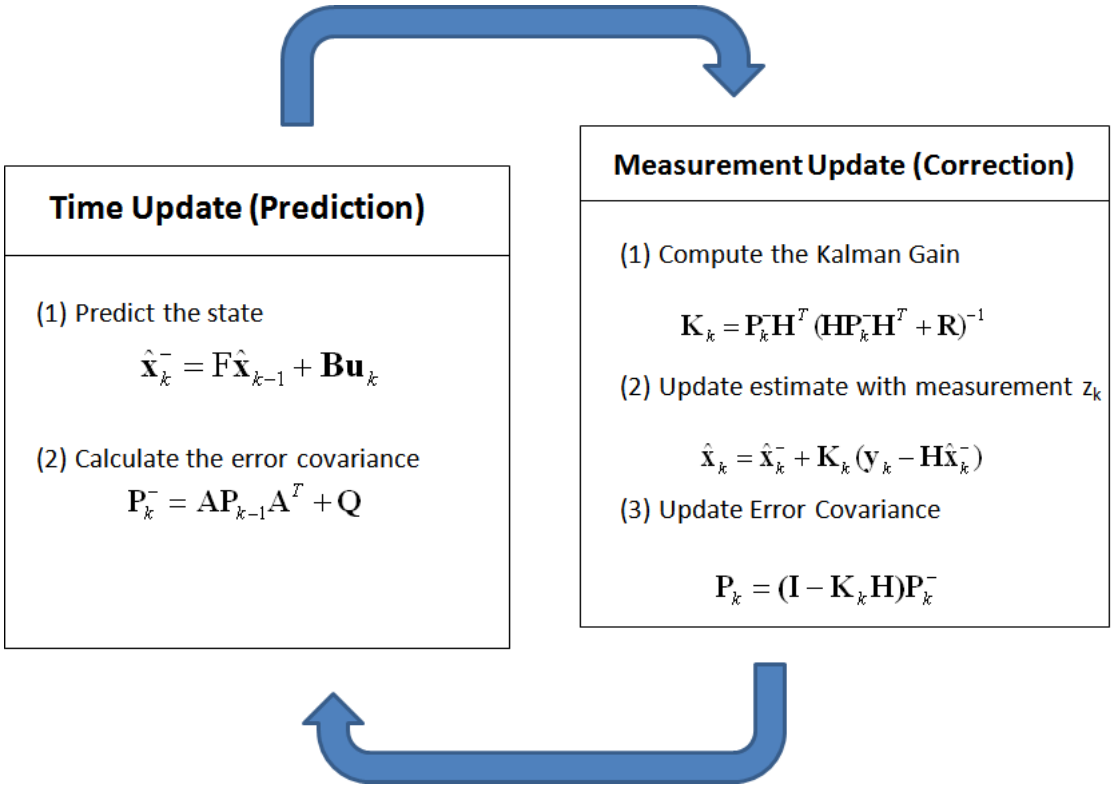

FIGURE 5.3: Kalman Filter: A recursive algorithm [88]

Kalman Filter is a recursive algorithm. At the beginning, initialization is required for the initial states estimate $\hat{x_k^-}$ and error covariance matrix P_k^-. In case of error states the initial states estimate $\hat{x_k^-}$ is usually set to zero and the error states variance is kept maximum which means that the initial estimate is completely unknown [5].

The Kalman Filter Equations and flow is shown in Figure 5.3. Kalman Filter is an extension of the least square estimation for systems which can be represented by linear differential equations. For linear systems, it provides optimal estimate between the time propagated estimate from the previous time instant and the present measurements. The optimal estimate depends upon the error variance of the time propagated estimate and the present measurements.

Kalman Filter Time Update Equations
$\hat{x_k^-} = \mathbf{F}x_{k-1} + Bu_k$
$P_k^- = \mathbf{F}P_{k-1}\mathbf{F}^t + Q$

Kalman Filter Measurement Update Equations
$K_k = P_k^-\mathbf{H}^t[\mathbf{H}P_k^-\mathbf{H}^t + R_k]^{-1}$
$\hat{x_k} = \hat{x_k^-} + K_k(y_k - \mathbf{H}\hat{x_k^-})$
$P_k = [I - K_k\mathbf{H}]P_k^-$

TABLE 5.1: Discrete Kalman Filter Equations

5.2.2 Extended Kalman Filter

Most of the systems in the Universe are nonlinear in nature. However, Kalman Filter requires a linear model of the system. Therefore, nonlinear systems need to be linearized for optimal estimate. If the system model is linearized about a nominal trajectory where the nominal trajectory is taken as the latest estimate of the states, the Kalman Filter is called Extended Kalman Filter [1, 2].

5.3 Improved Attitude via Kalman Filter

In the present research, attitude is computed by two methods using three types of sensors. The first method is by rate integration of gyros as discussed in section 4.2 and the second is by vector matching using three axes accelerometers and magnetometers. For the vector matching technique, we used Davenport q-method as discussed in section 4.1.3. Hence, we have attitude information from two different sources. Kalman Filter can be used to combine both sources of information, appropriately weight them and estimate the better attitude.

Kalman Filter can be used in two configurations, either direct and indirect. In direct configuration the state variables are the attitude parameters, i.e. roll, pitch and heading which are directly estimated using Kalman Filter. In indirect configuration, Extended Kalman Filter is used to estimate the error states which are

used as state variables. Both configurations are discussed in details. In the inertial navigation systems, Kalman Filter is mostly used in indirect configuration. Therefore, we will first discuss the indirect and then the direct configuration.

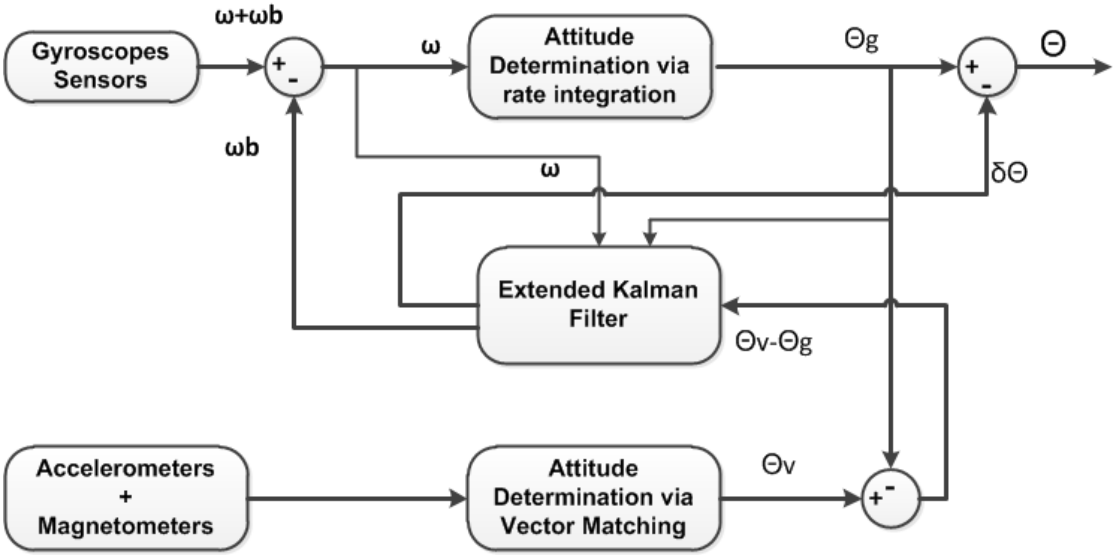

FIGURE 5.4: Extended Kalman Filter Implementation (Indirect Configuration)

5.3.1 Indirect Configuration

The block diagram of Kalman Filter's implementation in indirect configuration is shown in Figure 5.4. In this configuration, we linearized the attitude error dynamics around the nominal trajectory and used Extended Kalman Filter. As shown in the block diagram, the gyro rates and the initial estimate of the attitude parameters (roll, pitch and yaw) are used in the error dynamics equation to model the attitude and bias errors. This is performed in the first step "time update" of the Kalman Filter's cycle. In the second step, the attitude error (difference between the attitude computed by rate integration and by vector matching) is used as the measurement update for correction. The Kalman Filter's estimated states are fed to the attitude computer for compensation. This configuration has the advantage that the fast dynamic response of the attitude computer is not affected by the Kalman Filter as the Kalman Filter estimates the attitude error not the attitude output.

5.3.1.1 System Model for Extended Kalman Filter

To implement Kalman Filter for state estimation, the first step is to derive the system's state space model. In deriving system model for attitude error estimation, we used Euler angles representation of the attitude in which the roll, pitch and yaw are represented by ϕ, θ and ψ respectively. The Euler angles update relation with the body angular rates is given by [2]

$$\dot{\Theta}_{(t)} = W_B(\theta(t))\Omega_{(t)} \tag{5.17}$$

where

$$\dot{\Theta}_{(t)} = \begin{bmatrix} \dot{\phi} \\ \dot{\theta} \\ \dot{\psi} \end{bmatrix} \quad W_B(\theta(t) = \begin{bmatrix} 1 & \sin\phi\tan\theta & \cos\phi\tan\theta \\ 0 & \cos\phi & -sin\phi \\ 0 & \frac{\sin\phi}{\cos\theta} & \frac{\cos\phi}{\cos\theta} \end{bmatrix}$$

and

$$\Omega_{(t)} = \begin{bmatrix} \omega_x \\ \omega_y \\ \omega_z \end{bmatrix}$$

$\begin{bmatrix} \phi & \theta & \psi \end{bmatrix}^t$ is the attitude vector and $\begin{bmatrix} \omega_x & \omega_y & \omega_z \end{bmatrix}^t$ is the angular rate vector in the body frame. Since the goal is to get a drift free attitude from the gyros, the attitude error $\delta\phi$, $\delta\theta$ and $\delta\psi$ are included in the state vector. Gyro biases is the largest source of attitude error, therefore the state vector is also augmented with gyro biases $\delta\omega_x$, $\delta\omega_y$ and $\delta\omega_z$. On the measurement side, we have the attitude from gyros and from a combination of accelerometers and magnetometers through vector matching, therefore, the attitude error between these two measurements is taken as measurement vector. For the Kalman Filter's implementation the state and measurement vector are

$$x = \begin{bmatrix} \delta\phi & \delta\theta & \delta\psi & \delta\omega_x & \delta\omega_y & \delta\omega_z \end{bmatrix}^t \tag{5.18}$$

$$y = \begin{bmatrix} \phi_{vm} - \phi_{gyro} & \theta_{vm} - \theta_{gyro} & \psi_{vm} - \psi_{gyro} \end{bmatrix}^t \tag{5.19}$$

To derive the attitude error dynamics, we linearize Equation 5.17 about a nominal path with respect to the attitude error $\partial\Theta$ and gyro bias error $\partial\Omega$ [8] i.e. $\frac{\partial}{\partial\Theta}[W_B(\theta(t))\Omega_(t)] = A1$

$$= \begin{bmatrix} \frac{\cos\phi\sin\theta}{\cos\theta}\omega_y - \frac{\sin\phi\sin\theta}{\cos\theta}\omega_z & \frac{\sin\phi}{\cos^2\theta}\omega_y + \frac{\cos\phi}{\cos^2\theta}\omega_z & 0 \\ -\sin\phi\omega_y - \cos\phi\omega_z & 0 & 0 \\ \frac{\cos\phi}{\cos\theta}\omega_y - \frac{\sin\phi}{\cos\theta}\omega_z & \frac{\sin\phi\sin\theta}{\cos^2\theta}\omega_y + \frac{\cos\phi\sin\theta}{\cos^2\theta}\omega_z & 0 \end{bmatrix} \tag{5.20}$$

and $\frac{\partial}{\partial\Omega}[W_B(\theta(t))\Omega_(t)] =$

$$B1 = \begin{bmatrix} 1 & \sin\phi\tan\theta & \cos\phi\tan\theta \\ 0 & \cos\phi & -sin\phi \\ 0 & \frac{\sin\phi}{\cos\theta} & \frac{\cos\phi}{\cos\theta} \end{bmatrix} \tag{5.21}$$

Every time, when a MEMS gyro is powered on, it shows some bias offset. In case of low grade, this error is further enhanced. As in the proposed research, we are using low grade MEMS gyros, their turn on bias is more severe. Therefore, we have modeled this bias error as a random constant. Hence

$$\delta\dot{\Omega} = 0 \tag{5.22}$$

The complete error dynamics for the attitude error and bias error is given by [9].

$$\begin{bmatrix} \delta\dot{\Theta} \\ \delta\dot{\Omega} \end{bmatrix} = \begin{bmatrix} A1 & B1 \\ 0_{3\times3} & 0_{3\times3} \end{bmatrix} \begin{bmatrix} \delta\Theta \\ \delta\Omega \end{bmatrix} \tag{5.23}$$

where $\delta\Theta = \begin{bmatrix} \delta\phi & \delta\theta & \delta\psi \end{bmatrix}^t$ and $\delta\Omega = \begin{bmatrix} \delta\omega_x & \delta\omega_y & \delta\omega_z \end{bmatrix}^t$. or

$$\dot{\delta x} = \mathbf{A(t)}\delta x \tag{5.24}$$

where

$$\mathbf{A(t)} = \begin{bmatrix} A1 & B1 \\ 0_{3\times3} & 0_{3\times3} \end{bmatrix} \tag{5.25}$$

A(t) is called the dynamic matrix. It propagates error over time [1]. From the dynamic matrix, the state transition matrix can be computed as

$$\mathbf{F} = e^{\mathbf{A}\Delta t} \tag{5.26}$$

using the Taylor series expansion and taking the first two terms gives

$$\mathbf{F} = \mathbf{I} + \mathbf{A}\Delta t \tag{5.27}$$

where Δt is the sampling time $\mathbf{I}$ shows the identity matrix.
In discrete form the error dynamics can be written as

$$x_{k+1} = \mathbf{F}_k x_k + w_k \tag{5.28}$$

$$y_k = \mathbf{H} x_k + v_k \tag{5.29}$$

$\mathbf{H} = \begin{bmatrix} I_{3\times3} & 0_{3\times3} \end{bmatrix}$ is called the system observation matrix. w_k is the process and v_k is the measurement noise vector as mentioned earlier. At each time interval, the system error dynamics are linearized about the nominal trajectory and state transition matrix is calculated. Once the state transition matrix is calculated, the standard Kalman Filter's equations as shown in section 5.2.1 for the time update and observation update have been used for implementation. The observation model is already linear as, a subset of the states is already available for measurements.

5.3.1.2 Process and Measurement Noise Matrices (Q *and* R)

Generally, in Kalman Filter's implementation, it is assumed that the process and measurement noises are uncorrelated, zero mean white Gaussian processes. Therefore, the covariance matrices Q and R are diagonal. The selection of Q and R are very important because, although, Kalman Filters can be used for nonlinear states estimation, the convergence or stability cannot be guaranteed and it strongly depends upon the selection of covariance matrices Q and R.

In inertial navigation system, if all the error sources are properly modeled in the state transition matrix, then the process noise mainly depends on the noise density and drift of the sensors used. In the present situation, the first three states of the state vector correspond to the attitude error while the other three states correspond to the gyro bias errors. If the bias errors of the gyros are properly estimated and compensated, then the attitude error depends on the noise density σ_N of the gyros. To get the noise density and in-run drift of the gyros, an experimental test is performed. The IMU is placed in a disturbance free environment in static condition and data of the gyros are acquired for 10 minutes. The noise density and in-run drift of the gyros are calculated from this data. The average noise density of the gyros is found $0.04\ ^\circ/sec/\sqrt{Hz}$ or $6.97 \times 10^{-4}\ rad/sec/\sqrt{Hz}$. Therefore the first three diagonal elements of the process covariance matrix are set to the variance σ_N^2. The other three states of the state vector depend on the average in-run drift σ_g of the gyros which was computed experimentally and found $0.03\ ^\circ/sec$ or $5.34 \times 10^{-4}\ rads/sec$. Therefore, the last three diagonal elements of the process noise matrix are set to σ_g^2. Hence the process noise matrix is given by

$$Q = \begin{bmatrix} \sigma_N^2 & 0 & 0 & 0 & 0 & 0 \\ 0 & \sigma_N^2 & 0 & 0 & 0 & 0 \\ 0 & 0 & \sigma_N^2 & 0 & 0 & 0 \\ 0 & 0 & 0 & \sigma_g^2 & 0 & 0 \\ 0 & 0 & 0 & 0 & \sigma_g^2 & 0 \\ 0 & 0 & 0 & 0 & 0 & \sigma_g^2 \end{bmatrix}$$

The measurement covariance matrix R depends on the standard deviation of the measurement sensors used. In our case, we are using attitude error as a measurement which is computed from gyros and a combination of accelerometers and magnetometers. It has been observed experimentally that the roll and pitch computed by the accelerometers have a standard deviation of $0.3^\circ(0.005\ rad)$ and the heading computed by magnetometers has a maximum deviation of $1^\circ(0.018\ rad)$. Therefore the measurement noise matrix contains first two elements with variance $\sigma_a^2 = (0.005)^2$ corresponding to the attitude error introduced by accelerometers'

noise and the third element with variance $\sigma_m^2 = (0.018)^2$ corresponding to the heading error introduced by the magnetometers noise. Hence the measurement covariance matrix is given by

$$R = \begin{bmatrix} \sigma_a^2 & 0 & 0 \\ 0 & \sigma_a^2 & 0 \\ 0 & 0 & \sigma_m^2 \end{bmatrix}$$

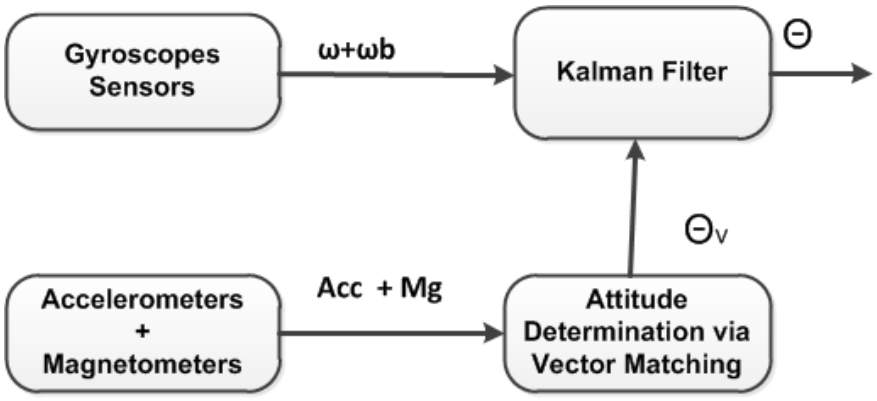

FIGURE 5.5: Kalman Filter Implementation (Direct Configuration)

5.3.2 Direct Configuration

The block diagram of Kalman Filter's implementation in direct configuration is shown in Figure 5.5. In direct configuration, we are estimating the attitude parameters directly in the form of quaternion instead of the attitude error. The attitude update relation given by Equation 4.22 in quaternion form is used as the time update (prediction step) in Kalman Filter's implementation. The attitude computed by vector matching is used as the measurement update for correction. For vector matching, we used Davenport q-method as discussed in section 4.1.3. This method provides attitude directly in the form of quaternion.

The state vector contains attitude in the form of quaternions and the measurement vector is also an attitude in the form of quaternion computed by the vector

matching i.e.

$$\begin{aligned} x &= \begin{bmatrix} q_1 & q_2 & q_3 & q_4 \end{bmatrix}^t \\ y &= \begin{bmatrix} q_{1vm} & q_{2vm} & q_{3vm} & q_{4vm} \end{bmatrix}^t \end{aligned} \tag{5.30}$$

The state space model used for the attitude estimation in quaternion form is given by

$$\dot{\mathbf{q}} = \begin{bmatrix} \dot{q_1} \\ \dot{q_2} \\ \dot{q_3} \\ \dot{q_4} \end{bmatrix} = 0.5 \begin{bmatrix} 0 & -\omega_x & -\omega_y & -\omega_z \\ -\omega_x & 0 & \omega_z & -\omega_y \\ \omega_y & -\omega_z & 0 & \omega_x \\ \omega_z & \omega_y & -\omega_x & 0 \end{bmatrix} \begin{bmatrix} q_1 \\ q_2 \\ q_3 \\ q_4 \end{bmatrix} \tag{5.31}$$

ω_x, ω_y and ω_z are the outputs of the gyros used. The above equation is the same as equation 4.22. The difference is, the rate vector is written in the matrix form instead of quaternion. Equation 5.31 can be written as

$$\dot{\mathbf{q}} = \mathbf{W}\mathbf{q} \tag{5.32}$$

where

$$\mathbf{W} = 0.5 \begin{bmatrix} 0 & -\omega_x & -\omega_y & -\omega_z \\ -\omega_x & 0 & \omega_z & -\omega_y \\ \omega_y & -\omega_z & 0 & \omega_x \\ \omega_z & \omega_y & -\omega_x & 0 \end{bmatrix} \tag{5.33}$$

The solution to the above equation in discrete form with Δt as sampling interval

$$\mathbf{q}_{k+1} = e^{\mathbf{W}\Delta t}\mathbf{q}_k \tag{5.34}$$

Expanding by the Taylor series and taking the first two terms gives

$$\mathbf{q}_{k+1} = [\mathbf{I} + \mathbf{W}\Delta t]\mathbf{q}_k \tag{5.35}$$

where **I** is the identity matrix.

$$\mathbf{q}_{k+1} = \mathbf{F}_k \mathbf{q}_k \tag{5.36}$$

Equation 5.36 is used as the time update. If the state and measurement vectors are denoted by x and y as defined in equation 5.30, the Kalman's Filter equations can be written as

Time update (Prediction)

$$\begin{aligned} \hat{x_k^-} &= F_k x_{k-1} \\ P_k^- &= F P_{k-1} F^t + Q \end{aligned} \tag{5.37}$$

Measurement update(Correction)

$$\begin{aligned} K_k &= P_k^- H^t [H P_k^- H^t + R_k]^{-1} \\ \hat{x_k} &= \hat{x_k^-} + K_k (y_k - H \hat{x_k^-}) \\ P_k &= [I - K_k H] P_k^- \end{aligned} \tag{5.38}$$

As the measurement and the estimated states are the same, the observation matrix is

$$H = \begin{bmatrix} 1 & 0 & 0 & 0 \\ 0 & 1 & 0 & 0 \\ 0 & 0 & 1 & 0 \\ 0 & 0 & 0 & 1 \end{bmatrix}$$

Another important step is to set the process and measurement co-variance matrices. In the prediction step, gyros are used as inputs so the variations in the estimated attitude depends upon the variations in the gyro outputs. Therefore, the process noise matrix is initiated with the variance of the gyros' bias drift σ_g^2 i.e.

$$Q = \begin{bmatrix} \sigma_g^2 & 0 & 0 & 0 \\ 0 & \sigma_g^2 & 0 & 0 \\ 0 & 0 & \sigma_g^2 & 0 \\ 0 & 0 & 0 & \sigma_g^2 \end{bmatrix}$$

For setting the measurement co-variance matrix, experimental test is performed. The IMU is placed in a disturbance free environment in static condition. Data of the IMU sensors, i.e. gyros, accelerometers and magnetometers are acquired for 10 minutes. Using the acquired data, attitude is computed by q-method offline and variances of quaternion parameters provided by q-method are calculated. The diagonal elements of the matrix are set with the computed variances. The measure covariance matrix becomes

$$R = \begin{bmatrix} \sigma_{q1_{vm}}^2 & 0 & 0 & 0 \\ 0 & \sigma_{q2_{vm}}^2 & 0 & 0 \\ 0 & 0 & \sigma_{q3_{vm}}^2 & 0 \\ 0 & 0 & 0 & \sigma_{q4_{vm}}^2 \end{bmatrix}$$

Chapter 6

Experimental Test, Results and Discussion

6.1 Development of Experimental Setup

For implementation and testing of the algorithms, an experimental setup is developed. A commercially available inertial module LSM9DS0 from ST Microelectronic is used which contains three axes gyroscope, accelerometer and magnetometer sensors. The sensors' chip is stuffed on a printed circuit board and interfaced with Xilinx Sparatan III series field programmable gate array (FPGA). The firmware to read the sensors is coded in varilog hardware description language (Verilog HDL). This electronics assembly is packaged in a rectangular box which can be mounted in different orientations to build an IMU. The data from the IMU can be continuously acquired and stored in Personal Computer (PC) at 51Hz and 1Hz for post processing using data acquisition software. The data acquisition software is built in visual C++ which acquires data through a serial port of a PC and stores sensors' calibrated data. The sensors' calibration process adopted is discussed in the next section. The algorithm for quaternion feedback and Kalman filters are implemented in Matlab and applied offline to the acquired data. The

specifications of the sensors available in MEMS IMU are summarized in table 6.1.

Gyroscopes	
Measurement Range	$\pm 250\ ^\circ/sec$
Bias	$\pm 10\ ^\circ/sec$
Bias Drift(Fixed Temperature)	$110\ ^\circ/h$
Noise Density	$0.04\ ^\circ/sec/\sqrt{Hz}$
Accelerometers	
Measurement Range	$\pm 4\ g$
Bias	$\pm 60\ mg$
Bias Drift (Fixed Temperature)	$0.9mg$
Noise Density	$0.768\ mg/\sqrt{Hz}$
Magnetometers	
Measurement Range	$\pm 4\ Gauss$
Noise Density	$0.55\ mGauss/\sqrt{Hz}$

TABLE 6.1: Sensors Specifications

6.2 Sensors Calibration

The gyros, accelerometers and magnetometers in MEMS IMU are calibrated first before use. Although, the accelerometers and gyros in the MEMS IMU used are factory calibrated, however, calibration is recommended for applications that require measurement of tilt angle better than 1 degree [90].

For proper calibration of an IMU, a precise multi-axes rate table is required. However, in the present research, because of the non-availability of the multi-axes rate table and keeping the quality of the sensors used in mind, approximate calibration methods are adopted which will be discussed in details. The three types of sensors are calibrated independently and will be discussed separately. First, the gyros, then the accelerometers and finally the magnetometers calibration processes are discussed.

6.2.1 Rate Gyro Calibration

For gyroscope calibration, the IMU is mounted on a single axis rate table. Each gyro in the X, Y and Z axes is calibrated independently, The rate table used consists of a platform that can be rotated at different preset rotation rates. Data is acquired for 5 minutes in static condition. The outputs of the gyros are recorded and the mean values of each in the X, Y and Z directions are calculated. The mean values show offsets at the gyro outputs which need to be subtracted to make the gyro outputs approximately equal to zero [91]. Because the gyros are of low quality which cannot sense Earth's rate, this method of fixed bias calculation is accurate enough for this class.

To calculate the scale factor, the rate table is rotated at a rate of $5°/sec$. In the initial configuration, only Z-gyro should sense the rotation as X, and Y are orthogonal to the axis of rotation. The output of Z-gyro is recorded for repeated cycles in clockwise and counter clockwise directions. The scale factor of Z-gyro is calculated as

$$\begin{aligned} Rate_{applied} &= G_{S.F} \times Rate_{sensed} \\ G_{S.F} &= \frac{Rate_{applied}}{Rate_{sensed}} \end{aligned}$$

The scale factor calculated is multiplied with the output of the Z-gyro. To calculate the scale factor of X-gyro, the IMU is placed on the rate table such that X-axis of the IMU becomes parallel to the axis of rotation. The same procedure is repeated as done for Z-gyro to calculate the Scale factor of X-gyro. Similarly for Y-gyro, Y-axis is made parallel to the axis of rotation and the same procedure is repeated. After calculating the fixed biases and scale factors of the gyros, these parameters are permanently stored in the data acquisition software and the gyros calibrated outputs are acquired whenever the IMU is used. The calibrated gyro output is given by

$$G_{cal} = (G_{out} - G_{bias})G_{S.F}$$

The calibration parameters calculated for gyros are shown in table 6.2.

Axis	**Bias** $(^\circ/sec)$	**Scale Factor**
X	0.5	0.98
Y	1.1	0.98
Z	-0.6	0.99

TABLE 6.2: Gyros Calibration Parameters

6.2.2 Accelerometer Calibration

Accelerometers are also approximately calibrated by placing the IMU in different positions. First, the Z-axis accelerometer is calibrated. The IMU is placed on a flat surface such that the Z-axis accelerometer senses gravitational acceleration g. In this case, the other two accelerometers X and Y will sense approximately zero acceleration. The Z-accelerometer will measure the gravity plus bias at the output. Let this value is

$$a_{out} = g + a_{bias}$$

where a_{out} is the accelerometer's output, g is the acceleration due to gravity and a_{bias} is the accelerometer's bias. This output is recorded and its average value is noted. Now the IMU is placed 180 degrees opposite to its position. The accelerometer will now measure gravitational acceleration g with opposite sign plus accelerometer bias as given below

$$a_{out} = -g + a_{bias}$$

This value is also recorded. If we add these two values, then the gravity component will be canceled out and remaining will show twice the bias value [91]. Mathematically, it can be seen that

$$a_{out} = g + a_{bias} + a_{out} - g + a_{bias}$$

$$a_{bias} = a_{out}/2$$

Once the bias value is calculated, the output of the accelerator is corrected by subtracting this value. After subtracting the accelerometer's bias, the next step is to calculate the accelerometer's scale factor. As the accelerometer's output is in

g, under static condition it should read $1g$ i.e.

$$1 = a_{S.F} \times a_{out}$$

Hence $a_{S.F}$ is given by

$$a_{S.F} = 1/a_{out}$$

After bias and scale factor determination, the calibrated output of the accelerometer is given by

$$a_{cal} = (a_{out} - a_{bias})a_{S.F}$$

X and Y accelerometers are also calibrated in the similar way. The calibration parameters as shown in table 6.3 are stored in the data acquisition software and the accelerometers' calibrated outputs are recorded.

Axis	**Bias** (g)	**Scale Factor**
X	-0.0515	0.99
Y	-0.019	0.98
Z	-0.0425	0.99

TABLE 6.3: Accelerometers Calibration Parameters

6.2.3 Magnetometer Calibration

In the present work, a three axes magnetometer is used to measure the Earth's magnetic field. It should be able to provide the Earth's magnetic field measurement correctly without any ambiguity. However, the output of a magnetometer is strongly affected by nearby ferrous material, magnetic fields and disturbances. Therefore, once the magnetometer is fixed in some housing or casing, the effect of disturbances must be compensated before use [40]. To properly calibrate and estimate the effects of disturbances, the IMU is fixed on a rate table such that the X and Y magnetometers are in the horizontal plane. Under no disturbance condition, the plot of X and Y magnetic components against each other rotated 360 degrees in the Earth's magnetic field will show a circle with center at the origin as

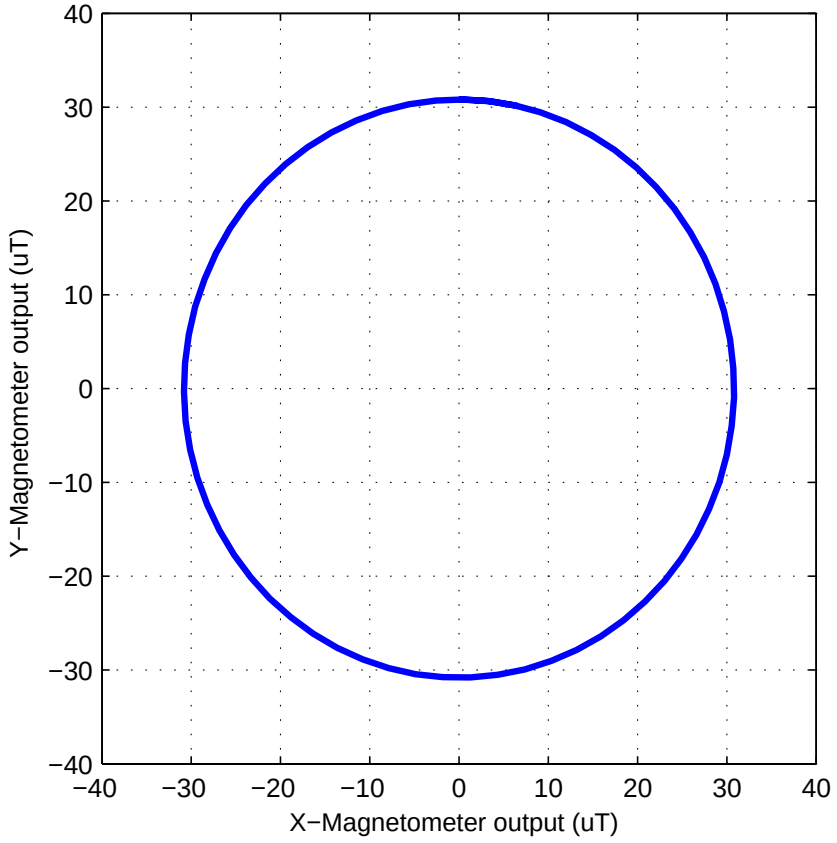

FIGURE 6.1: Rotation in Earth's Magnetic Field with no Disturbance

shown in Figure 6.1. However, any type of nearby disturbance will add constant offset in the X and Y magnetometer outputs. This will result a shift of the circle from the origin. To find the fixed offsets added in X and Y magnetometer outputs due to disturbance, the rate table is rotated 360 degrees at $1°/sec$ in the Earth's magnetic field. The X and Y magnetometers will measure the Earth's magnetic field in the horizontal plane, which will change their magnitudes with rotation as shown in Figure 6.2. It can be observed that maximum and minimum intensity of the magnetic field is different for X and Y components. This is because of the fixed offsets added in X and Y components. If the X component is plotted against Y as shown in Figure 6.3, the resulting circle is also shifted from the origin. The fixed offsets in X and Y components are calculated as

$$X_{Bias} = (max(X) + min(X))/2$$

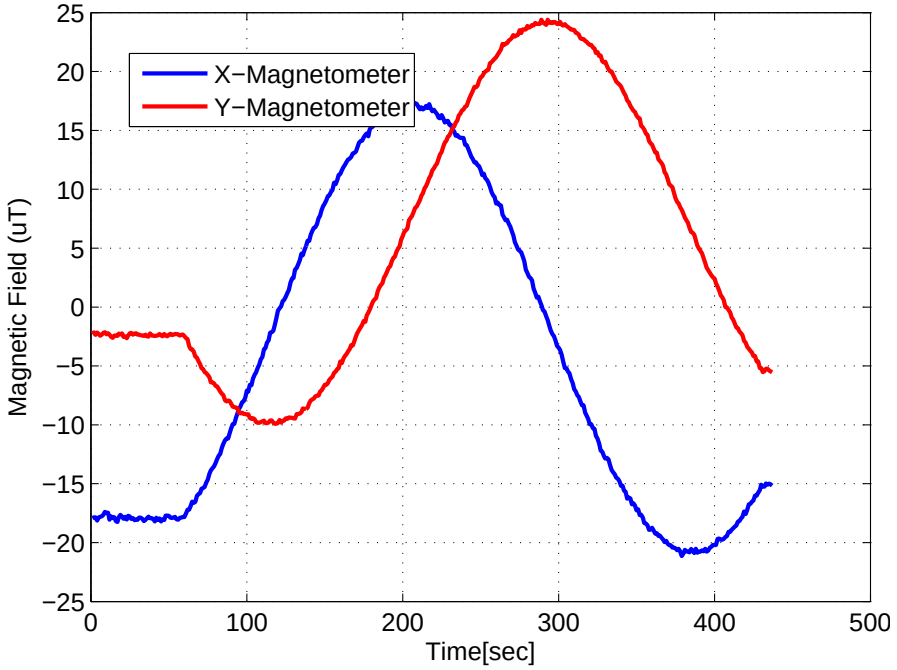

FIGURE 6.2: X-Y Magnetic Field (un-calibrated)

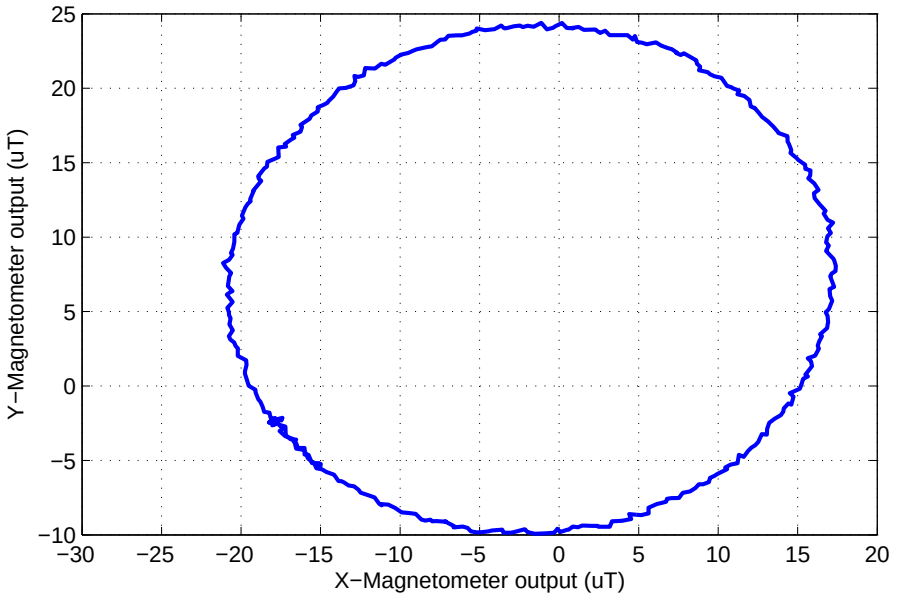

FIGURE 6.3: Rotation in Earth's Magnetic Field (un-calibrated)

$$Y_{Bias} = (max(Y) + min(Y))/2$$

The calculated X and Y offsets are subtracted from the X and Y magnetometer outputs respectively. To find the scale factor, the horizontal field intensity is required, which can be taken from the IGRF model at any locations. With horizontal field intensity H_{IGRF}, the X and Y magnetometers scale factor can be

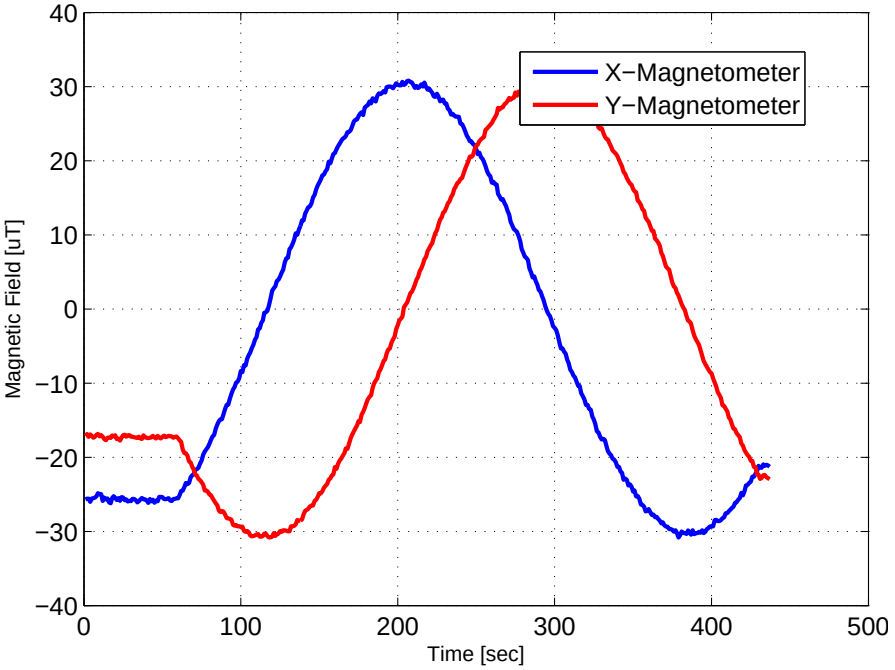

FIGURE 6.4: X-Y Magnetic Field (Calibrated)

calculated as

$$Mx_{SF} = H_{IGRF}/max(X)$$

$$My_{SF} = H_{IGRF}/max(Y)$$

After offsets and scale factors determination, the calibrated outputs of X and Y magnetometers are given by

$$Mx_{cal} = (Mx_{out} - X_{bias})Mx_{SF}$$

$$My_{cal} = (My_{out} - Y_{bias})My_{SF}$$

With calibrated outputs, the plot of X and Y components of Earth's magnetic field can be seen in Figure 6.4. It can be observed that now the peak values of X and Y magnetometers are equal. The plot of X component along Y also shows a circle with center at the origin as shown in Figure 6.5. After X and Y magnetometers' calibration, the Z magnetometer can be calibrated by placing the IMU on the rate table in such way that X and Z magnetometers are in the horizontal plane now. The same procedure is repeated. It can be noted that while finding the offset of Z-magnetometer, we will also find the offset of X-magnetometer

Axis	**Bias** (uT)	**Scale Factor**
X	-1.86	1.60
Y	7.24	1.79
Z	8.94	1.63

TABLE 6.4: Magnetometers Calibration Parameters

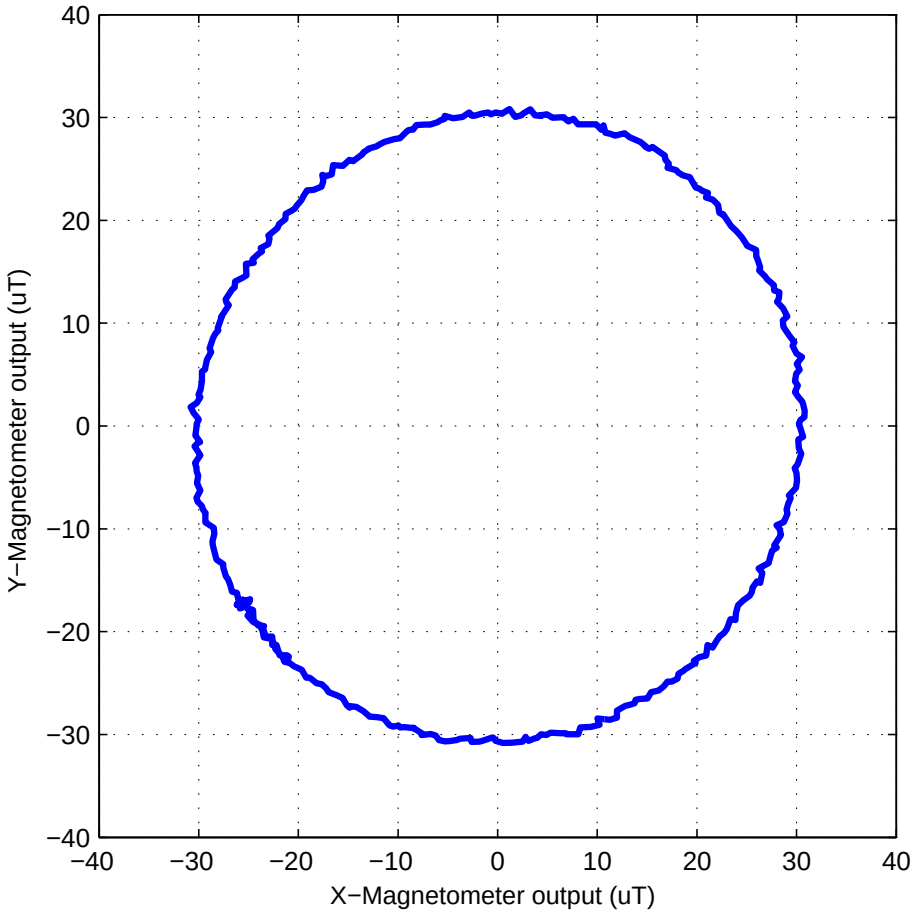

FIGURE 6.5: Rotation in Earth's Magnetic Field (Calibrated)

which we have already determined. The two offsets of X-magnetometer should be nearly equal or close to each other. This will also verify our offset determination method. A similar confirmation for Y and Z magnetometer's offsets can also be done if the IMU is placed on the rate table such that Y and Z magnetometers are in the horizontal plane. The magnetometers calibration parameters calculated are shown in table 6.4 which are stored in the data acquisition software and the magnetometers' calibrated outputs are recorded.

6.3 Experimental Tests

After the sensors' calibration, two types of tests are performed in which the IMU is mounted in different orientations and data is acquired. The details of the tests performed are discussed in the following.

6.3.1 Motion Test

In this test, the IMU is mounted on a single axis rate table such that its X-axis is aligned to the north. The rate table is rotated in Z-axis. Initially, the IMU is kept in a static condition for 50 seconds, then the rate table is operated in synthesis mode in which 14 cycles of sine wave are applied. Then, again the IMU is kept in static conditions for 50 seconds. Data is acquired at 51 Hz during the test. As the rotation is applied only along the Z-axis, only the Z-axis gyro will sense the angular rate. The X and Y-axes gyros being orthogonal to the axis of rotation will sense no rotation.

6.3.2 Static Test

In static test, the IMU is placed on a fixed table at room temperature under no disturbance environment i.e. no vibrations and nearby magnetic field. Under static conditions, data is acquired for 30 minutes. Because of uncontrolled room temperature and MEMS gyros intrinsic behaviour, the gyro outputs will drift with time and significant bias error will be introduced. Hence, the static test is a useful check for the algorithm's performance against time growing bias errors of the gyros.

6.4 Attitude Computation

Using the acquired data in the static and motion conditions, attitude is computed by the following methods.

- Rate integration of the gyros
- Davenpot's q-method (Vector Matching)
- Quaternion Feedback Configuration
- Sensors data fusion through Extended Kalman Filter (Indirect Configuration)
- Sensors data fusion through Kalman Filter (Direct Configuration)

6.4.1 Rate Integration of the Gyros

The attitude computed by rate integration using the acquired data for motion test is shown in Figure 6.6. It can be seen in the heading angle plot that the heading starts initially at 0.40 degrees and drifts to 1.8 degrees in the first 50 second under static condition. After 50 second there are sinusoidal variation in the heading which corresponds to the rotation around Z-axis. After the rotation stopped, the heading angle should return to its initial value, but it drifts to 4.9 degrees. This change in heading value is due to the bias error which introduced the total error of 6 degrees in just 160 seconds. The roll and pitch should also remain at their initial values as there are no variations in the roll and pitch axes. However, the roll angle drift and peaks at -14 degrees and pitch angle reaches 10.5 degrees.
The dynamic response is very good in the heading axis during the time in which rotation is applied around Z-axis. The attitude computed is also low noise because noise of the gyros are filtered out during the integration process.
The static test results are shown in Figure 6.7. Under static condition, the response of gyros becomes worst. The heading angle drifts with time and reaches to 180 degrees after 23 minutes. The roll angle also peaks at -30 degrees and pitch angle at -36 degrees.
Before performing the test, the fixed biases of the gyros were calculated and subtracted. It means that, the in-run drifts of the gyros have introduced unacceptable errors in the computed attitude. Hence, this type of gyros are not suitable for attitude determination without bias correction. In order to use them for drift free

Rate Integration	Vector Matching
Low noise	High noise
Drift with time	No drift with time
Good dynamic response	Poor dynamic response
Poor static response	Good static response
Disturbance free	Disturbance sensitive

TABLE 6.5: Comparison of Vector Matching and Rate Integration

attitude, we have to detect and correct the bias error of the gyros continuously during the operation.

6.4.2 Vector Matching

Attitude computed by vector matching (Davenport q-method) using the acquired data for the motion and static test is shown in Figure 6.6 and Figure 6.7 respectively. It can be observed that the attitude computed both for the static and motion test has no drift as observed in the rate integration of gyros. However, the attitude computed contains noise. This is because of the sensors' noise. In this method, the attitude is computed sample by sample using the available sensor measurements independent of the previous measurement. Hence, no initial estimate of the attitude is required at the start up. As no integration or filtering is performed during the computation process, the sensors' noise directly reflects on the computed attitude. This is one major drawback of the vector matching when compared to the rate integration.

Other drawback of the vector matching is the disturbance during dynamic motion. For sensing the gravity vector, we are using a triad of accelerometers, which will measure linear acceleration during dynamic motion also in addition to the gravity. This linear acceleration acts as a disturbance and the gravity vector measurement will not be accurate enough depending upon the extent of the linear acceleration. Hence, the dynamic response of the vector matching technique is not good as compared to the rate integration.

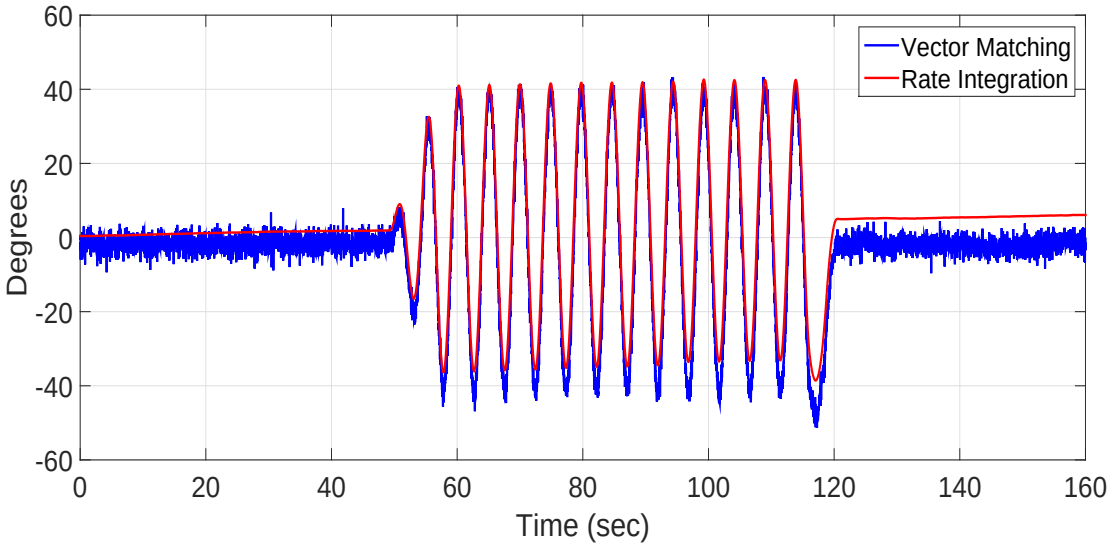

(A) Heading angle

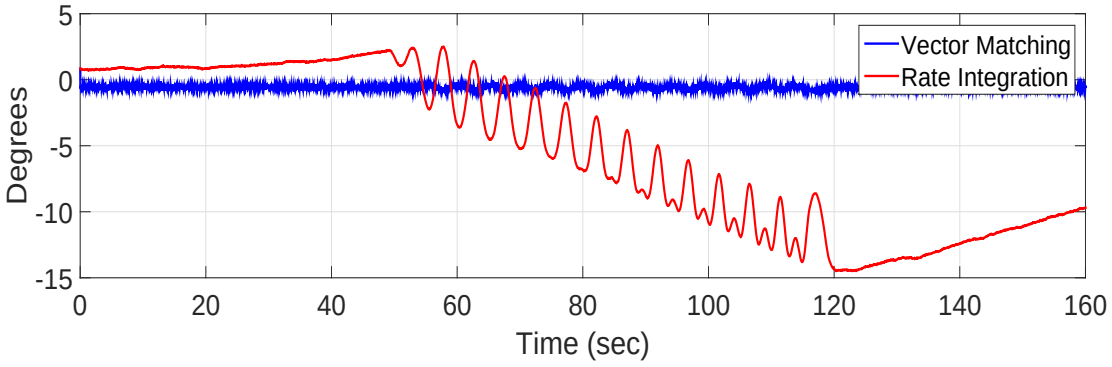

(B) Roll angle

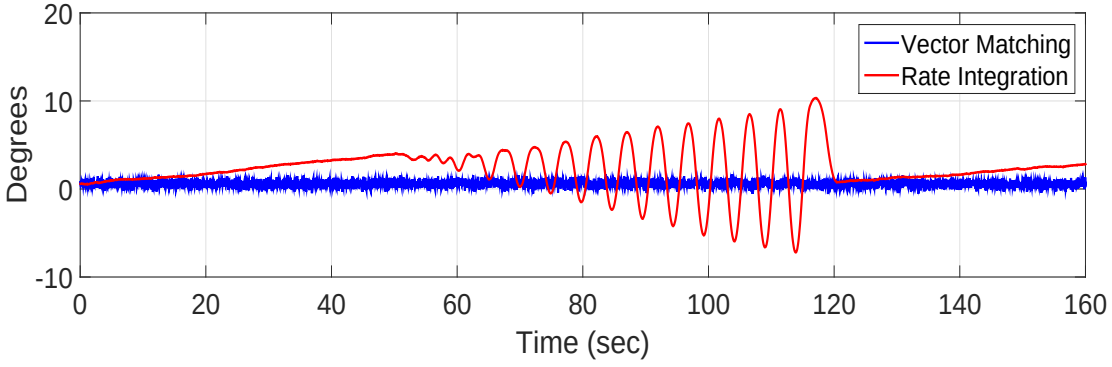

(C) Pitch Angle

FIGURE 6.6: Attitude Determination by Rate integration and Vector Matching for motion test

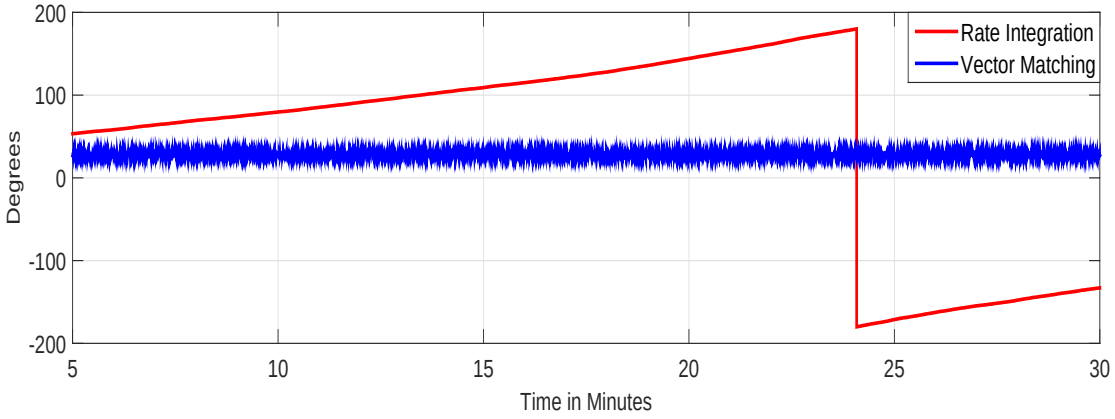

(A) Heading angle

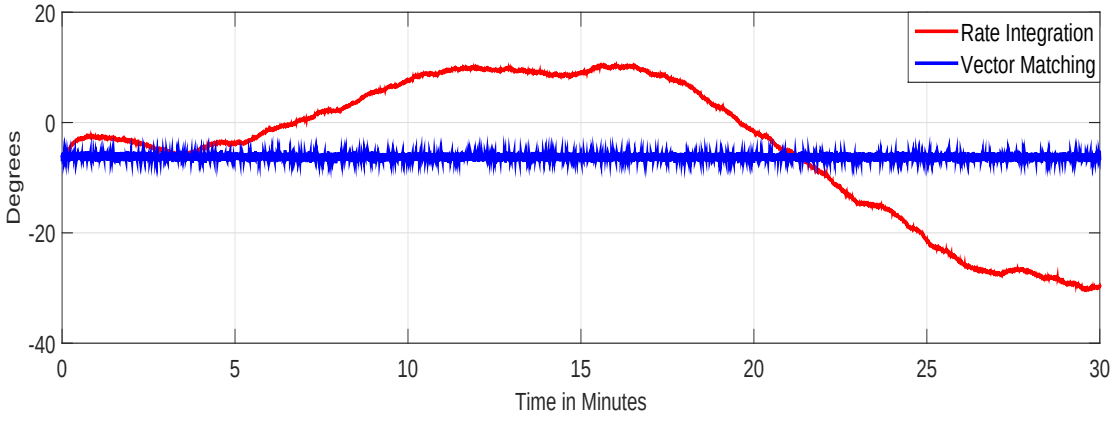

(B) Roll angle

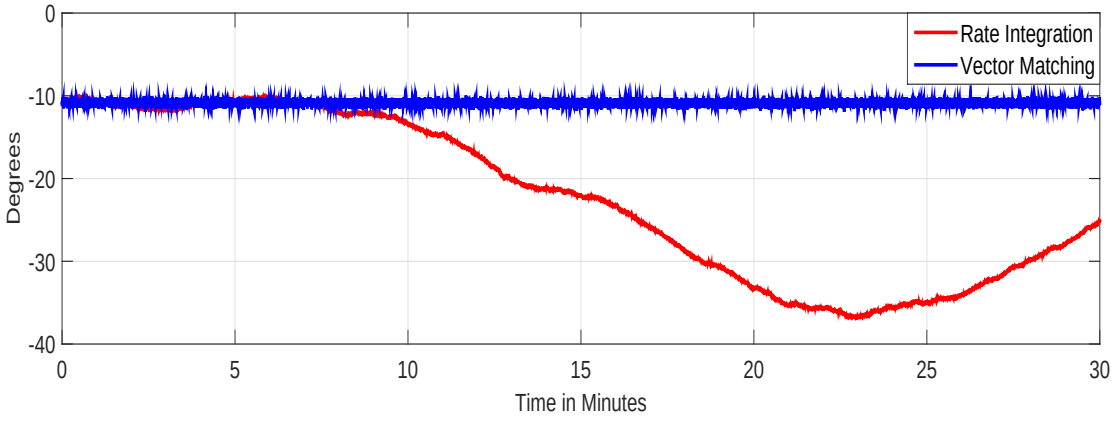

(C) Pitch Angle

FIGURE 6.7: Attitude Determination by Rate integration and Vector Matching for static test

	Axis	Before motion(deg)	After motion(deg)	Attitude error(deg)
Rate Integration	Roll	2.33	-14	16.33
	Pitch	4.08	0.84	3.18
	Heading	0.95	4.25	3.45
Vector Matching	Roll	-0.54	-0.56	0.02
	Pitch	-0.33	-0.31	0.02
	Heading	-1.6	-.88	0.20

TABLE 6.6: Attitude Error Comparison between Rate integration and Vector Matching For motion test

6.4.3 Rate Integration Vs Vector Matching

To compare the attitude computed by rate integration and by vector matching, results are tabulated in table 6.6 and table 6.8 for motion and static tests respectively.

In table 6.6 for the motion test comparison, the attitude has been noted before the start and at the end of the motion. The difference between these two values is taken as the attitude error. This error is 16.33, 3.18 and 3.45 degrees in the roll, pitch and heading respectively, for the attitude computed by the rate integration. This shows the error introduced in the attitude during the dynamic motion. The noise is, however, very low. On the other hand, the attitude error is very small and remains within 0.2 degrees for vector matching. However, the noise is high, especially in the heading as shown in figure 6.6.

For static test, the IMU is placed in a disturbance free environment in certain orientations. As no dynamic motion or magnetic disturbance is involved, the attitude computed by vector matching will be accurate enough to be used as a reference. Therefore, the mean value of the attitude for the first five minutes computed by vector matching is calculated and taken as the reference attitude. The roll, pitch and heading found are -6.27, -10.87 and 29.20 degrees respectively. These values are assumed as our actual orientation in which the IMU is placed. To calculate the attitude error, these values are subtracted from the computed attitude and the difference is taken as the attitude error whose RMS is calculated

Attitude Error [deg](Motion Test)	Attitude [(Before motion)-(After motion)]
Attitude Error [deg] (Static Test)	RMS[Attitude- Reference Attitude])
Noise (1σ) [deg]	STD [Attitude- mean(Attitude)]

TABLE 6.7: Statistical Parameters Calculation

and tabulated in table 6.8. For noise calculation, mean value of the computed attitude is calculated. This mean value is subtracted from the computed attitude and standard deviation (1σ) of the difference is taken. For the rate integration, the roll, pitch and heading drift with time, therefore their mean values used for noise calculation are computed using moving average filter. The calculation of performance parameters used for comparison for the static and motion test are shown in table 6.7.

	Axis	Attitude error rms(deg)	Noise std (deg)
Rate Integration	Roll	12.75	0.05
	Pitch	15.80	0.04
	Heading	108	0.03
Vector Matching	Roll	0.19	0.18
	Pitch	0.27	0.27
	Heading	0.95	0.94

TABLE 6.8: Attitude Error Comparison between Rate integration and Vector Matching for static test

The comparison shows that the attitude error grows with time for rate integration. The maximum error introduced is in the heading which RMS value reaches 108 degrees. The roll and pitch errors also grow and reach 12.78 and 15.80 respectively in 30 minutes. The noise, however, is very small and remains with 0.05 degree. For vector matching, the attitude error remains within bound. The maximum error introduced is 0.95 degrees in the heading. The error in the other two axes

is even smaller. The noise, however, is high as compared to rate integration. The maximum noise noted, is 0.94 degrees in the heading. The merits and demerits of both methods are summarized in table 6.5.

6.5 Multi-sensor Fusions

As discussed earlier, in the present research both rate integration and vector matching techniques are merged together to make use of the merits of both methods. For the data fusion from gyros, accelerometers and magnetometers the following methods are used.

- Quaternion Feedback Configuration
- Extended Kalman Filter (Indirect Implementation)
- Kalman Filter (Direct Implementation)

These methods are implemented in Matlab and the data acquired for both static and motion tests are used for simulation. It is observed that, if the drift effects of gyros are properly compensated, then gyros are more suitable for attitude determination both under dynamic and static conditions. Therefore, in all multi-sensor integration methods, the objective is to use gyros as primary sensors for attitude determination and all other auxiliary sensors like accelerometers and magnetometers for estimation and correction of the drifting effect of the gyros.
In the preceding sections, results are shown for the above mentioned fusion methods. To compare the results, we have taken the attitude computed by rate integration as a reference. Because the target is, how much improvement we have achieved using multi-sensor integration schemes in the computed attitude as compared to that computed by rate integration. We know the actual attitude both in the motion and static tests. Because in the motion test, we have placed the IMU in a known orientation and applied predefined motion only the around Z-axis. Similarly in the static test, the IMU is placed in predefined orientation.

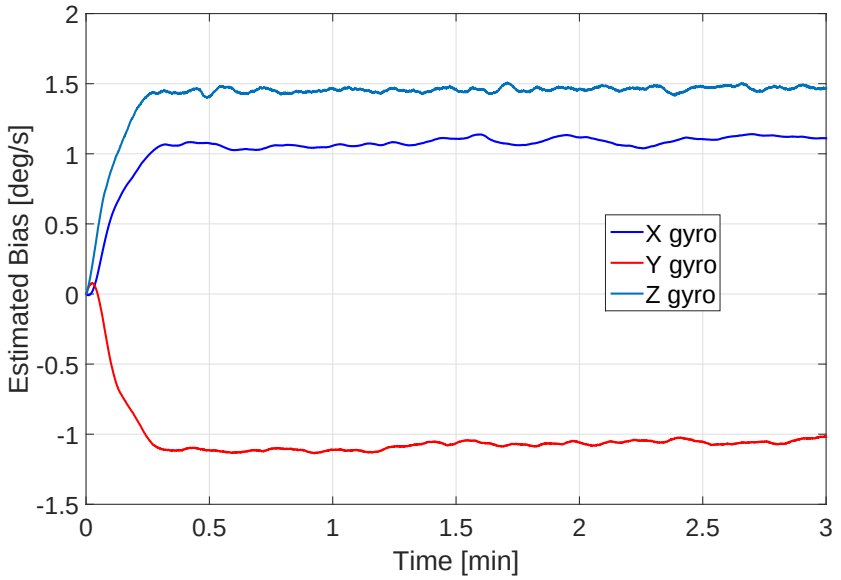

FIGURE 6.8: Bias Estimation

6.5.1 Quaternion Feedback

In quaternion feedback configuration, the bias errors of gyros are estimated and compensated continuously by a bias compensator. Therefore, at first the performance of bias compensator is evaluated. For this purpose, static test is performed for a few minutes and fixed biases of 1,-1 and 1.5 deg/sec are intentionally added in x, y and z-axes gyros' data. The data with added biases is then used for evaluation of the bias compensator. It has been observed as shown in Figure 6.8 that the estimated biases converge to the bias values which were added for evaluation. Results for attitude computation by quaternion feedback using the data for motion and static tests are shown in Figure 6.9 and 6.10 respectively. The algorithm works in close loop and compensates the drift affect of the attitude. It can be observed that the attitude variations remain within ± 1.5 degrees under static and dynamic conditions. For comparison, we have also plotted the attitude computed by the rate integration. It can be seen that quaternion feedback technique provides better attitude with no drift effect with time, clean and low noise unlike the attitude provided by rate integration and vector matching respectively. Specially the static test shows that after estimating and correcting the gyro biases, the rising trend with time vanishes and drift free attitude is available throughout the test.

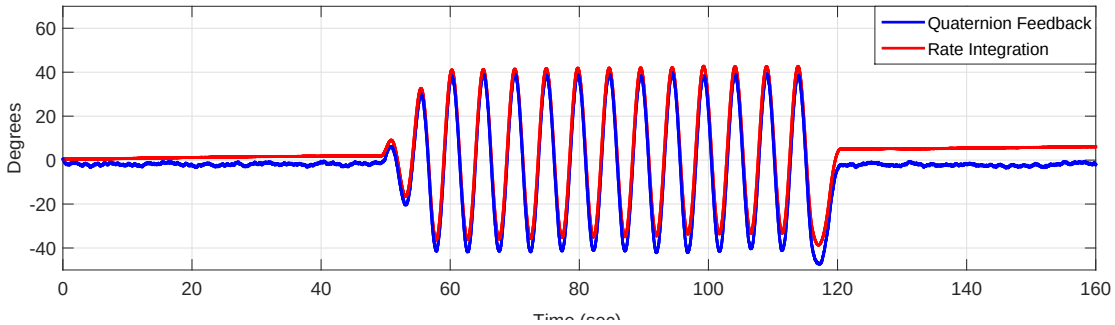

(A) Heading angle

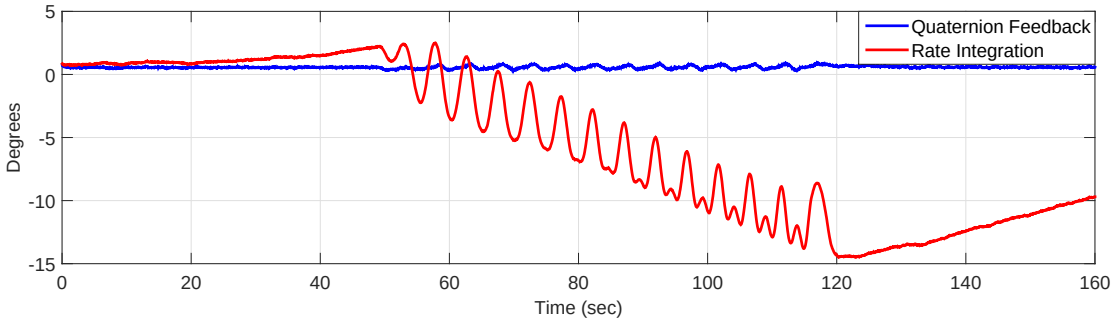

(B) Roll angle

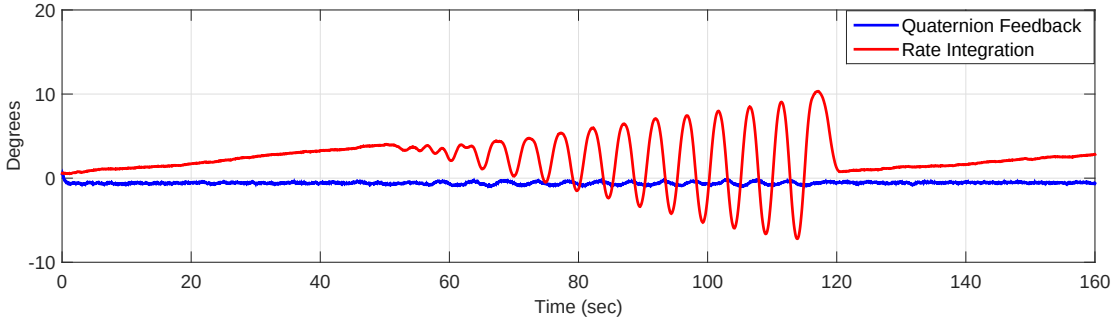

(C) Pitch angle

FIGURE 6.9: Attitude Comparison between Quaternion Feedback and Rate Integration for motion test

It has also been observed that, when bias drift of the gyros in static data was calculated, it was found around 100 deg/h. Gyros with this bias errors cannot be used for attitude determination as within a few minutes, the attitude error will grow beyond the acceptable limits. However, after compensation of the bias error of gyros, the drift is reduced to 1-2 deg/h resulting in improved attitude. Hence, it can be concluded that the algorithm not only compensates fixed biases, but also the in-run drift of the gyros.

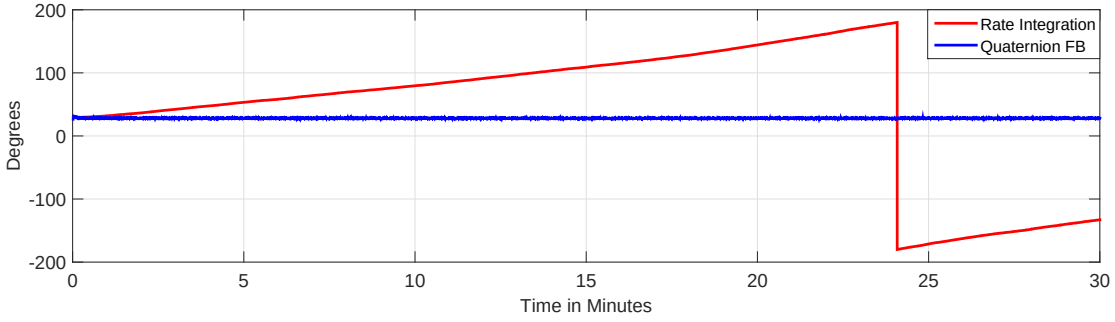

(A) Heading angle

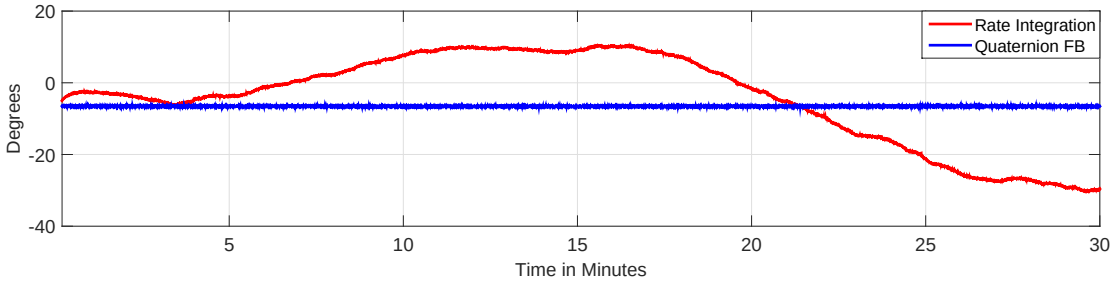

(B) Roll angle

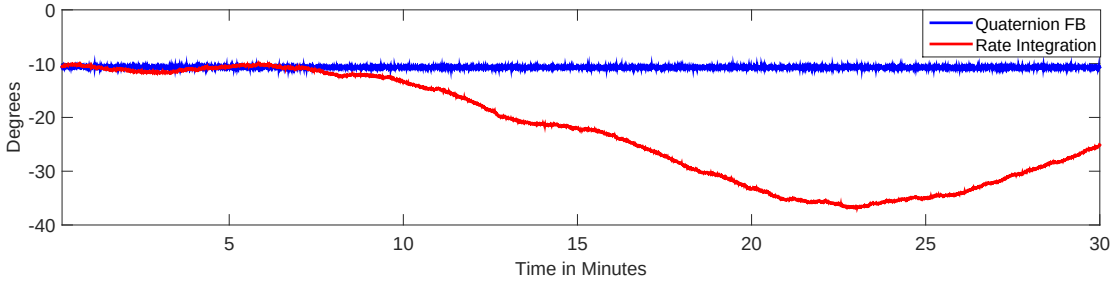

(C) Pitch angle

FIGURE 6.10: Attitude Comparison between Quaternion Feedback and Rate Integration for static test

6.5.2 Extended Kalman Filter (Indirect Implementation)

In the indirect Extended Kalman Filter's implementation, the error states are estimated which are then used for correction. A six states Extended Kalman Filter is implemented in which three states correspond to the attitude error and the other three states to the gyro biases.

To check the estimated error states in the Extended Kalman Filter implementation, fixed rates of 1, -2 and 3 deg/sec are added in the x, y and z-axes gyros' data

respectively. The estimated bias and attitude error states are plotted in Figure 6.12 and 6.11 respectively. In these Figures, the data for the motion test is used for simulation. The attitude error remains within bounds and the estimated biases converge to the fixed biases added in the gyros' data.

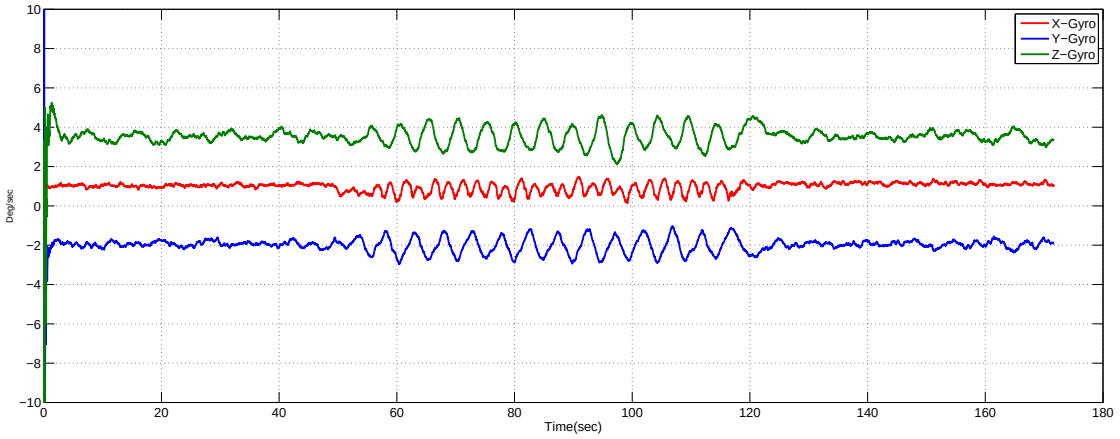

FIGURE 6.11: Bias Estimation using EKF

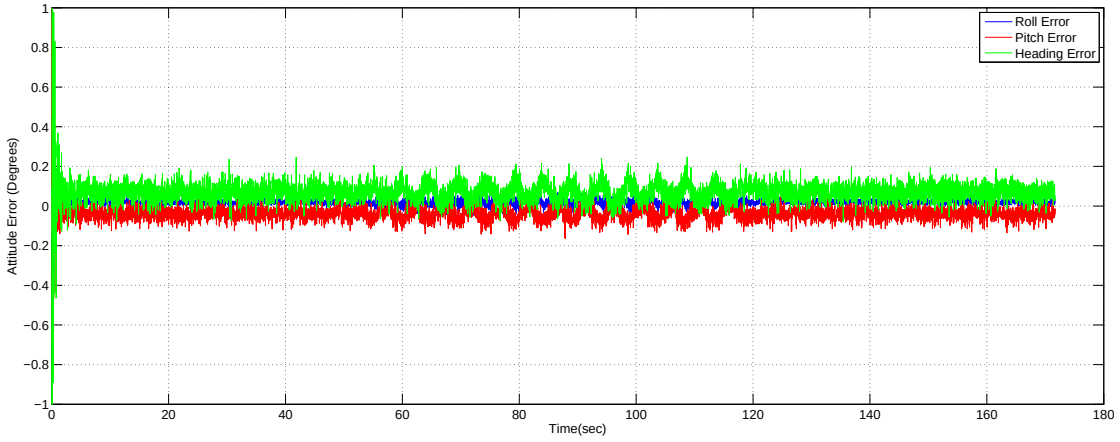

FIGURE 6.12: Attitude Error Estimation using EKF

The Extended Kalman Filter based algorithm runs in a close loop, the attitude and bias errors at each time step are calculated. The attitude update relation given by Equation 4.20 or 4.22 can used to compute the attitude by rate integration. The attitude error estimate is subtracted from the attitude computed by rate integration and reset to zero. For the next time step, corrected attitude computed during the previous time step is used in the error dynamics equation to estimate the errors states. In close loop the attitude error states remain within ± 1.

The Extended Kalman Filter based fusion algorithm is applied to the data acquired for the motion and static tests and the results are shown in Figure 6.13 and 6.14. In both tests, it has been observed that the Extended Kalman Filter estimates the error states which, when subtracted from the outputs results in a better attitude. The attitude variations remain within ±1.5 degrees for both static and motion tests. The noise in the computed attitude is also reduced as compared to the vector matching methods. Hence, both objectives of drift free and low noise attitude are achieved using all available sensors in the IMU chip by multi-sensor fusion.

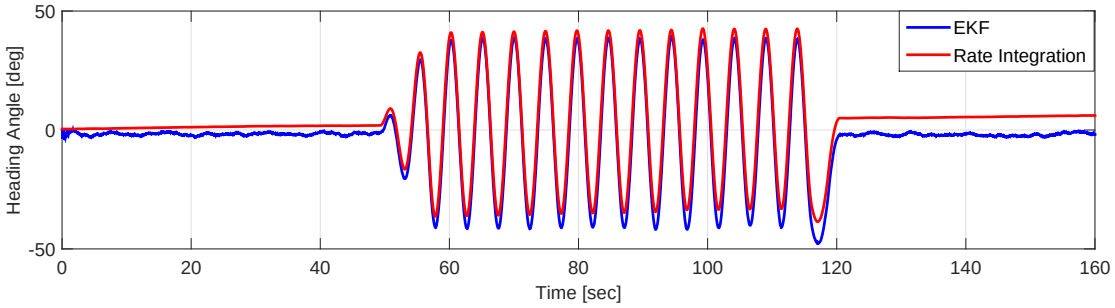

(A) Heading angle

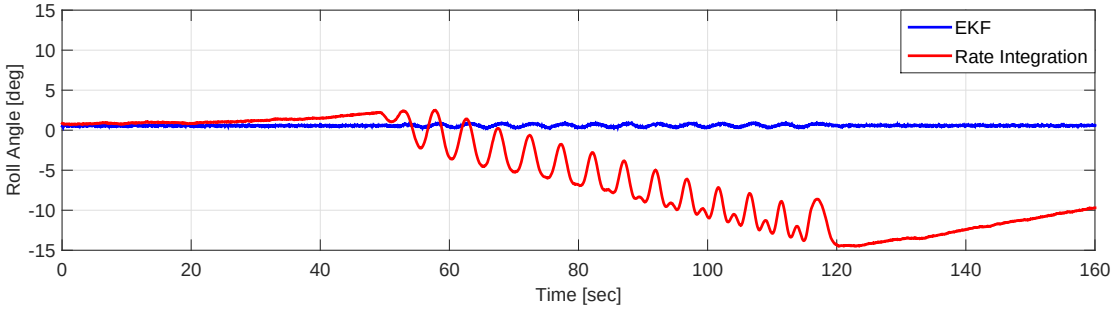

(B) Roll angle

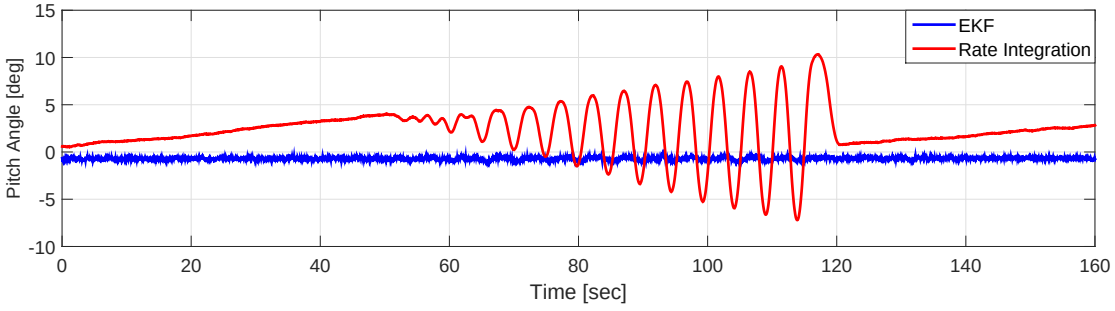

(C) Pitch Angle

FIGURE 6.13: Attitude Comparison between Rate integration and EKF for motion test

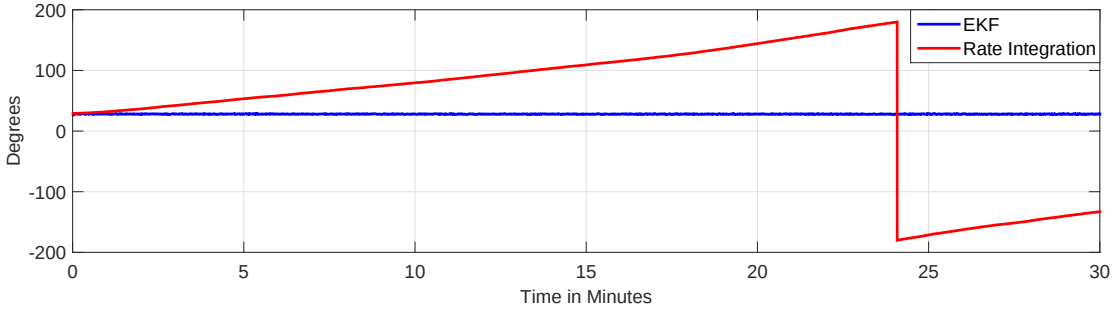

(A) Heading angle

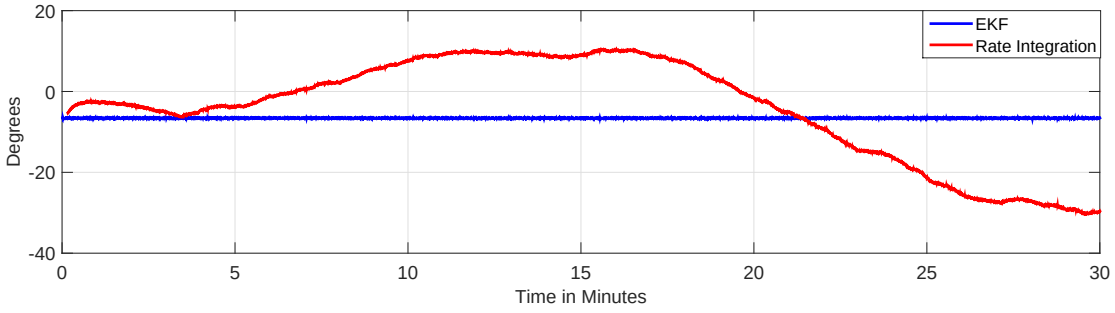

(B) Roll angle

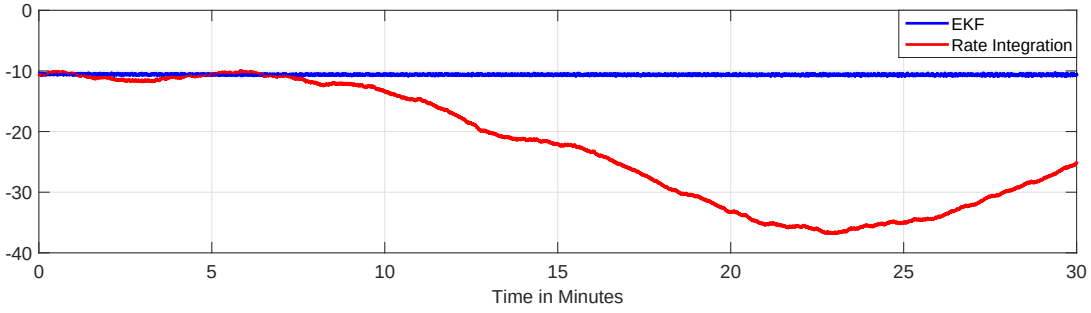

(C) Pitch Angle

FIGURE 6.14: Attitude Comparison between Rate integration and EKF for static Test

6.5.3 Direct Implementation

In the direct implementation, instead of the error states the attitude parameters in quaternion form are taken as the Kalman Filter's states. Therefore a four state Kalman Filter is implemented. Results are shown in Figure 6.15 and 6.16 for the motion and static tests respectively. It can be seen that the results are comparable

to the indirect EKF implementation with less no of states. The final attitude is low noise and drift free for both tests as desired.

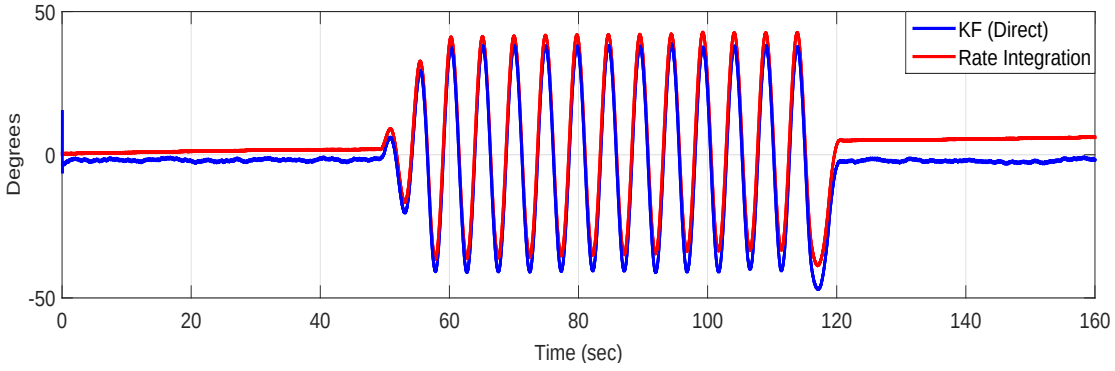

(A) Heading angle

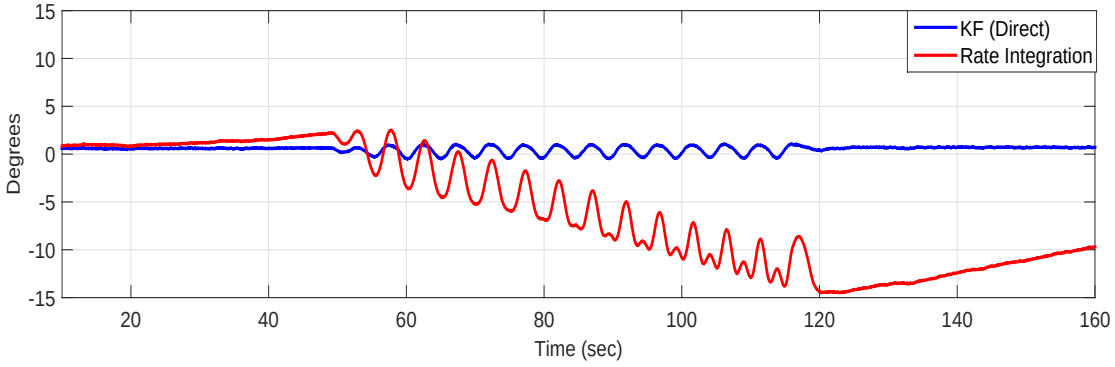

(B) Roll angle

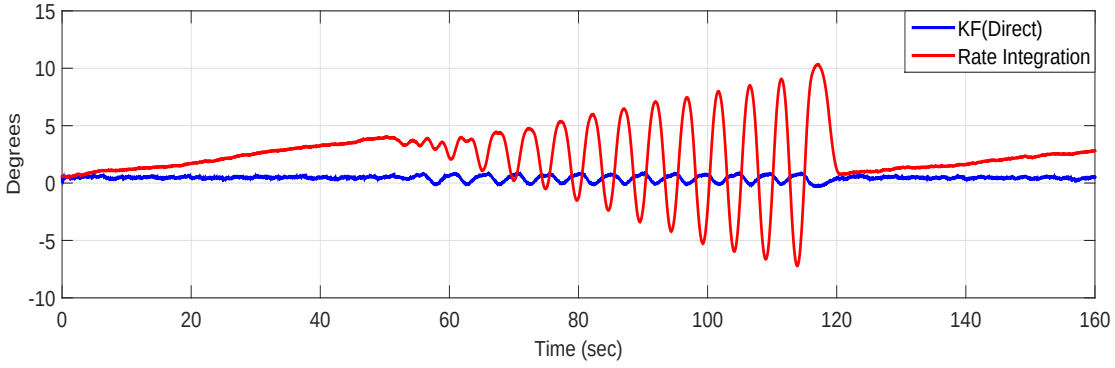

(C) Pitch Angle

FIGURE 6.15: Attitude Comparison between Rate integration and KF(Direct Implementation) for motion test

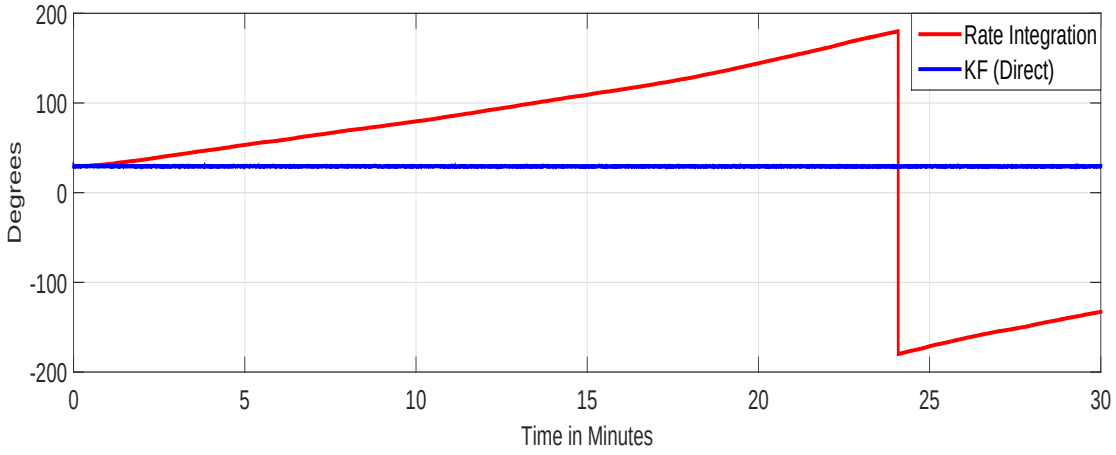

(A) Heading angle

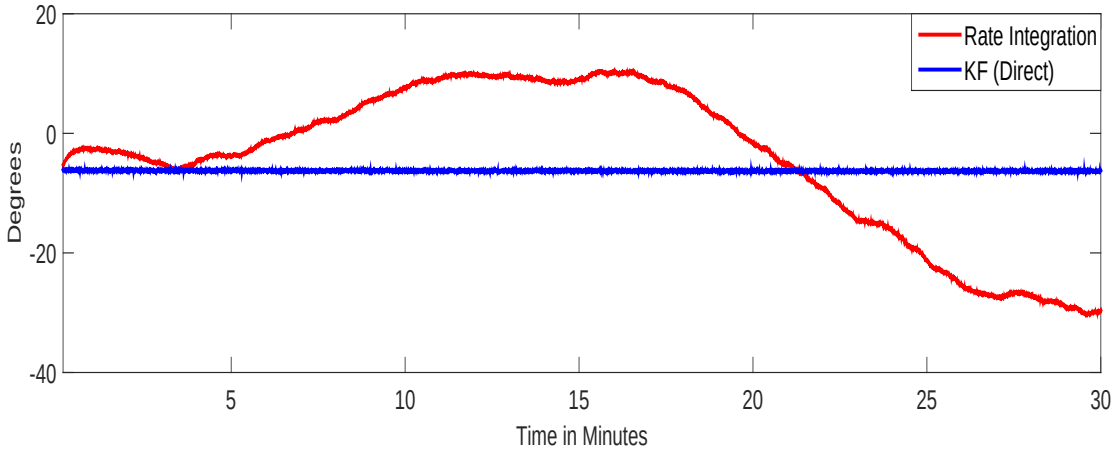

(B) Roll angle

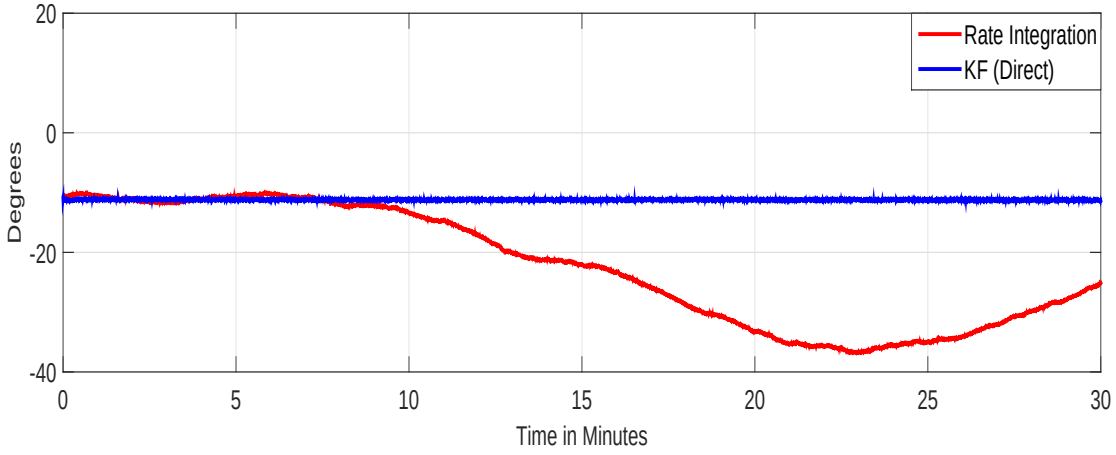

(C) Pitch Angle

FIGURE 6.16: Attitude Comparison between Rate integration and KF(Direct Implementation) for static test

	Axes	RI	EKF	KF Direct	QFB
Motion Test	Roll	16.33	0.017	0.28	0.078
	Pitch	3.18	0.01	00.03	0.01
	Heading	3.45	0.31	0.22	0.09
Static Test	Roll	12.75	0.30	0.34	0.317
	Pitch	15.80	0.26	00.07	0.19
	Heading	108	01.23	0.25	1.22

TABLE 6.9: Attitude Error Comparison of Multi-sensor Integration Techniques

6.6 Comparison of Multi-sensor Fusion Schemes with Rate Integration

The comparison of Multi-sensor fusion schemes with the rate integration is shown in table 6.9 and 6.10. For comparison, we have selected two performance parameters. The first parameter is the attitude error, and the second is the noise. For the attitude error, data of both the motion and static tests are used and the results are tabulated in table 6.9. The attitude error for the static and motion tests is calculated as mentioned in table 6.7. For the motion test, it can be seen that the attitude error is significantly reduced as compared to the rate integration. The error in the roll is less than 0.08 degree for the EKF and QFB. In the KF direct implementation, this error is 0.28 degree which is slightly higher as compared to the EKF and QFB. The error in pitch is less than 0.03 degree for all fusion methods. The error in heading touches 0.31 degree for the EKF and 0.22 for the KF direct. For QFB this error is 0.09 degree. The maximum errors for Multi-sensor integration techniques in roll, pitch and heading are 0.28,0.03 and 0.3 degrees which are very small as compared to 16.33, 3.18 and 3.45 in the same axes by the rate integration.

For static test, the attitude error is also very small as compared to the rate integration. The maximum error in roll is 0.34 degree observed in the KF direct method. In the pitch and heading, the maximum errors are 0.26 and 1.23 degrees respectively in the EKF method. The errors in all other axes remain less than these by other Multi-sensor integration methods.

For noise comparison, we used the data for static test and computed the noise for

each Multi-sensor integration technique as tabulated in table 6.10. The noise for all Multi-sensor integration techniques are smaller than the vector matching in all axes. The maximum noise introduced is 0.25 degrees in the heading for quaternion feedback. The noise in the other two axes is less 0.06 degrees. Similarly the noise by other two Kalman Filter methods are also less, with a maximum of 0.154 degrees in the heading.

From the table 6.9 and 6.10 it can be observed that the attitude error and the noise in the heading is a little bit higher as compared to the two other axes i.e. the roll and pitch. The reason is, the magnetometers available in the IMU are not as good as compared to the accelerometers. As the correction in the heading depends upon the magnetometers, we observed slightly higher attitude error and noise.

The above comparison shows that by using Multi-sensor integration schemes the attitude error and noise have been significantly improved as compared to the rate integration and vector matching respectively.

Axes	RI	VM	EKF	KF Direct	QFB
Roll	0.05	0.18	0.035	0.055	0.055
Pitch	0.04	0.27	0.071	0.051	0.049
Heading	0.03	0.94	0.12	0.154	0.253

TABLE 6.10: Noise Comparison of Multi-sensor Integration Techniques

6.7 Extended Kalman Filter Vs Quaternion Feedback

After implementation of the Extended Kalman Filter based integration scheme and Quaternion feedback and performing simulations using the available data for the motion and static tests, it is interesting to compare the results of the two schemes. Figure 6.17 and 6.18 show the results comparison of both schemes for

the motion and static test.

It has been observed that both algorithms provide similar results. The main objectives of the drift compensations and low noise are achieved by both algorithms. The attitude plots superimpose on each other showing comparable results.

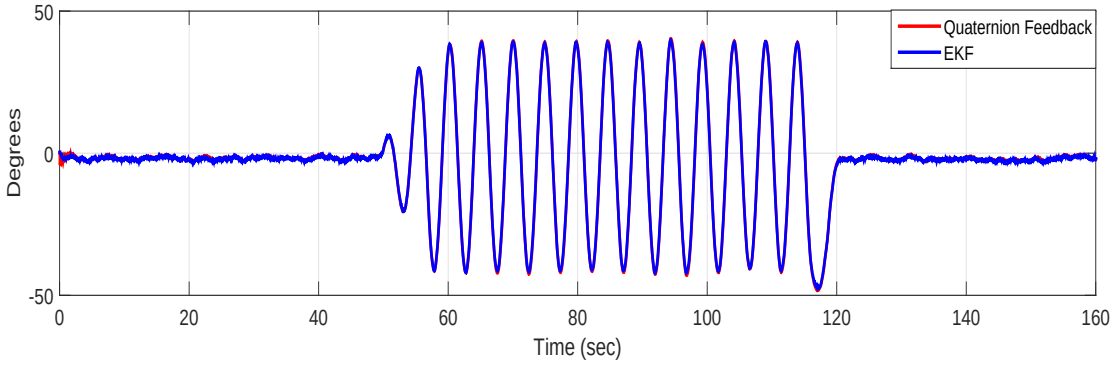

(A) Heading angle

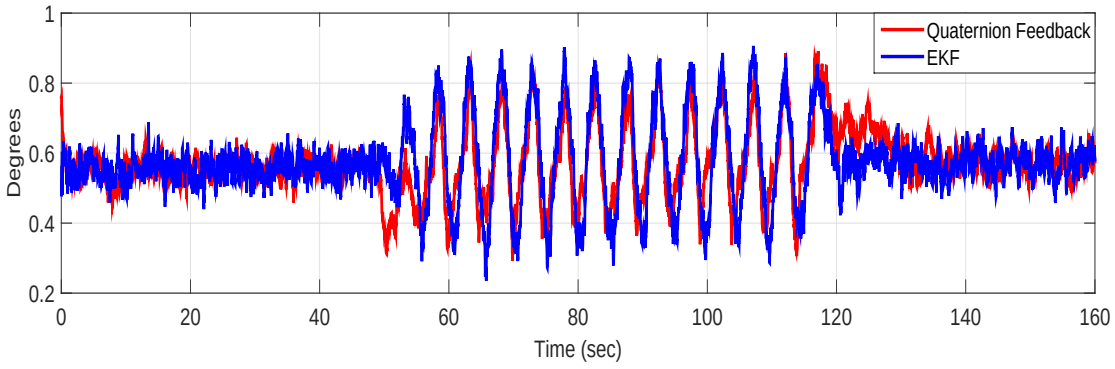

(B) Roll angle

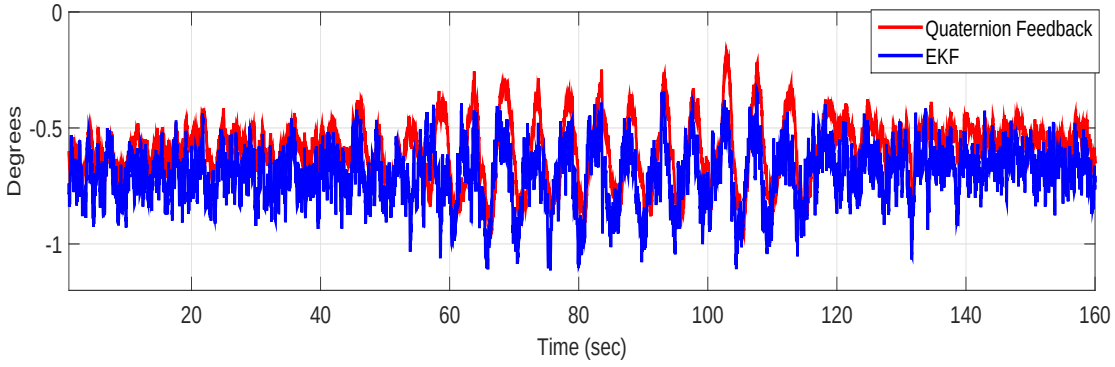

(C) Pitch Angle

FIGURE 6.17: Attitude Comparison between Quaternion Feedback and Extended Kalman Filter for motion test

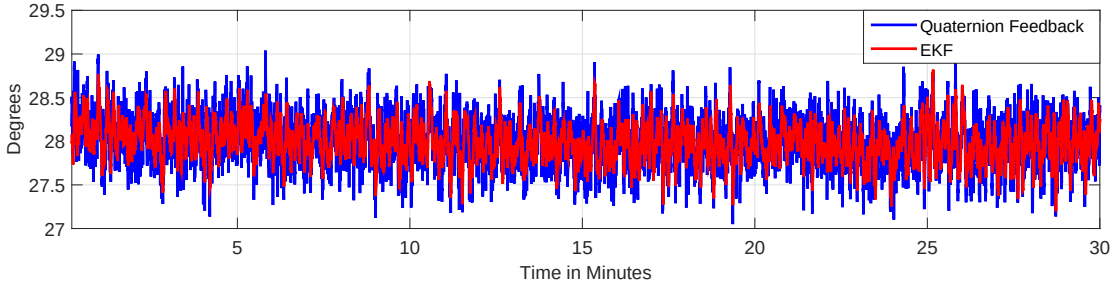

(A) Heading angle

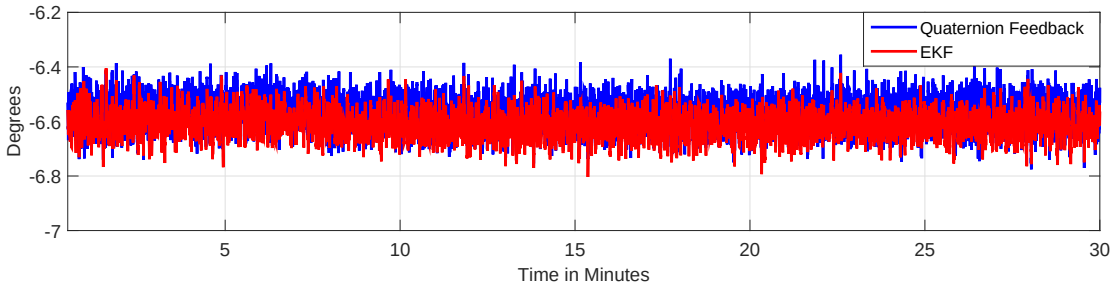

(B) Roll angle

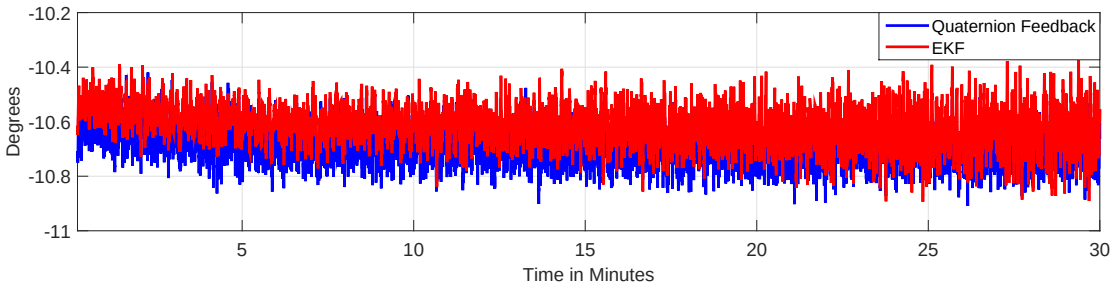

(C) Pitch Angle

FIGURE 6.18: Attitude Comparison between Quaternion Feedback and Extended Kalman Filter for static test

6.8 Road Test

The experimental tests described in section 6.3 are performed in the Laboratory to test and characterize the multi-sensors integration schemes. In these tests, the changes in real time environment like vibrations, temperature etc are not considered. The rotation in the motion test is also given only along the z-axis and limited to ± 40 degrees. In static condition, the test performed is also at room temperature in control environment.

To check and test the algorithms' performance in real time environment, a data

set acquired in road test is used. The road test in real time environment is not performed. Instead, an already available data of road test is used. The data used has been taken from a MEMS based IMU mounted on a van and a road test performed for 33 minutes. The data contain variations in Roll, Pitch and Heading axes and also vibration noise coupled in all axes. The variation in heading is specially large and switches direction from +180 to -180 degrees. The gyros in x, y and z direction contain large bias error. The reference attitude is available which can be used to compare the results. Hence, this data set can be a good check to test the performance of any multi-sensors fusion scheme.
Using the road test data, both Quaternion feedback and Kalman Filter based multi-sensors integration schemes are tested. Results are discussed in the following section.

6.8.1 Quaternion Feedback

When the road test data is used, the Quaternion feedback technique proposed in section 5.1 showed some variations. It has been observed that the computed attitude track the reference attitude, but shows divergence momentarily at different intervals. On investigation, it has been found that the attitude computed by vector matching in quaternion form needs to be modified before being used for generating the attitude error. The q-method of vector matching techniques returns the attitude in the form of quaternion $\mathbf{q} = \begin{bmatrix} q_1 & q_2 & q_3 & q_0 \end{bmatrix}'$, the first three elements of the quaternion show the vector part while the fourth shows the real part. It has been observed that the real part switches between positive and negative values. This sign inversion does not affect when the attitude is computed in terms of Euler angles from this quaternion. But if this quaternion is multiplied with another quaternion to generate the attitude error which has been used for bias estimation, it create spikes in the estimated biases and results divergence in the computed attitude. Hence, the quaternion generated by q-method needs to be modified, if the real part of the quaternion becomes negative. In this case, all the four elements of the quaternion need to be multiplied by -1. This variation in the

algorithm does not affect the results shown in section 6.5.1.

Figure 6.19 shows that results of Quaternion feedback algorithm for the road test data. The attitude computed by vector matching is also plotted along with the reference attitude. It can be observed that the attitude computed by Quaternion feedback follow the reference attitude. The heading computed is very close to the reference. The roll and pitch show some minor variations around the reference at some intervals but mostly follow the reference. The noise in the computed attitude is also small as compared to that computed by the vector matching.

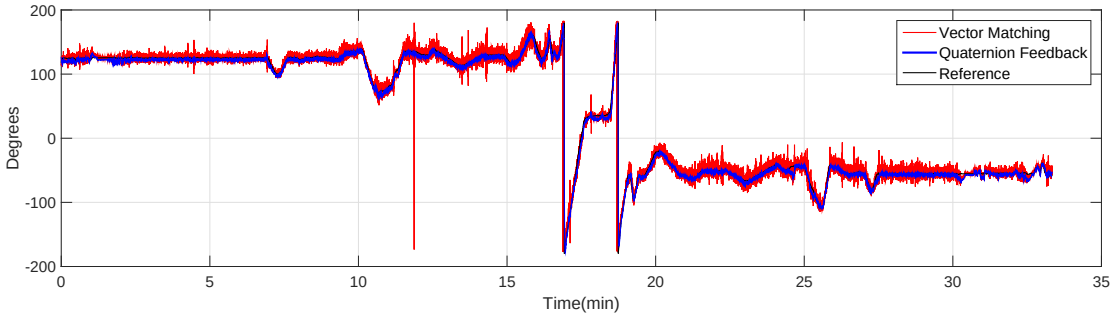

(A) Heading angle

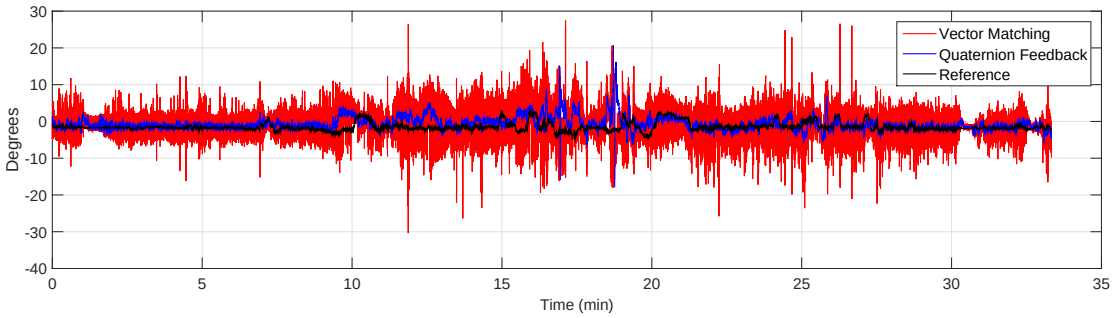

(B) Roll angle

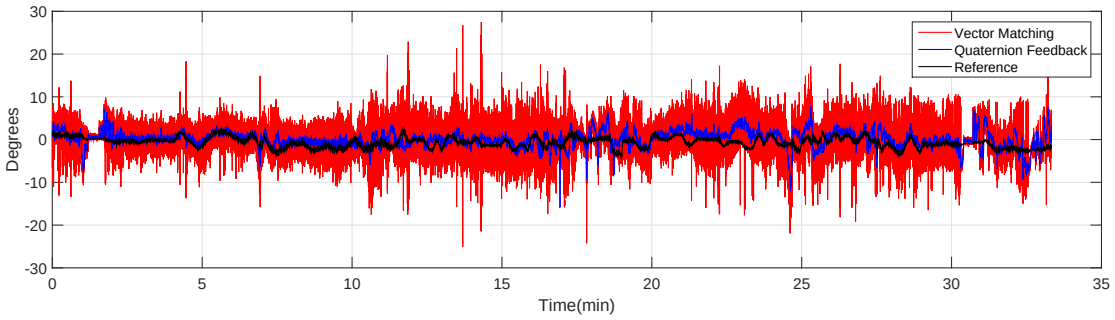

(C) Pitch Angle

FIGURE 6.19: Attitude Computation by Quaternion Feedback For Road Test

6.8.2 Extended Kalman Filter

The Extended Kalman Filter based algorithm is also tested using the road test data. In the data, it has been observed that the changes in heading touches the boundaries i.e. the heading angle changes from +180 deg to -180 deg. These boundary conditions should be specially handled in the implementation of Extended Kalman Filter.

In the Kalman Filter's Implementation, Equation 4.20 or 4.22 can be used for attitude update with angular rates in terms of the Euler angles or quaternion respectively. If Equation 4.20 is used, then the roll and heading must be limited to the range of ±180 degree because this equation generates these parameters continuously without reseting at ±180 degree. The pitch is, however, in the range (± 90). On the other hand, the roll and heading computed by the vector matching are in the range of ±180 degree. As the difference between these two attitudes is used as measurement update in the Kalman Filter's implementation, both should be in the same range. The roll and heading updated by Equation 4.20 can be brought in the range using the relation

$$\begin{aligned} \phi &= atan2(\sin(\phi), \cos(\phi)) \\ \psi &= atan2(\sin(\psi), \cos(\psi)) \end{aligned} \tag{6.1}$$

In addition, before the measurement update, the attitude error (difference between the attitude computed by rate integration and vector matching) must be brought in the range of ±180. For example, if the heading angle computed by the rate integration and vector matching are 179 and -180 degrees receptively. Their difference generates -359 degrees, while the actual difference is only 1 degree. If the heading error of -359 degrees is fed to the Kalman Filter in the measurement update, then in case of using Equation 4.20 for attitude update, the algorithm will not generate correct values at the boundaries. Similarly, in case of using Equation 4.22 for attitude update, the Kalman Filter may diverge. Hence, the attitude error $y = \begin{bmatrix} \phi_{vm} - \phi_{gyro} & \theta_{vm} - \theta_{gyro} & \psi_{vm} - \psi_{gyro} \end{bmatrix}^t = \begin{bmatrix} y_1 & y_2 & y_3 \end{bmatrix}^t$ must be brought in the limits of ±180 before the measurement update. This can be done using the

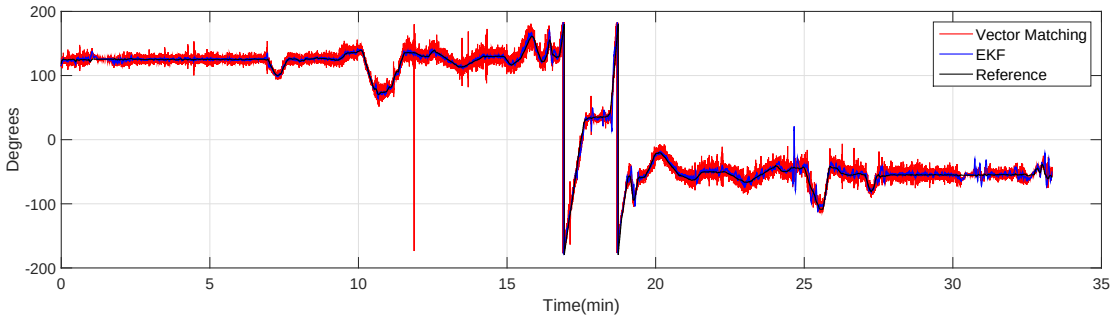

(A) Heading angle

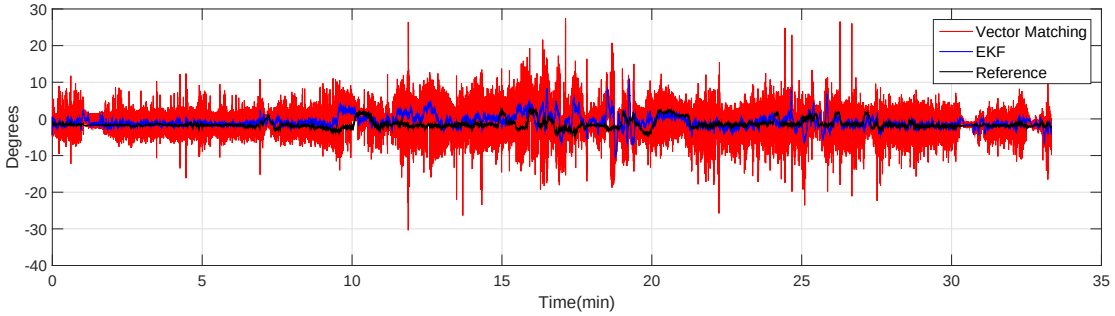

(B) Roll angle

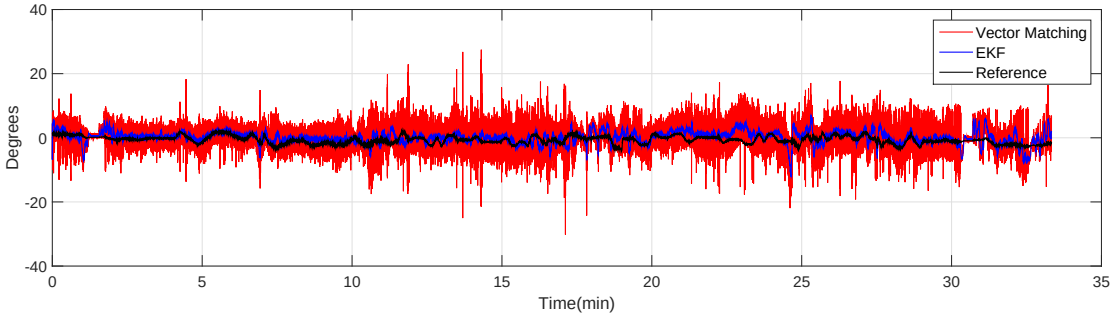

(C) Pitch Angle

FIGURE 6.20: Attitude Computation by Extended Kalman Filter For Road Test

relation

$$\begin{aligned} y_1 &= atan2(\sin(y_1), \cos(y_1)) \\ y_2 &= atan2(\sin(y_2), \cos(y_2)) \\ y_3 &= atan2(\sin(y_3), \cos(y_3)) \end{aligned} \tag{6.2}$$

With these considerations in the implementation, the Extended Kalman Filter estimates the errors states correctly without going into divergence and generate correct values at the boundaries.

Figure 6.20 shows the results of Extended Kalman Filter based multi-sensors

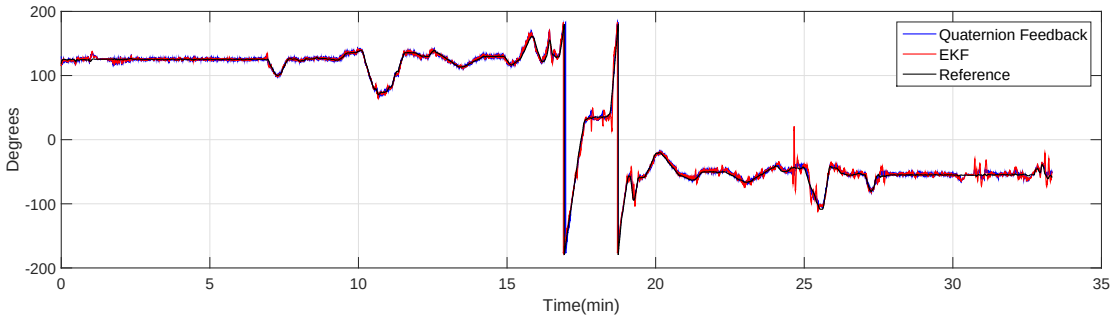

(A) Heading angle

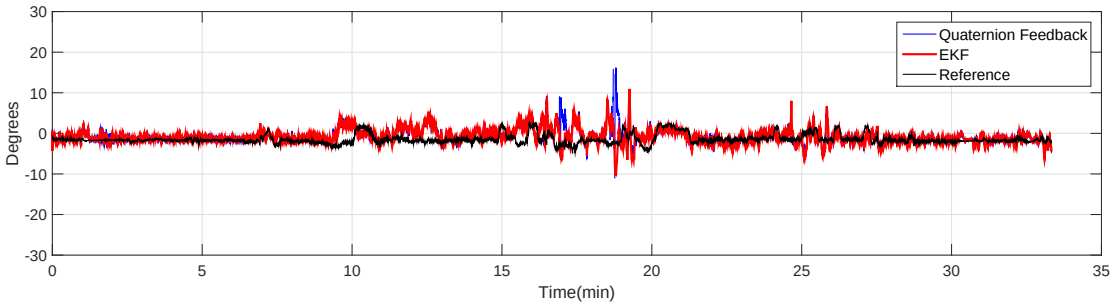

(B) Roll angle

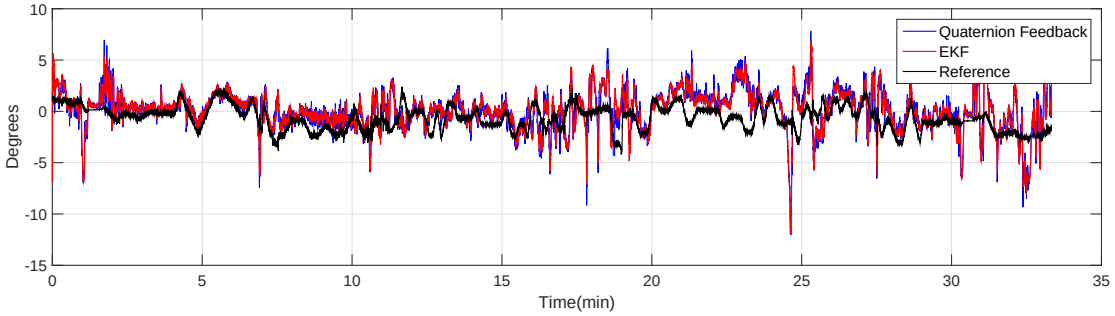

(C) Pitch Angle

FIGURE 6.21: Attitude Comparison between Quaternion Feedback and Extended Kalman Filter for Road Test

fusion algorithm for the road test data. The roll, pitch and heading follow the reference attitude and less noisy as compared to that computed by vector matching. Figure 6.21 shows the comparison between Quaternion feedback and Extended Kalman Filter using the road test data. It can be observed that both algorithm shows comparable results.

Chapter 7

Conclusions and Future Work

In this research, two methods of attitude determinations are discussed. These are conventional rate integration of gyroscopes and vector matching using directional vectors. Both methods have their own merits and demerits. The vector matching technique is good for static applications, but not suitable for dynamic applications where accelerated motion occurs. The computed attitude also contains high noise as the sensors' noise directly reflect on the attitude. The gyroscope integration method is more suitable for dynamic applications, but suffers from drift effect. The attitude drifts with time and reaches beyond limits within a short period of time. The reason is integration in the computation process which also integrates undesirable error at the sensor outputs. The sensors' noise, however, is filtered during the process and low noise attitude output is achieved. The integration acts as a low pass filter and removes high frequency noise at the gyro outputs.

In order to achieve accurate attitude information, external aiding is required for error estimation and correction. Conventionally, GPS is used for external aiding. However,a GPS receiver is an expensive component and not suitable for low cost applications. GPS has also a tendency toward jamming and unavailability for indoor applications and also under certain environmental conditions.

With the advancement of MEMS technology, multiple MEMS sensors are available in small size single chip with very low cost. This opened a door for multi-sensor

integration of all available sensors in a single chip for improved navigation parameters. In this work, we have targeted computation of attitude using multiple sensors available in a single chip. The techniques results in self aiding schemes which does not require any inputs from any external source.

We presented self aiding three techniques for improved attitude determination both from noise and drift point of view. These techniques are suitable for MEMS based Inertial Measurement unit containing magnetometers in addition to gyros and accelerometers. In all three schemes, gyros are used for attitude determination and the gyro errors are estimated and corrected using the accelerometers and magnetometers as aiding sensors. As all the sensors are available within the same chip, the integrated solution becomes self aiding without external dependency.

The first scheme, Quaternion feedback works in close loop. The algorithm continuously estimates and compensates the gyro bias errors which cause the drift effect in the computed attitude. The attitude is primarily computed by the rate integration of gyro outputs and the attitude computed by vector matching is used as a reference. The bias compensator continuously adjusts the gyro outputs by minimizing the attitude error between the reference and computed attitude. To perform both under static and dynamic conditions, the effect of linear acceleration is also incorporated because under accelerated motion conditions, the attitude computed via vector matching will not be accurate enough to be used as a reference.

The second scheme uses Extended Kalman Filter for error estimation and correction. The Kalman Filter is implemented in an indirect way to estimate the error states which are used for compensation. Six error states are defined which corresponds to bias and attitude error. The difference between the attitudes computed from the rate integration and vector matching is used as measurement update. Kalman Filter estimates the error states and after correction, the drift effect in the computed attitude is minimized.

In the third scheme Kalman Filter is used in direct configuration. The attitude parameters are used as states of the Kalman Filter. Since we are using attitude in

the form of quaternion, four states are defined in the Kalman Filter. The quaternion update relation with angular rates is used as a prediction step in the Kalman Filter. The attitude computed by vector matching is used as the measurement update.

If we compare the results of the last two schemes, i.e. Kalman Filter with indirect and direct configuration, it is observed that the results are comparable. However, the states are reduced from six to four from indirect to direct configuration.

A Kalman Filter is an optimal linear estimator which provides optimal state estimation. However, Kalman Filter has associated stability issues. Also, the Kalman Filter is computationally complex. The algorithm involves solution of high dimension matrices and vectors which require sufficient hardware resources. The situation becomes challenging when cost and hardware resources are the governing parameters.

If we compare Kalman Filter based scheme with Quaternion feedback configuration, we found comparable results with low computational requirement and less probability of being unstable. Quaternion feedback does not require tuning of parameters. The two gains k_1 and k_2 needs to be properly selected which are then valid for all types of motion and static conditions. In this scheme, the effect of linear acceleration is also catered for, during which the accelerometers (sensing a linear acceleration in addition to the gravity) will not provide accurate measurement of the gravity vector.

The quaternion feedback technique can be further improved by adding disturbance rejection against variations in the magnetometer outputs due to environmental changes. As it has been discussed that during motion, if the accelerometers measures linear acceleration in addition to the gravity, then it will introduce error in the computed attitude. Similarly, if the magnetometers sense magnetic field other than the Earth's magnetic field, then they will not be accurate enough to be used as a measurement vector in the vector matching. Magnetometers are very sensitive devices whose output are strongly disturbed by any nearby magnetic material structure and currents flowing through the circuits in close vicinity. Therefore, the magnetometer reading changes with location and installation place. For error free

attitude determination, the disturbances in magnetic field should be estimated and corrected which is recommended for future work.

Also, for attitude determination using vector matching, we have used Davenport q method. There are also other methods like Shuster's QUEST, Markley's SVD methods and Triad algorithm which can be evaluated in future work. The method with the best results and low computational requirement should be used for vector matching in quaternion feedback configuration.

Bibliography

[1] A. Noureldin, T. Karamat, and J. Geogy, *Fundamentals of Inertial Navigation, Satellite-based Positioning and their Integration*. Springer, 2013.

[2] D. H. Titerton and J. L. Weston, *Strapdown Inertial Navigation Technology*, 2nd ed. AIAA, 2004.

[3] K. Gade, "A Non-singular Horizontal Position Representation," *The Journal of Navigation*, vol. 63, no. 03, pp. 395–417, 2010.

[4] R. Collinson, *Introduction to Avionics Systems*, 3rd ed. Springer, 2011.

[5] J. Farrel and M. Barth, *The Global Positioning System and Inertial Navigation*. McGraw-Hills, 1998.

[6] A. Lawrence, *Modern Inertial Technology, Navigation, Guidance and Control*, 2nd ed. Springer, 1998.

[7] M. Euston, P. Coote, R. Mahony, J. Kim, and T. Hamel, "A Complementary Filter for Attitude Estimation of a Fixed-Wing UAV," in *2008 IEEE/RSJ International Conference on Intelligent Robots and Systems*, 2008, pp. 340–345.

[8] E. Foxlin, "Inertial Head-Tracker Sensor Fusion by a Complementary Separate-Bias KalmanFilter," in *IEEE Virtual Reality Annual Int. Symposium, Santa Clara, USA*, 1996, pp. 185–194.

[9] P. Setoodeh, A. Khayatian, and E. Frajah, "Attitude Estimation by Separate-Bias Kalman Filter-Based Data Fusion," *The Journal of Navigation*, vol. 57, no. 2, pp. 261–273, 2004.

[10] M. Grewal, L. R. Weill, and A. P. Andrews, *Global Positioning Systems, Inertial Navigation and Integration*, 2nd ed. WILEY, 2007.

[11] O. J. Woodman, "An introduction to inertial navigation," Computer Laboratory, Universiy of Cambridge, Tech. Rep. 696, 2007.

[12] M. Ilyas, Y. Yang, Q. S. Qian, and R. Zhang, "Low-cost IMU/Odometer/GPS Integrated Navigation Aided with two Antennae Heading Measurement for Land Vehicle Application," in *25th Chinese Control and Decision Conference*, 2013, pp. 4521–4526.

[13] K. Prasad, B. Kumudha, and P. Keerthana, "Mechznization and Error analysis of Aiding Systems in Civilian and Military Vehicle Navigation using Matlab," *International Journal of Control Theory and Computer Modeling (IJCTCM)*, vol. 5, no. 1, pp. 15–31, 2015.

[14] J. Pan, C. Zhang, and X. Zhang, "Real-time Accurate Odometer Velocity Estimation Aided by Accelerometers," *Measurement*, vol. 91, pp. 468–473, 2016.

[15] S. Liu, M. M. Atia, T. B. Karamat, and A. Noureldin, "A LiDAR-Aided Indoor Navigation System for UGVs," *The Journal of Navigation*, vol. 68, no. 2, pp. 253–273, 2015.

[16] H. Zhao, L. Miao, and H. Shao, "Adaptive Two-stage Kalman Filter for SINS/Odometer Integrated Navigation Systems," *The Journal of Navigation*, vol. 70, no. 2, pp. 242–261, 2017.

[17] C. Kebler, C. Ascher, M. Flad, and G. F. Trommer, "Multi-Sensor Indoor Pedestrian Navigation System with Vision Aiding," *Gyroscopy and Navigation*, vol. 3, no. 2, pp. 79–90, 2012.

[18] L. Ruotsalainen, H. Kuusniemi, M. Z. H. Bhuiyan, L. Chen, and R. Chen, "A two-dimensional pedestrian navigation solution aided with a visual gyroscope and a visual odometer," *GPS Solut*, vol. 17, no. 4, pp. 575–586, 2013.

[19] F. Baklanov and J. Dambeck, "Observability Analysis and Concept of Usage of Air Data Attitude and Heading Reference Systems," *Journal of the Institute of Navigation*, vol. 64, no. 4, pp. 427–446, 2017.

[20] Q. Fan, B. Sun, Y. Sun, Y. Wu, and X. Zhuang, "Data Fusion for Indoor Mobile Robot Positioning Based on Tightly Coupled INS/UWB," *The Journal of Navigation*, vol. 70, no. 5, pp. 1079–1097, 2017.

[21] K. Wang, T. Zhu, Y. Qin, C. Zhang, and Y. Li, "Integration of Star and Inertial Sensors for Spacecraft Attitude Determination," *The Journal of Navigation*, vol. 70, no. 6, pp. 1335–1348, 2017.

[22] Novtel, "Application note on IMU errors and their effects, Apn064," 2014.

[23] Y. Zhang, X. Yang, X. Xing, Z. Wang, and Y. Xiong, "The Standing Calibration Method of MEMS Gyro Bias for Autonomous Pedestrian Navigation System," *The Journal of Navigation*, vol. 70, no. 3, pp. 607–917, 2017.

[24] P. Aggarwal, Z. Syed, X. Niu, and N. El-Sheimy, "A Standard Testing and Calibration Procedure for Low Cost MEMS Inertial Sensors and Units," *The Journal of Navigation*, vol. 61, no. 2, pp. 323–336, 2008.

[25] A. R. Khairi, "Heading Drift Mitigation for Low-cost Inertial Pedestrian Navigation," Ph.D. dissertation, University of Nottingham, 2012.

[26] P. F. Partnership, "An Introduction to MEMS," Wolfson School of Mechanical and Manufacturing Engineering, Loughborough University, Loughborough, Leics LE11 3TU, Tech. Rep., 2002.

[27] H. Xie and G. K. Fedder, "Integrated Microelectromechanical Gyroscopes," *Journal of Aerospace Engineering*, vol. 16, no. 2, pp. 65–75, 2003.

[28] M. Park and Y. Gao, "Error and Performance Analysis of MEMS-based Inertial Sensors with a Low-cost GPS Receiver," *Sensors*, vol. 8, no. 4, pp. 2240–2261, 2008.

[29] Z. Fu, G. Zhang, Y. Lin, Y. Liu, and J. Tan, "Calibration and compensation of inertial sensor errors in portable applications - a review," in *UKACC 11th International Conference on Control Belfast, UK*, 2016, pp. 1–4.

[30] M. Kirkko-Jaakkola, J. Collin, and J. Takala, "Bias Prediction for MEMS Gyroscopes," *IEEE Sesnsors Journal*, vol. 12, no. 6, pp. 2157–2163, 2012.

[31] S. Y. Cho and C. G. Park, "MEMS Based Pedestrian Navigation System," *The Journal of Navigation*, vol. 59, no. 1, pp. 135–153, 2006.

[32] M. Andrejasi, "MEMS accelerometer," University of Ljubljana, Faculty for mathematics and physics, Department of physics, Tech. Rep., 2008.

[33] K. Narayanan, "Performance Analysis of Attitude Determination Algorithms for Low-cost Attitude Heading Reference Systems," Ph.D. dissertation, Auburn University, Alabama, 2010.

[34] S. K. Hong and S. Park, "Minimal-Drift Heading Measurement using a MEMS Gyro for Indoor Mobile Robots," *Sensors*, vol. 8, no. 11, pp. 7287–7299, 2008.

[35] Z. Wu, Z. Sun, W. Zhang, and Q. Chen, "Attitude and gyro bias estimation by the rotation of an inertial measurement unit," *Measurement Science and Technology*, vol. 26, no. 12, 2016.

[36] N. Metni, J. M. Pfimlin, T. Hamel, and P. Soueres, "Attitude and gyro bias estimation for a VTOL UAV," *Elsevier Control Engineering Practice*, vol. 14, no. 12, pp. 1511–1520, 2006.

[37] P. Petkov and T. Slavov, "Stochastic Modeling of MEMS Inertial Sensors," *Cybernatics and Information Technology*, vol. 10, no. 2, pp. 31–40, 2010.

[38] J. Borenstein and L. Ojeda, "Heuristic Drift Elimination for Personnel Tracking Systems," *The Journal of Navigation*, vol. 63, no. 4, pp. 591–606, 2010.

[39] V. M. Tereshkov, "An Intuitive Approach to Inertial Sensor Bias Estimation," *International Journal of Navigation and Observation*, vol. 2013, 2012.

[40] M. J. Caruso, "Applications of Magnetic Sensors for Low-cost Compass Systems," in *IEEE Position Location and Navigation Symposium*, 2000, pp. 177–184.

[41] S. Han and J. Wang, "A Novel Method to Integrate IMU and Magnetometers in Attitude and Heading Reference Systems," *The Journal of Navigation*, vol. 64, no. 4, pp. 727–738, 2011.

[42] X. Niu, S. Nasser, C. Goodall, and N. El-Sheimy, "A Universal Approach for Processing any MEMS Inertial Sensor Configuration for Land-Vehicle Navigation," *The Journal of Navigation*, vol. 60, no. 2, pp. 233–245, 2007.

[43] H. Rehbinder and X. Hu, "Drift Free Attitude Estimation for Accelerated Rigid Bodies," *Automatica*, vol. 40, no. 4, pp. 653–659, 2004.

[44] Y. S. Suh, S. K. Park, H. J. Kang, and Y. S. Ro, "Attitude Estimation Adaptively Compensating External Acceleration," *JSME International Journal Series C Mechanical Systems*, vol. 49, no. 1, pp. 172–179, 2006.

[45] A. Ali and N. El-Sheimy, "Low-cost MEMS-Based Pedestrian Navigation Technique for GPS-Denied Areas," *Journal of Sensors*, vol. 2013, 2013.

[46] W. Li and J. Wang, "Effective Adaptive Kalman Filter for MEMS-IMU/Magnetometers Integrated Attitude and Heading Reference Systems," *The Journal Navigation*, vol. 66, no. 1, pp. 99–113, 2013.

[47] L. Wang, B. Song, X. Han, and Y. Hao, "Attitude Determination Method by Fusing Single Antenna GPS and Low Cost MEMS Sensors using Intelligent Kalman Filter Algorithm," *Mathematical Problems in Engineering*, vol. 2017, pp. 1–14, 2017.

[48] R. Munguia, "A GPS-aided Inertial Navigation System in Direct Configuration," *Journal of Applied Research and Technology*, vol. 12, no. 1, pp. 803–814, 2014.

[49] N. Li, W. Ma, W. Man, L. Cao, and H. Zhang, "Multiple Robust High-degree Cubature Kalman Filter for Relative Position and Attitude Estimation of

Satellite Formation," *The Journal of Navigation*, vol. 72, no. 5, pp. 1254–1274, 2019.

[50] R. M. Rogers, *"Applied Mathematics in Integrated Navigation Systems"*, 2nd ed. AIAA, 2003.

[51] Q.-Q. Yang, L.-L. Sun, and L. Yang, "A Fast Adaptive-Gain Complementary Filter Algorithm for Attitude Estimation of an Unmanned Aerial Vehicle," *The Journal of Navigation*, vol. 71, no. 6, pp. 1478–1491, 2018.

[52] L. Zhao and Q. Yunwang, "Design of an Attitude and Heading Reference System Based on Distributed Filtering for Small UAV," *Mathematical Problems in Engineering*, vol. 2013, pp. 1–8, 2013.

[53] Y. Xu, W. Sun, and P. Li, "A Miniature Integrated Navigation System for Rotary-Wing Unmanned Aerial Vehicles," *International Journal of Aerospace Engineering*, vol. 2014, pp. 1–13, 2014.

[54] H. Fourati, N. Manamanni, L. Afilal, and Y. Handrich, "A Rigid Body Attitude Estimation for Bio-Logging Application: A Quaternion-Based Nonlinear Filter Approach," in *2009 IEEE/RSJ International Conference on Intelligent Robots and Systems*, 2009, pp. 558–563.

[55] M. Hua, "Attitude Estimation for Accelerated Vehicles using GPS/INS measurements," *Control Eng. Practice*, vol. 18, no. 7, pp. 723–732, 2010.

[56] H. F. Grip, "Globally Exponentially Stable Attitude and Gyro Bias Estimation with Application to GNSS/INS integration," *Automatica*, vol. 51, no. 1, pp. 158–166, 2014.

[57] H. An, J. Li, J. Wang, J. Wang, and H. Ma, "Second-Order Geometric Sliding Mode Attitude Observer with Application to Quadrotor on a Test Bench," *Mathematical Problems in Engineering*, vol. 2013, 2013.

[58] H. Yamato and T. Furuta, "Attitude Determination by Globally and Asymptotically Stable Estimation of Gyroscope Bias Error with Disturbance Attenuation and Rejection," *Journal of Robotics and Mechatronics*, vol. 24, no. 2, pp. 389–398, 2012.

[59] G. Wahba, "Problem 65-1, A Least Squares Estimation of Satellite Attitude," *SIAM Review*, vol. 7, no. 3, p. 409, 1965.

[60] P. Davenport, "A Vector Approach to the Algebra of Rotations with Applications," Goddard Space Flight Center NASA TN D-4696, Technical note, 1968.

[61] J. Keat, "Analysis of Least-Square Attitude Determination Routine DOAOP," NASA-CR183450, Tech. Rep., 1977.

[62] M. D. Shuster and S. D. Oh, "Three-Axis Attitude Determination from Vector Observations," *AIAA Journal of Guidance and Control*, vol. 4, no. 1, pp. 70–77, 1981.

[63] F. L. Markley, "Attitude Determination using Vector Observations and the Singular Value Decomposition," *Journal of the Astronautical Sciences*, vol. 36, no. 3, pp. 245–258, 1988.

[64] ——, "Attitude Determination using Vector Observations: A Fast Optimal Matrix Algorithm," *Journal of the Astronautical Sciences*, vol. 41, no. 2, pp. 261–280, 1993.

[65] C. Hide, T. Moore, and M. Smith, "Adaptive Kalman Filtering for Low-cost INS/GPS," *The Journal of Navigation*, vol. 56, no. 1, pp. 143–152, 2003.

[66] Z. Zheng, S. Han, J. Yue, and L. Yuan, "Compensation for Stochastic Error of Gyros in a Dual-axis Rotational Inertial Navigation System," *The Journal of Navigation*, vol. 69, pp. 169–182, 2016.

[67] S. Han and J. Wang, "Land Vehicle Navigation with the Integration of GPS and Reduced INS: Performance Improvement with Velocity Aiding," *The Journal of Navigation*, vol. 63, no. 1, pp. 153–166, 2010.

[68] K. Abdulrahim, C. Hide, T. Moore, and C. Hill, "Aiding Low Cost Inertial Navigation with Building Heading for Pedestrian Navigation," *The Journal of Navigation*, vol. 64, no. 2, pp. 219–233, 2011.

[69] W. W. Ding, Jinling, and C. Rizos, "Improving Adaptive Kalman Estimation in GPS/INS Integration," *The Journal of Navigation*, vol. 60, no. 3, pp. 517–529, 2007.

[70] A. V. Nebylov and J. Watson, *"Aerospace Navigation Systems"*, 1st ed. Wily, 2016.

[71] J. Diebel, "Representing attitude: Euler angles, Unit Quaternions and Rotation Vectors," Stanford University Stanford, California 94301-9010, Tech. Rep., 2006.

[72] M. B. Ari, "A Tutorial on Euler Angles and Quaternions," Department of Science Teaching, Weizmann Institute of Science, Tech. Rep., 2018.

[73] N. Madinehi, "Rigid Body Attitude Estimation: An Overview and Comparative Study," Master's thesis, The University of Western Ontario, 2013.

[74] E. Bakir, *"Introduction to Modern Navigation Systems "*, 1st ed. World Scientific, 2007.

[75] L. Fei, L. Jie, W. Haifu, and L. Chang, "An improved quaternion Gauss-Newton algorithm for attitude determination using magnetometer and accelerometer," *Chinese Journal of Aeronautics*, vol. 27, no. 4, pp. 986–993, 2013.

[76] T. B. Rinnan, "Development and Comparison of Estimation Methods for Attitude Determination," Master's thesis, Norwegian University of Science and Technology, 2012.

[77] J. Wu, Z. Zhou, B. Gao, R. Li, Y. Cheng, and H. Fourati, "Fast Linear Quaternion Attitude Estimator using Vector Observations," *IEEE Transactions on Automation Science and Engineering*, vol. 15, no. 1, pp. 307–319, 2018.

[78] R. O. Duarte, L. S. Martins-Filho, and H. K. Kuga, "Performance comparison of Attitude Determination Algorithms Developed to Run in a Microprocessor Environment," in *20th International Conference of Mechanical Engineering, Gramado, RS, Brazil*, 2009.

[79] Z. Shao-yu, H. An-yi, Y. Yong-an, D. Dong-mei, K. Dong-mei, and S. Xia, "Research on Attitude Determination using Adaptive Optimal-Request," in *Proceedings of 2014 IEEE Chinese Guidance, Navigation and Control Conference*, 2014, pp. 2537–2541.

[80] *Magnetic Components*, 2019 (accessed November 6, 2019). [Online]. Available: https://www.geomag.nrcan.gc.ca/mag_fld/comp-en.php

[81] A. Wahdan, W. F. Abdelfatah, and A. Noureldin, "Magnetometer Calibration for Portable Navigation Devices in Vehicles using a Fast and Autonomous Technique," *IEEE Transactions on Intelligent Transportation Systems*, vol. 15, no. 5, pp. 2347–2352, 2014.

[82] *IGRF Magnetic Field Calculator*, 2017 (accessed March 9, 2017). [Online]. Available: https://geomag.nrcan.gc.ca/calc/mfcal-en.php

[83] J. B. Kuipers, *"Quaternions and Rotation Sequences"*. Princeton University Press, 1999.

[84] W. F. Trench, "The method of lagrange multiplier," Department of Mathematics, Trinity University San Antonio, Texas, USA, Tech. Rep., 2013.

[85] D. J. Siminovitch, "Rotations in NMR: Part I Euler-Rodrigues parameters and quaternions," *Concepts in Magnetic Resonance*, vol. 9, pp. 149 – 171, 01 1997.

[86] G. Stange, *Introduction to Linear Algebra*, 2nd ed. Wellesley Cambridge Press, 1998.

[87] R. E. Kalman, "A New Approach to Linear Filtering and Prediction Problems," *Journal of Basic Engineering*, vol. 82, no. 1, pp. 35–45, 1960.

[88] G. Welch and G. Bishop, "An Introduction to the Kalman Filter," Department of Computer Science University of North Carolina at Chapel Hill, Tech. Rep. TR 95-041, 2006.

[89] M. H. Hayes, *"Statistical Digital Signal Processing and Modeling"*, 1st ed. John Wiley and Sons, Inc., 1996.

[90] *Parameters and calibration of a low-g 3-axis accelerometer, AN4508*, ST Microelectronics, 2014.

[91] B. Vaglienti, *MEMs Inertial Measurement Unit Calibration*, 2017 (accessed November 6, 2019). [Online]. Available: http://www.fivebyfivedevelopment.com/Downloads/IMU%20Calibration.pdf

[92] V. Sokolovic, G. Dikic, G. Markovic, R. Stancic, and N. Lukic, "INS/GPS Navigation System Based on MEMS Technologies," *Journal of Mechanical Engineering*, vol. 61, pp. 448–458, 2015.

[93] J. K. Bekkeng, "Calibration of a Novel MEMS Inertial Reference Unit," *IEEE Transactions on Instrumentation and Measurement*, vol. 58, no. 6, pp. 1967–1974, 2009.

[94] A. Ali, S. Siddharth, Z. Syed, C. Goodall, and N. El-Sheimy, "An efficient and robust maneuvering mode to calibrate low cost magnetometer for improved heading estimation for pedestrian navigation," *Journal of Applied Geodesy*, vol. 7, no. 1, pp. 65–73, 2013.

[95] Y. Li, J. Georgy, X. Niu, Q. Li, and N. El-Sheimy, "Autonomous Calibration of MEMS Gyros in Consumer Portable Devices," *Journal of Sensors*, vol. 15, no. 7, pp. 4062–4072, 2015.

[96] D. M. Ma, J. K. Shiau, C. Wang, and Y. H. Lin, "Attitude Determination Using a MEMS-Based Flight Information Measurement Unit," *Journal of Sensors*, vol. 12, no. 1, pp. 1–23, 2012.

[97] E. Foxlin, M. Harrington, and Y. Altshuler, "Miniature 6-DOF inertial system for tracking HMDs," in *Helmet- and Head-Mounted Displays III*, 1998, pp. 214–228.

[98] H. Luinge and P. Veltink, "Measuring orientation of human body segments using miniature gyroscopes and accelerometers," *Journal of Medical, Biological Engineering and Computing*, vol. 43, no. 2, pp. 273–282, 2005.

[99] X. Yun and E. R. Bachmann, "Design, Implementation, and Experimental Results of a Quaternion-Based Kalman Filter for Human Body Motion Tracking," *IEEE Transactions on Robotics*, vol. 22, no. 6, pp. 389–398, 2006.

[100] H. Wu, X. Zhao, C. Pang, L. Zhang, and B. Feng, "Multivariate Constrained GNSS Real-time Full Attitude Determination Based on Attitude Domain Search," *The Journal of Navigation*, vol. 72, no. 2, pp. 483–502, 2018.